ÇUKUROVA UNIVERSITY
INSTITUTE OF NATURAL AND APPLIED SCIENCES

MSc THESIS

Oğur İYNEN

THE INFLUENCE OF SINTERING AND SHOT PEENING PROCESSES ON ALUMIX 431 POWDER MATERIALS

DEPARTMENT OF MECHANICAL ENGINEERING

ADANA, 2009

UNIVERSITY OF CUKUROVA

INSTITUTE OF NATURAL AND APPLIED SCIENCES

THE INFLUENCE OF SINTERING AND SHOT PEENING PROCESSES ON ALUMIX 431 POWDER MATERIALS

Oğur İYNEN

MSc THESIS

DEPARTMENT OF MECHANICAL ENGINEERING

We certified that the thesis titled above was reviewed and approved for the award of degree of master of science by the board of jury on ..... /..... / 2009

Signature:	Signature:	Signature:
Prof. Dr. Abdul Kadir EKŞİ	Assist. Prof. Dr. Ali KOKANGÜL	Lecturer. Dr. Durmuş Ali BİRCAN
Advisor	Member	Member

This MSc Thesis is performed in Department of Mechanical Engineering of Institute of Natural and Applied Sciences of Cukurova Universty.

Registration Number:

Prof. Dr. Aziz ERTUNÇ

Director The Institute of Natural and Applied Sciences

This study is supported by Unit of Scientific Research Projects of Cukurova University. Project Number: MMF2008BAP2

Note: The usage of the presented specific declarations, figures, and photographs either in thesis or in any other reference without citation is subject to "The law of Arts and Intellectual Products" numbered 5846 of Turkish Republic.

ABSTRACT

MSc THESIS

THE INFLUENCE OF SINTERING AND SHOT PEENING PROCESSES ON ALUMIX 431 POWDER MATERIALS

Oğur İYNEN

DEPARTMENT OF MECHANICAL ENGINEERING INSTITUTE OF NATURAL AND APPLIED SCIENCES UNIVERSITY OF ÇUKUROVA

Supervisor : Prof. Dr. Abdul Kadir EKŞİ
Year : 2009, **Pages:** 95
Jury : Prof. Dr. Abdul Kadir EKŞİ
Assist. Prof. Dr. Ali KOKANGÜL
Lecturer. Dr. Durmuş Ali BİRCAN

In this work, Alumix 431 metal powders have been chosen for study due to widely used in the industrial applications. First, Alumix 431 powders were pressed at 400 MPa pressure and room temperature (RT). Then, pressed specimens were sintered at 600 ºC and 620 ºC temperatures for 1h separately. In order to examine effects of sintering operation to density, densities have been measured in per different temperature. After sintering operation, a group of specimen was shot peened in 12A and 16A intensities. To investigate mechanical properties of sintered and shot peened Alumix 431 powders, tensile and fatigue tests were performed. In addition, fractured specimens after tensile tests were used for Micro-Hardness tests. For metallographic researches of specimens, Optic Microscopy (OM) and Scanning Electron Microscopy (SEM) test were examined.

Key Words: Powder metallurgy, Alumix 431, Sintering, Shot peening, Fatigue strength

ÖZ

YÜKSEK LİSANS TEZİ

SİNTERLEME VE BİLYALI DÖVME İŞLEMLERİNİN ALUMİX 431 TOZ MALZEMELER ÜZERİNDEKİ ETKİSİ

Oğur İYNEN

ÇUKUROVA ÜNİVERSİTESİ
FEN BİLİMLERİ ENSTİTÜSÜ
MAKİNA MÜHENDİSLİĞİ ANABİLİM DALI

Danışman : Prof. Dr. Abdul Kadir EKŞİ
Yıl : 2009, **Sayfa :** 95
Juri : Prof. Dr. Abdul Kadir EKŞİ
Yrd. Doç. Dr. Ali KOKANGÜL
Öğr. Gör. Dr. Durmuş Ali BİRCAN

Bu çalışmada, endüstriyel uygulamalarda yaygın olarak kullanılan Alumix 431 tozları seçilmiştir. Alumix 431 tozları 400 MPa basınç ve oda sıcaklığında sıkıştırılmıştır. Daha sonra, sıkıştırılan numuneler 600 ºC ve 620 ºC sıcaklıklarda 1 saat sinterlenmiştir. Sinterleme işleminin yoğunluğa etkisini araştırmak için, sinterlenmiş numuneler farklı sıcaklıklarına göre her biri ayrı olarak ölçülmüştür. Sinterleme işleminden sonra, bir grup numuneye 12A ve 16A yoğunluklarında bilyalı dövme uygulanmıştır. Sinterlenme ve bilyalı dövme yapılmış Alumix 431 toz malzemelerinin mekanik özelliklerini incelemek için çekme ve yorulma testleri yapılmıştır. Bununla birlikte, çekme deneylerinden sonra kırılmış numuneler Mikro-Sertlik testleri için kullanılmıştır. Metalografik araştırmalar için, Optik Işık Mikroskobu (OIM) ve Taramalı Elektron Mikroskobu (TEM) değerlendirilmiştir.

Anahtar Kelimeler: Toz metallurjisi, Alumix 431, Sinterleme, Bilyalı dövme, Yorulma dayanımı

ACKNOWLEDGEMENTS

I am so grateful to my supervisor Prof. Dr. Abdul Kadir EKŞİ for his guidance, inspiration and encouragement during all my thesis studies.

I also thank my special committee members, my supervisor Prof. Dr. Abdul Kadir EKŞİ, Assist. Prof. Dr. Ali KOKANGÜL, and Lecturer. Dr. Durmuş Ali BİRCAN their enthusiasms and many helpful suggestions.

I would like to thank to all my friends for their endless support: Research Assistant. Çetin CANPOLAT, Murat DİLEK, Bilal ÇALIK and Project Assistant. Engin PINAR and Project Assistant. İsmail Yasin SÜLÜ, Musa KABURCUK, Sibel TAHMAZOĞLU, Arif Rüstem ZALOĞLU.

I would like to thank to TEMSA GLOBAL Sanayi ve Ticaret A. Ş., Işın Technical Machine Industry Limited Company, Air Supply and Maintanence Center and Uzeller Machine Industry Limited Company for their technical contribution to my thesis.

I have to thank to Prof. Dr. Remzi VAROL in Süleyman Demirel University; Assoc. Prof. Dr. Halil ARIK, Project Assistant. Arif UZUN, Project Assistant. Uğur GÖKMEN in Gazi University; Assoc. Prof. Dr. Mustafa Kemal KÜLEKCİ, Lecturer. Ercan KÖSE, Research Assistant. Şeref ÖCALIR and Research Assistant. İbrahim Aslan ŞEHİTOĞLU in Tarsus Technical Education Faculty/Mersin University; Prof. Dr. Mahmut D. MAT and Assist. Prof. Dr. Fahrettin ÖZTÜRK in Niğde University for their special attention during my laboratory works. They have let me use all possibilities of University Laboratories for pressing, sintering, hardness, and scanning electron microscope operations, respectively.

Finally, special thanks to my family for their endless supports, and I am so grateful to Lecturer. Dr. Durmuş Ali BİRCAN for his endless interest and support during all my thesis studies.

TABLE OF CONTENTS **Pages**

ABSTRACT…… I
ÖZ..... II
ACKNOWLEDGEMENTS……. III
TABLE OF CONTENTS…… IV
LIST OF TABLES ……..……..……... VII
LIST OF FIGURES……...…….. VIII
NOMENCLATURE…… XIII
1. INTRODUCTION……...……... 1
1.1. Powder Metallurgy Manufacturing Techniques……. 1
1.2. Powder Metallurgy Technology……. 3
1.2.1. Powder Production……... 3
1.2.2. Blending or Mixing…….. 5
1.2.3. Pressing or Compacting…… 6
1.2.4. Sintering……... 8
1.2.4.1. Sintering of Aluminum PM Parts…….. 10
1.2.5. Finishing……... 11
1.3. Properties of PM Parts…… 12
1.4. Introduction to Shot peening……..... 13
1.5. Why Shot peening Prevents Fractures?..... 16
1.6. What are the Effects of Shot peening?..... 17
1.6.1. Comparison with other Manufacturing Processes of Shot Peening Method in terms of Fatigue Properties... 18
1.7. Application Areas of Shot peening..... 19
1.8. Fatigue Design for Powder Metallurgy…….. 20
1.8.1. Performance Properties of Aluminum PM Components……..... 21
1.8.1.1 Important on Fatigue Design of Aluminum Powder Metallurgy…….. 22
2. PREVIOUS STUDIES……... 25

2.1. Processing, Properties, and Aplications of Powder Metallurgy Materials……. 25
2.2. Characteristic Properties of Fatigue Strength of Powder Matallurgical Materials…….. 32
2.3. Improvement of Fatigue Properties of PM Materials by Shot peening……... 38
3. MATERIAL AND METHOD…….…….. 44
3.1. Material……..... 44
3.2. Method……..... 45
3.2.1. The Pressing Process of Aluminum Alloys Powder Used in This Study……... 45
3.2.2. The Sintering Process of Compacted Aluminium Alloy Used in This Study……. 46
3.2.3. Density Measurement of Green and Sintered Aluminium Alloy……. 48
3.2.4. The Machining and Polishing Operations of Test Specimens……. 49
3.2.5. Shot Peening……. 51
3.2.6. Mechanical Tests…….. 52
3.2.6.1. Tensile and Fatigue Tests…….. 52
3.2.6.2. Hardness Tests……... 57
3.2.7. Microstructure Analysises…… 59
3.2.7.1. Optical Microscopy (OM)……. 59
3.2.7.2. Scanning Electron Microscopy (SEM)….. 61
4. RESULTS AND DISCUSSION……..... 62
4.1. Evaluation of Physical, Chemical, Metallurgical and Mechanical Properties…… 62
4.1.1. Evaluation of Density Measurements……... 62
4.1.2. Evaluation of Tensile and Hardness Test……. 63
4.1.3. Evaluation of Fatigue Test…….. 68
4.1.4. Evaluation of Optical Microscope Images……... 75

4.1.5. Evaluation of Scanning Electron Microscope Images. 81
5. CONCLUSIONS AND FUTURE STUDIES…… 85
5.1. Conclusion…….. 85
5.2. Future Studies……. 87
5.3. Recommendation Future Studies……..... 87
REFERENCES……..……... 89
CIRRICULUM VITAE……... 95

LIST OF TABLES **Pages**

Table 1.1.	Advantages and disadvantages of PM…….....	13
Tablo 1.2.	Comparison with other methods of powder processing.....	13
Table 1.3.	Comparison with other manufacturing processes of shot peening method……..	18
Table 2.1.	Typical tensile datas for aluminum…….	26
Table 2.2.	Mechanical properties obtained on specimens with a cross section of 5x5 mm……..	34
Table 3.1.	Chemical composition and particle size characteristics of the Alumix 431……..	45
Table 3.2.	Sintering conditions…….	47
Table 3.3.	Typical materials properties of the Alumix 431……..	48
Table 3.4.	Typical compacting and sintering properties of the Alumix 431…….....	48
Table 3.5.	Shot peening parameters used in this study…….....	51
Table 3.6.	Typical materials properties of sintered parts…….....	53
Table 4.1.	Density values of prismatic samples compacted with axial die at RT formed from the Alumix 431……..	62
Table 4.2.	Symbols of material used in this work……	63
Table 4.3.	Characteristic properties of specimen used in this study…….....	66
Table 4.4.	S-N datas for all unpeened specimens at 600 ºC…….....	69
Table 4.5.	S-N datas for all unpeened specimens at 620 ºC…….....	70
Table 4.6.	S-N datas for all peened specimens at 600 ºC…….....	70
Table 4.7.	S-N datas for all peened specimens at 620 ºC.....	71

LIST OF FIGURES **Pages**

Figure 1.1.	Typical iron and copper based PM parts…….....	1
Figure 1.2.	Worldwide market share of PM parts…….	2
Figure 1.3.	Distribution of PM parts in a car…….....	3
Figure 1.4.	PM process flow diagram……...	4
Figure 1.5.	Mixing stage of production of PM parts; a) Mixing powders and other additives, b) Mixing machine ……	6
Figure 1.6.	Pressing stage of production of PM parts; a) Pressing machine, b) Compaction operation to create a green molded part……..	7
Figure 1.7.	Compaction of metal powders; a) Raw powder, b) Compacted powder…….	7
Figure 1.8.	Sintering process; a) Steps of sintering processes, b) Sintered powder……..	8
Figure 1.9.	Shrinkage versus time after sintering process…….	10
Figure 1.10.	Typical sintering aluminum PM parts……...	11
Figure 1.11.	Shot peening process……..	14
Figure 1.12.	Shot material……...	14
Figure 1.13.	Compression residual stresses by shot peening……..	15
Figure 1.14.	Shot peening parameters and surface conditions on material; a) Elements of shot peening process, b) Peened and unpeened surfaces……...	16
Figure 1.15.	Fracture characteristic of material originated tension strength……	17
Figure 1.16.	Shot peening applications; a) Usage areas of shot peening, b) Parts produced by shot peened……...	20
Figure 2.1.	Process flow for aluminum PM Process…….....	25
Figure 2.2.	Fatigue curves for 201AB PM and 2014 aluminum alloys……..	27

Figure 2.3.	Fatigue curves for 601AB PM and 6061 aluminum alloys……..	27
Figure 2.4.	Unetched optical microstructures of Al–4Cu–0.6Si–0.1Mg without wax, compacted at 400 MPa with die wall lubricant and sintered in either nitrogen (a and b) or argon (c and d). Samples were either quenched as the sintering temperature was reached (a and c) or 1 h later (b and d). It is only the small pores that are removed under argon, whereas the large pores also disappear in nitrogen, except for those close to the surface……..	29
Figure 2.5.	Comparison of % densities for 20 min sintered Al parts.....	30
Figure 2.6.	Comparison of % green density and 600 °C/20 min sintered Al parts……	30
Figure 2.7.	Variation in green and sintered densities with compaction pressure for the premixed elemental 6061 Al powder compacts sintered at 620 °C for 1 h……	32
Figure 2.8.	SEM photographs of fracture surfaces……	37
Figure 2.9.	Influence of material strength on the increase of fatigue strength due to surface rolling…….....	38
Figure 2.10.	S-N curves for shot peened and unpeened specimens……...	40
Figure 2.11.	S-N comparative curves of the base materials and shot peening conditions……..	41
Figure 3.1.	Alumix 431 powder which have Al-5.5 Zn-2.5 Mg-1.5 Cu componenet powders…….....	45
Figure 3.2.	Compacted aluminium alloy used in this study……	46
Figure 3.3.	Protherm automatic controlled high temperature gas atmosphere tube furnace…….	47
Figure 3.4.	Fatigue and tensile test specimens; a) Fatigue test sample, b) Tensile test sample …….	50

Figure 3.5.	Technical representation of fatigue and tensile test specimens; a) Finished product (fatigue test sample), b) Finished product (tensile test sample) (Dimensions are in mm)…….....	50
Figure 3.6.	Shot peened specimen for fatigue test; a) Shot peened material, b) Technical representation of shot peened material……...	52
Figure 3.7.	Typical screen layout of Bluehill® 2 software…….....	53
Figure 3.8.	Typical main screen of SAX or MAX software…….	54
Figure 3.9.	Typical sinusoidal waveform……..	55
Figure 3.10.	The main equipment used to perform tensile and fatigue tests; a) General appearance of laboratory arranged for tensile and fatigue experiments, b) Set up of apparatus of specimen…….....	55
Figure 3.11.	Special apparatus machined for tests; a) Top view, b) Side view, c) Isometric view……...	57
Figure 3.12.	Fractured sample during tensile test for Vickers Micro-Hardness experiment……...	58
Figure 3.13.	Specimen preparation steps for Optical Microscopy……..	60
Figure 4.1.	The variations in hardness for sintered specimens at 600 ºC…….....	64
Figure 4.2.	The variations in hardness for sintered specimens at 620 ºC…….....	64
Figure 4.3.	Comparison of the variations in hardness for sintered specimens at 600 ºC and 620 ºC…….....	65
Figure 4.4.	Tensile stress curves of samples sintered at 600 ºC….....	66
Figure 4.5.	Tensile stress curves of samples shot peened at 600 ºC…….	67
Figure 4.6.	Tensile stress curves of samples sintered at 620 ºC….....	67
Figure 4.7.	Tensile stress curves of samples shot peened at 620 ºC…….	68
Figure 4.8.	Comparison of tensile stress curves……	68
Figure 4.9.	S-N curves for all unpeened specimens at 600 ºC……..	71

Figure 4.10.	S-N curves for all unpeened specimens at 620 ºC……..	71
Figure 4.11.	Comparison of S-N curves for all unpeened specimens at 600 ºC and 620 ºC……...	72
Figure 4.12.	S-N curves for all peened specimens at 600 ºC……..	73
Figure 4.13.	S-N curves for all peened specimens at 620 ºC……..	73
Figure 4.14.	Comparison of S-N curves for all peened specimens at 600 ºC and 620 ºC……..	74
Figure 4.15.	Comparison of S-N curves for all peened and unpeened specimens……	75
Figure 4.16.	Sintered specimen prepared in bakalite for Optical Microscope Images ……	76
Figure 4.17.	Optical Microscope analysis of unetched only sintered parts at 600 ºC; a) 50X, b) 100X ……	76
Figure 4.18.	Optical Microscope analysis of etched only sintered parts at 600 ºC; a) 50X, b) 100X…….	76
Figure 4.19.	Optical Microscope analysis of unetched only sintered parts at 620 ºC; a) 50X, b) 100X ……	77
Figure 4.20.	Optical Microscope analysis of etched only sintered parts at 620 ºC; a) 50X, b) 100X ……	78
Figure 4.21.	Optical Microscope analysis of unetched shot peened parts in 12A intensity at 600 ºC; a) 50X, b) 100X ……..	79
Figure 4.22.	Optical Microscope analysis of etched shot peened parts in 12A intensity at 600 ºC; a) 50X, b) 100X ……..	80
Figure 4.23.	Optical Microscope analysis of unetched shot peened parts in 16A intensity at 620 ºC; a) 50X, b) 100X……...	80
Figure 4.24.	Optical Microscope analysis of etched shot peened parts in 16A intensity at 620 ºC; a) 50X, b) 100X……...	81
Figure 4.25.	SEM views of fracture surface of unpeened specimen at 600 ºC; a) 50X, b) 500X……	82
Figure 4.26.	SEM views of fracture surface of peened specimen at 600 ºC in 12A; a) 50X, b) 500X……	82

Figure 4.27. SEM views of fracture surface of unpeened specimen at 620 ºC; a) 50X, b) 500X…… 83
Figure 4.28. SEM views of fracture surface of peened specimen at 620 ºC in 16A; a) 50X, b) 500X…… 84

NOMENCLATURE

a : Weight without Carrier Bond, g

A : Surface Area of the Resulting Indentation, mm^2

ASM : The American Society for Microbiology

ASME : The American Society for Mechanical Engineers

ASTM : The American Society for Testing and Materials

b : Difference of Weight, g

CIP : Cold Isostatic Pressing

d : The Average Length of the Diagonal Left by the Indenter, mm

E : Young's Modulus, GPa

ECM : Electro Chemical Machining

EDM : Electrical Discharge Machining

f : Frequency, Hz

F : The Force Applied to the Diamond, N

HIP : Hot Isostatic Pressing

HV : Vickers Hardness Scale, N/mm^2

K_t : Notch Factor

MIM : Metal Injection Molding

m_{green} : Green Mass of Specimen, g

$m_{sintered}$: Sintered Mass of Specimen, g

N_R : Cycles to Rupture, Number

OM : Optic Microscope

OIM : Optik Işık Mikroskobu

PM : Powder Metallurgy

PIM : Powder Injection Moulding

R : Reversing Loading, Load or Stress Ratio

SEM : Scanning Electron Microscope

TM : Toz Metallurjisi

TD : Theoretical Density, g/cm^3

TEM : Taramalı Elektron Mikroskobu

TPMA : Turkey Powder Metallurgy Association

UTS : Ultimate Tensile Strength, MPa

v_{green} : Green Volume of Specimen, cm^3

$v_{sintered}$: Sintered Volume of Specimen, cm^3

y : Carrier Material Weight, g

YS : Yield Strength, MPa

z : Weight of Specimen in the Water, g

x : Weight of Specimen, g

σ_{min} : Minimum Stress, MPa

σ_{max} : Maximum Stress, MPa

$\sigma_{a,n}$: Nominal Stress Amplitude, MPa

ρ_{green} : Green Density of Specimen, g/cm^3

$\rho_{sintered}$: Sintered Density of Specimen, g/cm^3

1. INTRODUCTION

1.1. Powder Metallurgy Manufacturing Techniques

Among the various metalworking technologies, Powder Metallurgy (PM) is the most diverse manufacturing approach. One attraction of PM is the ability to fabricate high quality, complex parts to close tolerances in an economical manner. In essence, PM takes a metal powder with specific attributes of size, shape, and packing, and then converts it into a strong, precise, high performance shape. Key steps include the shaping or compaction of the powder and the subsequent thermal bonding of the particles by sintering. The process effectively uses automated operations with low relative energy consumption, high material utilization, and low capital costs. These characteristics make PM well aligned with current concerns about productivity, energy, and raw materials. Consequently, the field is experiencing growth and replacing traditional metal-forming operations. Further, powder metallurgy is a flexible manufacturing process capable of delivering a wide range of new materials, microstructures, and properties. That creates several unique niche applications for PM such as wear resistant composites (German, 1994). The applications of PM are quite extensive. Typical iron and copper based on PM parts are shown in Figure 1.1.



Figure 1.1. Typical iron and copper based PM parts (Turkish Powder Metallurgy Association, 2009)

Consider the use of metal powders in the fabrication of tungsten lamp filaments, dental restorations, oil-less bearings, automotive transmission gears, armour piercing projectiles, electrical contacts, nuclear power fuel elements, orthopaedic implants, business machines, high-temperature filters, aircraft brake pads, rechargeable batteries, and jet engine components. Furthermore, metal powders find uses in such products as paint pigments, porous concretes, printed circuit boards, enriched flour, explosives, welding electrodes, rocket fuels, printing inks, brazing compounds, and catalysts. Worldwide market share in chart and distribution in a car of PM parts are shown in Figure 1.2 and 1.3, respectively. Automotive industry is leading with more than 75% of the share. American cars contain more than 16 kg of PM parts while European cars have 7 kg and Japan cars have 5 kg PM parts (Turkish Powder Metallurgy Association, 2009).

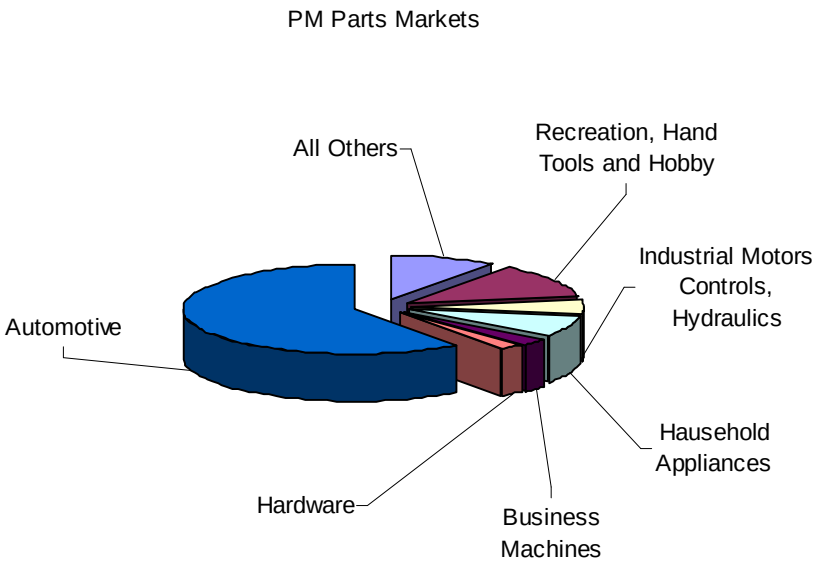


Figure 1.2. Worldwide market share of PM parts (Turkish Powder Metallurgy Association, 2009)

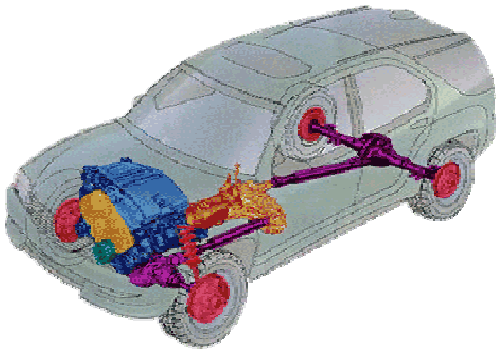


Figure 1.3. Distribution of PM parts in a car (Turkish Powder Metallurgy Association, 2009)

1.2. Powder Metallurgy Technology

Powder metallurgy uses raw material in the form of very fine powder. This is compacted (using a die) to the shape required, and then the powder particles are "joined" by heating the material to just below the melting point.

The basic steps of PM are: (i) powder production, (ii) powder blending, (iii) compaction in a die, (iv) sintering, and (v) finishing. PM process flow diagram is diplayed in Figure 1.4.

1.2.1. Powder Production

Metal powder can be produced by several processes.

i. Atomization

In this process, molten metal is broken up into small droplets and rapidly frozen before the drops come into contact with each other or with a solid surface. The principal method is to disintegrate a thin stream of liquid metal by subjecting it to the impact of high energy jets of gas or liquid. Air, nitrogen and argon are commonly used gases, and water is the liquid most widely used. By varying the several parameters; design and configurations of the jets, pressure and volume of the atomising fluid, thickness of the stream of metal, etc., it is possible to control the particle size distribution over a wide range.

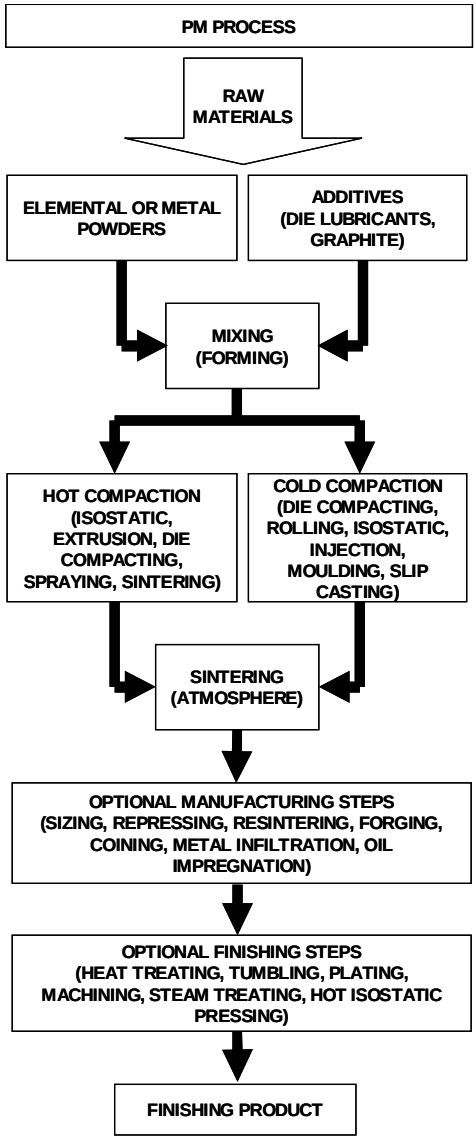


Figure 1.4. PM process flow diagram

The particle shape is determined largely by the rate of solidification and varies from spherical, if a low heat capacity gas is employed, to highly irregular if water is used. In principle, the technique is applicable to all metals that can be melted, and is commercially used for the production of iron, tool steels, alloy steels, copper, brass, bronze and the low-melting-point metals, such as aluminium, tin, lead, zinc, cadmium. The readily oxidising metals, for example chromium-bearing alloys, are being atomised on an increasing scale by means of inert gas, especially argon. Atomisation is particularly useful for the production of alloys in powder form, since

the constituent metals are fully alloyed in the molten state. Thus each powder particle has the same chemical composition.

ii. Chemical methods

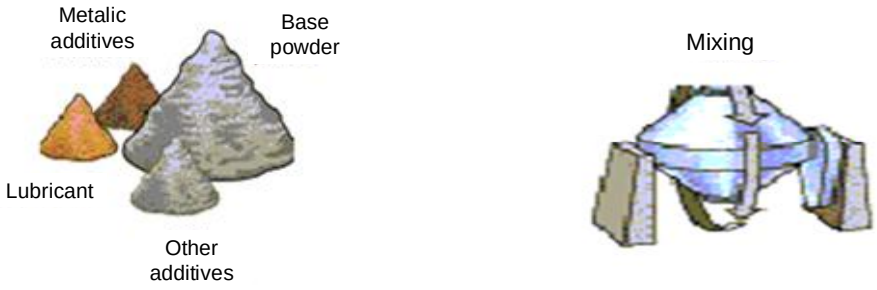
This has been for long the most widely used method for the production of iron powder. Selected ore is crushed, mixed with carbon, and passed through a continuous furnace where reaction takes place leaving a cake of sponge iron which is then further treated by crushing, separation of non-metallic material, and sieving to produce powder. Since no refining operation is involved, the purity of the powder is dependent on that of the raw materials. The irregular sponge-like particles are soft, and readily compressible, and give compacts of good green strength. Refractory metals are normally made by hydrogen reduction of oxides, and the same process can be used for copper.

iii. Electrochemical action

By choosing suitable conditions; composition and strength of the electrolyte, temperature, current density, etc., many metals can be deposited in a spongy or powdery state. Extensive further processing; washing, drying, reducing, annealing and crushing may be required. Copper is the main metal to be produced in this way, but chromium and manganese powders are also produced by electrolysis. In these cases, however, a dense and normally brittle deposit is formed and requires to be crushed to powder. Electrolytic iron was at one time produced on a substantial scale but it has been largely superseded by powders made by less costly processes. Electrolytic powders are very pure.

1.2.2. Blending or Mixing

If the PM part is being made form a mixture of metals, then the different powders must be mixed uniformly. Also, in some cases, a lubricant is added to the powder to improve the compaction of the powder in the die, as well as to improve the compaction die life. The mixing is done in shaking/rotating containers called blenders as displayed in Figure 1.5b. Figure 1.5 shows mixing stage of production of PM parts.



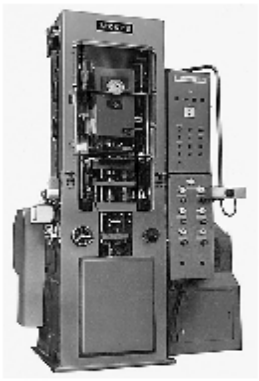
(a) (b)

Figure 1.5. Mixing stage of production of PM parts; a) Mixing powders and other additives, b) Mixing machine (Turkish Powder Metallurgy Association, 2009)

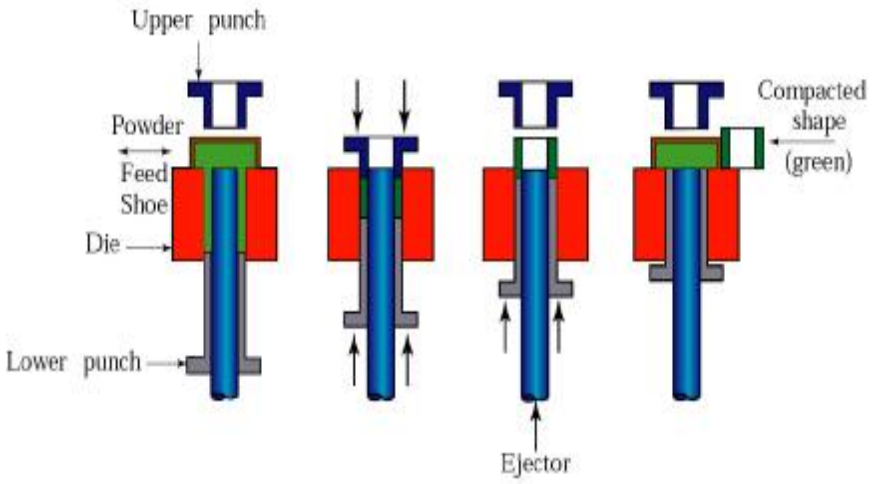
The main function of the lubricant is to reduce friction between the powder mass and the surfaces of the tool, die walls, core rods etc., along which the powder must slide during compaction. This assists the achievement of uniform density from top to bottom of the compact. Of equal importance is the fact that the reduction of friction also makes it easier to eject the compact. As an alternative to pre-alloyed powders, alloying elements can be added to the mix as powders. The high compressibility of a pure iron powder is thus maintained and the solution-hardening effect of the alloying elements is avoided. The most commonly used alloying element is carbon, which is added as graphite powder.

1.2.3. Pressing or Compacting

There are a lot of compacting systems such as cold and hot compaction. This is the step when the powder is given the shape of the part being produced. The method is similar to forming processes – the die is a cavity in the shape of the lower half of the part, and the powder is poured into the cavity. The upper portion of the shape is made by the punch, which is pressed down on the powder to achieve the required compaction as displayed in Figure 1.6b. Figure 1.6 shows pressing stage of production of PM parts.



(a)



(b)

Figure 1.6. Pressing stage of production of PM parts; a) Pressing machine, b) Compaction operation to create a green molded part (Kalpakjian and Schmid, 2008)

Increased compaction pressure provides better packing of particles, leads to decrease porosity and increase localized deformation allowing new contacts to be formed between particles as dislayed in Figure 1.7.



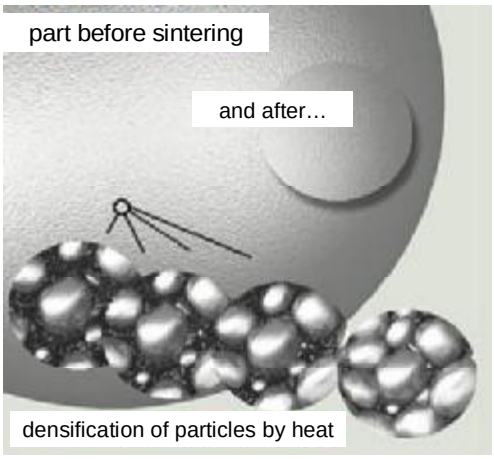
(a) (b)

Figure 1.7. Compaction of metal powders; a) Raw powder, b) Compacted powder

At higher pressures, the green density approaches density of the bulk metal, pressed density greater than 90% of the bulk density is difficult to obtain. Hence, compaction pressure used depends on desired density. Also, smaller particles provide greater strength mainly due to reduction in porosity. Introduction of finer particles will fill voids and result in increase of density.

1.2.4. Sintering

The compacted part is called a green part, or a green compact. It is weak, since the particles are held together mostly by friction. The green compact is put into an oven and heated to a high temperature approximately 70% to 90% of the melting point of the metal or alloy. The sintering process joins the metal particles together. There are two mechanisms for this. Firstly, at the interface between two particles, metal atoms diffuse across the boundary and re-crystallize. This diffusion process effectively forms a welded joint. Another phenomenon is that at the high temperature, some metal atoms get vaporized and then get re-deposited on the boundaries. If they re-deposit at an interface, a welded joint is formed as displayed in Figure 1.8.



(a)



(b)

Figure 1.8. Sintering process; a) Steps of sintering processes, b) Sintered powder

The time at temperature varies between 10 and 60 minutes, depending on the application. A sintering operation consists of de-waxing, sintering and cooling steps. In the de-waxing zone of the furnace, the lubricant is burned off. During the sintering, several reactions take place.

There are three stages of sintering. These are:

i. Burn-off (purge): Initially, the furnace atmosphere reduces oxides on the surface of the particles combusting any air and removing lubricants or binders, and an initial bond between particles in contact is formed.

ii. High temperature: The main mechanisms of sintering are surface and volume diffusion. By diffusion, a coherent body of metal is formed, and the admixed alloying elements are distributed into the base metal. Driven by the force to minimise free energy, stated by the laws of thermodynamics, rounding of pores takes place and small pores disappear in favour of larger.

iii. Cooling period: In the cooling zone of the sintering furnace, the parts are cooled under protective atmosphere in order to not oxidise in contact with air. The cooling speed, especially in the range 850 - 500°C, also affects the mechanical properties, due to phase transformations in the material. During the sintering, a moderate dimensional change takes place (Turkish Powder Metallurgy Association, 2009) and shrinkage always becomes. Therefore, when the shrinkage occurs, part transforms compacted mechanical bonds to much stronger metallic bonds as shown in Figure 1.9.

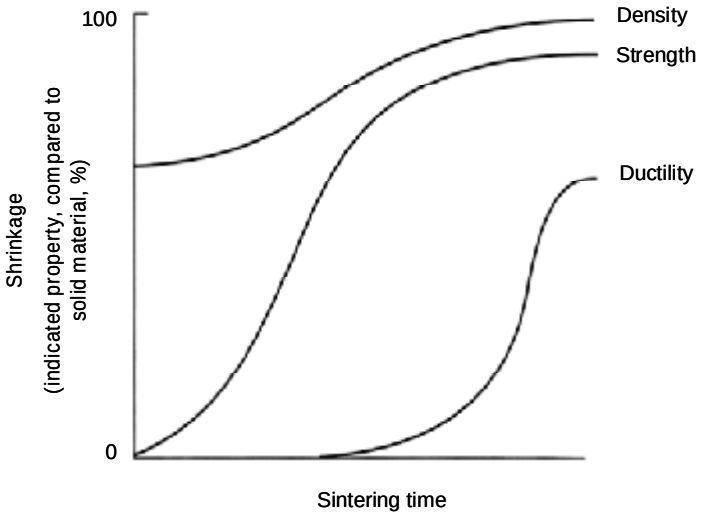


Figure 1.9. Shrinkage versus time after sintering process

Volume and linear shrinkage are calculated with formulas below:

$$\text{Volume shrinkage} = \frac{v_{\sin tered}}{v_{green}} = \frac{r_{green}}{r_{\sin tered}} \quad (1.1)$$

$$\text{Linear shrinkage} = \left(\frac{r_{green}}{r_{\sin tered}}\right)^{1/3} \quad (1.2)$$

where

$v_{sintered}$: Sintered volume of part, cm^3

v_{green}: Green volume of part, cm^3

ρ_{green}: Sintered density of part, g/cm^3

$\rho_{sintered}$: Green density of part, g/cm^3

1.2.4.1. Sintering of Aluminum PM Parts

Aluminum PM parts can be sintered in a controlled, inert atmosphere or in vacuum. Sintering temperatures are based on alloy composition and generally range from 595 to 625 °C (1100 to 1160 °F). Sintering time varies from 10 to 30 min. Nitrogen, dissociated ammonia, hydrogen, argon, and vacuum have been used for sintering aluminum; however, nitrogen is preferred because it results in high as sintered mechanical properties. It is also economical in bulk quantities, If a

protective atmosphere is used, a dew point of -40 °C (-40 °F) or below is recommended. This is equivalent to a moisture content of 120 mL/m^3 (120 ppm) maximum. A variety of pressed and sintered aluminum PM parts are shown in Figure 1.10 (ASM Metals Handbook, 1998).

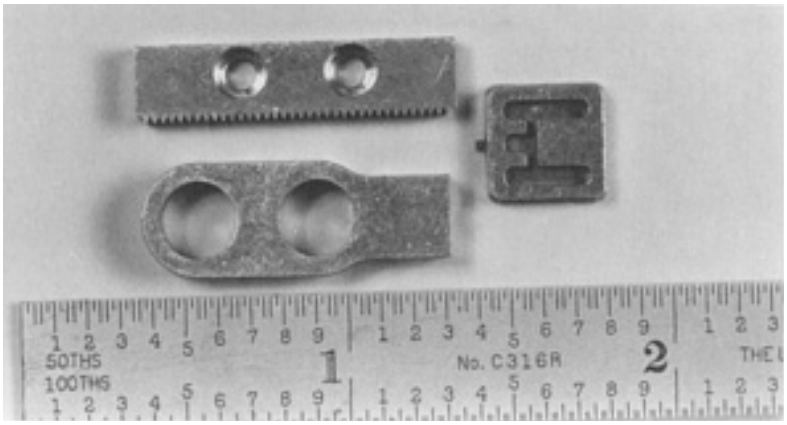


Figure 1.10. Typical sintered aluminum PM parts (ASM Metals Handbook, 1998)

1.2.5. Finishing

Most powder metallurgy products are ready to use after the sintering process. Some products may use secondary operation to provide enhanced precision, improved properties, or special characteristics. Distortion may occur during nonuniform cool-down so the product may be repressed, coined, or sized to improve dimensional precision. If massive metal deformation takes place in the second pressing, the operation is known as PM forging. Therefore, density increases and precision adds. Infiltration and impregnation- oil or other liquid is forced into the porous network to offer lubrication over an extended product lifetime. Metal infiltration fills in pores with other alloying elements that can improve properties. PM products can also be subjected to the conventional finishing operations: heat treatment, machining, and surface treatments.

1.3. Properties of PM Parts

i. Mechanical properties show a strong dependence on product density, with the fracture-limited properties of toughness, ductility and fatigue life being more sensitive than strength and hardness.

ii. The voids in the PM part act as stress concentrators and assist in starting and propagating fractures.

iii. The yield strength of PM products made from weaker metals is often equivalent to the same material in wrought form.

iv. If higher strength materials are used or the fracture-related tensile strength is specified, the PM properties tend to fall below those of wrought equivalents by varying but usually substantial amounts.

v. When larger presses or processes such as PM forging or Hot Isostatic Pressing (HIP) are employed to produce higher density, the strength of the PM products approaches that of the wrought material with full density and fine grain size.

vi. With full density and fine grain size, PM parts often have properties that exceed their wrought or cast equivalents.

vii. Since mechanical properties of powder metallurgy products are so dependent upon density, it is important that PM products be designed and materials selected so that the final properties will be achieved with the anticipated amount of final porosity.

viii. Physical Properties can also be affected by porosity.

ix. Corrosion resistance tends to be reduced due to the presence of entrapment pockets and fissures.

x. Electrical, thermal, and magnetic properties all vary with density.

xi. Porosity actually promotes good sound and vibration damping, and many PM parts are designed to take advantage of this feature.

Powder Metallurgy has many advantages and disadvantages. These are listed in Tablo 1.1.

Tablo 1.1. Advantages and disadvantages of PM

Advantages	Disadvantages
Elimination or reduction of machining	Inferior strength properties
High production rates	Relatively high die cost
Complex shapes to be produced	High material cost
Wide variations in compositions are possible	Design limitations
Wide variations in properties are possible	Density variations produce property variations
Scrap is eliminated or reduced	Healty and safety hazards

There are a lot of studies related to powder processing methods and comparison of these is given in Tablo 1.2.

Tablo 1.2. Comparison with other methods of powder processing

Characteristic properties	Conventional press, sinter (present process)	Metal injection molding (MIM)	Hot isostatic pressing	PM forging
Size of workpiece	Intermediate	Smallest	Largest	Intermediate
Shape complexity	Good	Excellent	Very good	Good
Production rate	Excellent	Good	Poor	Excellent
Production quantity	> 5000	> 5000	1-1000	> 10 000
Dimensional precision	Excellent	Good	Poor	Very good
Density	Fair	Very good	Excellent	Excellent
Mechanical properties	80-90% of wrought	90-95% of wrought	Greater than wrought	Equal to wrought
Cost	Low	Intermediate	High	Somewhat low

1.4. Introduction to Shot peening

In recent years, there has been a great interest the fatigue properties of powder metallurgy products. With improvement of the technology into dynamically loaded components, there appear potential performance limitations related to fatigue failure. In the first stages, these limitations were overcome by different processes

such as hot forging, rolling, carburizing, and polishing. Therefore, alternative methods are found for improving the fatigue properties of materials, so that they can be used directly without any further process required. The process of shot peening is used to produce a decorative finish and to modify mechanical properties of materials. Shot peening is a cold working process in which the surface of the material is bombarded with small spherical media called shot as shown in Figure 1.11 and Ø 6 mm shot material is displayed in Figure 1.12.

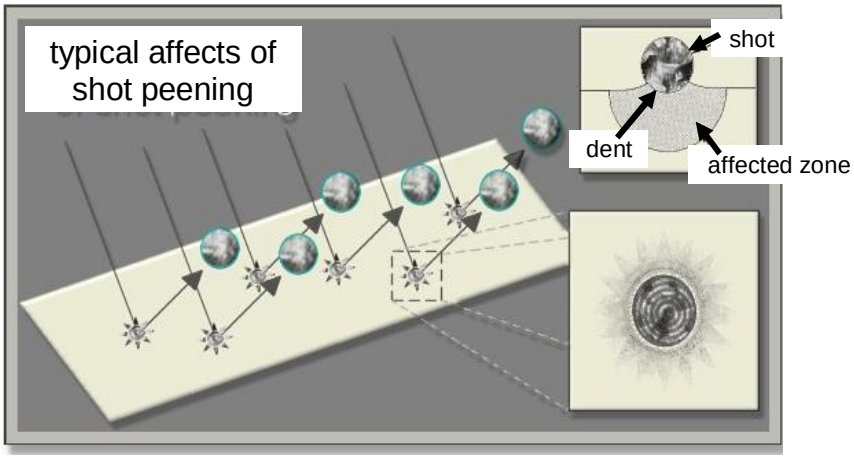


Figure 1.11. Shot peening process (Abrasive Finishing Company Inc., 2009)



Figure 1.12. Shot material (Abrasive Finishing Company Inc., 2009)

Each of piece of shot striking the material acts as a tiny peening hammer, imparting to the surface a small indentation or dimple. Because of the dimple to be created, the surface fibres of the material must be yielded in tension. Below the surface, the fibres try to restore the surface to its original shape, thereby producing

below the dimple, a hemisphere of cold worked material highly stressed in compression. There are many benefits of shot peening process on materials. One of these is effect of fatigue life because of compression residual streses as shown in Figure 1.13.

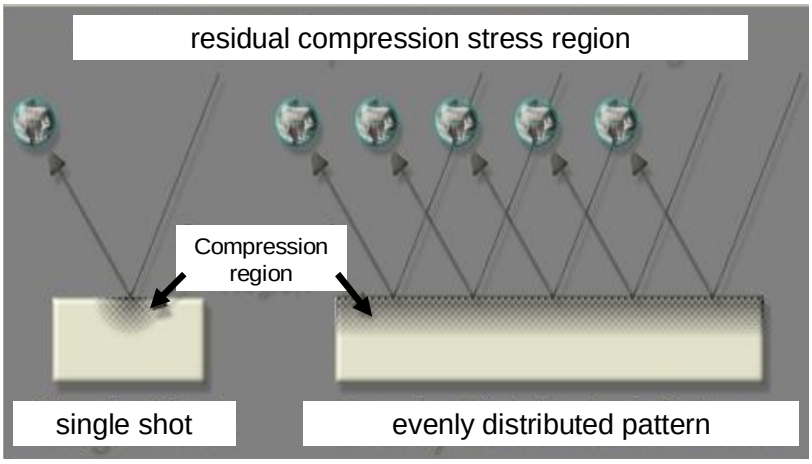


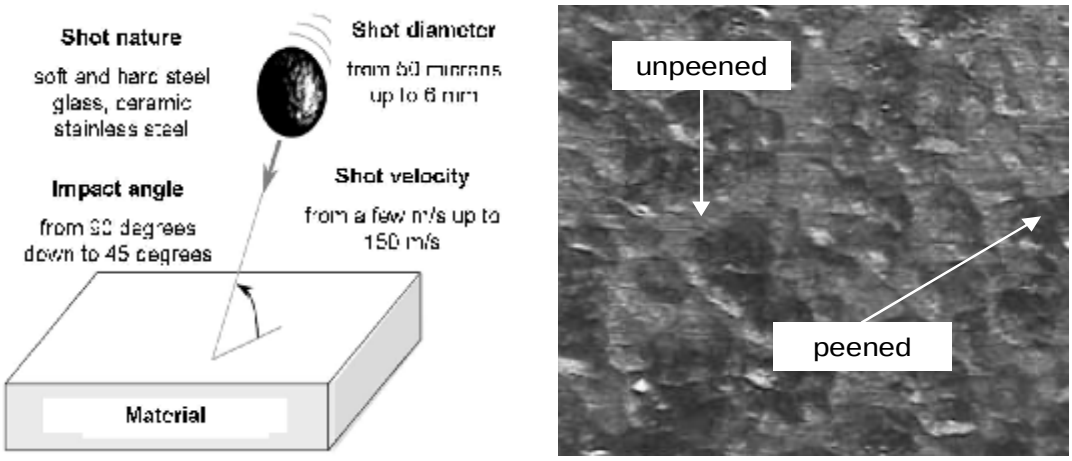
Figure 1.13. Compression residual streses by shot peening (Abrasive Finishing Company Inc., 2009)

Overlapping dimples develop an even layer of material in residual compressive stress parallel to the surface of the material. This compressive stress region may be several times greater than any imposed tensile stress, such as that encountered in bending, and markedly improves fatigue life of the part in service.

The principal parameters to control in shot peening process, which have influence on the residual stress profile, strain hardening and surface roughness are:

- shot, size, shape, and hardness,
- shot velocity and flow rate,
- distance from the nozzle to surface,
- impact angle,
- exposure time.

These parameters and peened, unpeened surfaces on material are shown in Figure 1.14a, 1.14b, respectively.



(a) (b)

Figure 1.14. Shot peening parameters and surface conditions on material; a) Elements of shot peening process, b) Peened and unpeened surfaces on material (Metal Improvement Co. Inc., 2009)

These parameters influence what is called the peening intensity. The shot peening intensity shows the amount of impact energy delivered to the part by the shots. It is measured with special strips produced from SAE 1070 spring steels, which are called almen (A) strips. There are three standard almen strips currently in use: A being 0.051 in, C being 0.094 in, and N being 0.031 in in thickness. The length and the width of an almen strip are 3.0 in and 0.75 in, respectively (Almen and Black, 1963).

1.5. Why Shot peening Prevents Fractures?

Material failures are mostly caused from fractures, or cracks, which start at the surface of the material. These fractures are caused from over stressing or bending past the materials yield strength, fatigue from continuous or repeated stresses, or from corrosion weakening the surface. When forces are applied to any material, tension stress and compressive stress regions form. Figure 1.15 shows stresses on material by shot peening and fractures only occur in tension stress regions, and they perform never in compression stress regions.

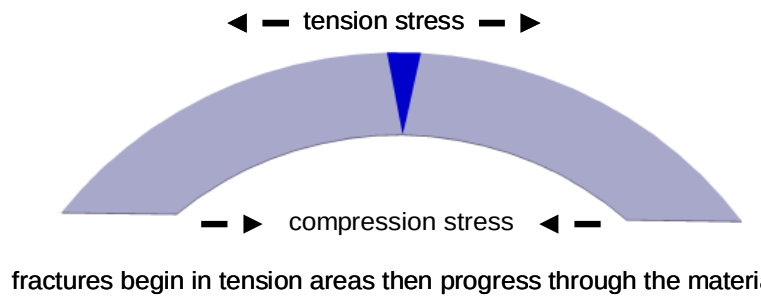


Figure 1.15. Fracture characteristic of material originated tension strength

By shot peening material, internal compressive stress areas are formed which oppose these tension stress regions and aid to prevent fractures in the material. The compressive stress areas in a shot peened surface are a residual effect and can profoundly increase the service life of the material (Abrasive Finishing Company Inc., 2009).

1.6. What are the Effects of Shot peening?

Benefits obtained by shot peening are the result of the effect of the compressive stress and the cold working induced. Compressive stresses are beneficial in increasing resistance to fatigue failures, corrosion fatigue, stress corrosion cracking, hydrogen assisted cracking, fretting, galling and erosion caused by cavitation. Benefits obtained due to cold working include work hardening, intergranular corrosion resistance, surface texturing, closing of porosity and testing the bond of coatings. Both compressive stresses and cold working effects are also benefits in the application of shot peening in forming metal parts. In addition, the shot peening action improves the distribution of stresses in surfaces that have been disturbed by grinding, machining, or heat treated. Particularly effective on ground surfaces, shot peening changes the tensile stresses that grinding imposes in a metal surface to beneficial compressive stresses. Also, especially effective in reducing the deleterious stress concentration effects of notches, fillets, forging pits, surface defects, and decarburization.

.

1.6.1. Comparison with other Manufacturing Processes of Shot peening Method in terms of Fatigue Properties

Manufacturing processes are known to have a significant effect on metal fatigue properties of parts. These effects can be either detrimental or beneficial, as represented according to applied process as listed in Table 1.3.

Table 1.3. Comparison with other manufacturing processes of shot peening method (Metal Improvement Co. Inc., 2009)

Detrimental	Beneficial
Hardening	Carburizing
Grinding	Honing
Machining	Polishing
Plating	Burnishing
Welding	Rolling
EDM and ECM	Shot peening

On the detrimental side; Grinding, Machining and Welding all can leave the surface of the part in tension, a seedbed for metal fatigue cracks. Hardening, Plating and Electrical Discharge Machining (EDM) can leave a hard brittle surface. Electro Chemical Machining (ECM) can damage or weaken surface grain boundaries. On the beneficial side all the listed processes improve metal fatigue life by virtue of the compressive stresses they induce. Shot peening is the most versatile of the list because it provides the highest magnitude of compressive stress in the greatest variety of materials and part configurations.

There are several ways of considering these benefits because of effects of shot peening:

i. First, shot peening allows an increased amount of stress to achieve the same component metal fatigue life.
ii. Second, shot peening extends the life of any part if the existing stress level is maintained.

iii. Thirdly, shot peening permits a greater range of acceptable manufacturing operations by providing a consistent surface compressive stress for combating metal fatigue (Metal Improvement Co. Inc., 2009).

1.7. Application Areas of Shot peening

The high level of performance of the jet plane and the modern automobile would be impossible without beneficial residual stresses gained from shot peening. Such stresses could be used to a much greater extent in the manufacture of industrial and domestic machinery, leading to savings in weight and greater serviceability along with lowering over-all cost. Springs are made stronger and lighter, hardware becomes stronger and more reliable, gears and bushings wear less, axles and shafts stay straighter, and structural parts resist fatigue and corrosion. However, the above explanation does not include every possible application of shot peening. The shot peening treatment can be applied to every kind of metal product and utilized in a wide range of technical fields. Shot peening applications are displayed in Figure 1.16a. In general, shot peening allows for stronger and more durable parts made with lighter and sometimes less material. In addition, to increase material strength helping shot peening, a lot of work were made in industry aplications. Parts machined in industry applications are displayed in Figure 1.16b (Improvement Co. Inc., 2009).



(a)



(b)

Figure 1.16. Shot peening applications; a) Usage areas of shot peening, b) Parts produced by shot peened (Improvement Co. Inc., 2009)

1.8. Fatigue Design for Powder Metallurgy

Powder metallurgy, among several competing mass production methods, plays an important role, not only as a means of saving material and energy, but also as a technique, delivering materials with good fatigue properties which are able to substitute for conventional materials. However, it is necessary to understand the

interaction between strength behaviour and design determining factors such as service loading, component geometry, and manufacturing. After presenting definitions of fatigue strength, which is divided into the areas of low cycle (endurance limit $N < 5 \times 10^4$), finite ($5 \times 10^4 < N < 2 \times 10^6$), and high cycle ($N > 2 \times l0^6$) fatigue under constant amplitude loading after the introduction of parameters which describe and determine S-N or fatigue life curves, relevant design data such as S-N curves, the effect of notches and mean stresses, and fracture mechanical properties are considered. The influence of manufacturing parameters (alloy composition, density, sintering temperature, post-sintering, mechanical and thermal surface treatments, and heat treatment) on the fatigue properties of sintered material is discussed. The need to determine material properties under different loading modes, i.e. axial, bending, different mean stresses, stress concentrations, and gradients, is outlined against the background of various service conditions and component geometries. Fatigue design starts by determining the local stresses and their distributions due to the service loading in the most critical areas of the part. For fatigue life assessment, the local stresses must then be compared with material properties to select design, material, and technology and to decide whether production can be started or further optimization is necessary (Sonsino, 1990).

1.8.1. Performance Properties of Aluminum PM Components

Increased demand for light weight components, primarily driven by the need to reduce energy consumption in a variety of societal and structural components, has led to increased use of aluminum. Additionally, the cost of fabrication coupled with a need to improve part recovery has led to significant growth in the net-shaped component manufacturing processes. Aluminum PM offers components with exceptional mechanical and fatigue properties, low density, corrosion resistance, high thermal and electrical conductivity, excellent machinability, good response to a variety of finishing processes, and which are competitive on a cost per unit volume basis. In addition, aluminum PM parts can be further processed to eliminate porosity and improve bonding yielding properties that compare favorably to those of

conventional wrought aluminum products. The primary driver for the use of Aluminum PM is the unique properties of aluminum coupled with the ability to produce complex net or near net shape parts which can reduce or eliminate the operational and capital costs associated with intricate machining operations. Aluminum PM can replace other PM in certain applications on a direct basis. However, in terms of the potential for ferrous based product substitution, each potential application needs to be considered on a case by case basis. Typical economics tend to favor iron parts but the unique characteristics of aluminum such as strength, weight, corrosion resistance, and machinability can make the aluminum parts economically viable.

1.8.1.1. Important on Fatigue Design of Aluminum Powder Metallurgy

Aluminum PM parts can be produced with a range of properties. Mechanical properties can vary from 110 MPa to 345 MPa depending upon composition, density, sintering practices and thermal treatments. Further secondary processing such as hot or cold forming can yield properties approaching those of conventional wrought aluminum materials. Aluminum PM mechanical properties are very good and typically dominate in the materials selection process. For certain applications, the dynamic properties as well as other performance properties are more critical and become the determinant criteria. These properties typically include, but are not limited to, fatigue, density, electrical and thermal conductivity, corrosion resistance and machinability. Fatigue is an important decision consideration for PM parts subject to dynamic stresses. The most commonly used fatigue property is the fatigue limit, which is the maximum reversed stress the material will withstand if cycled indefinitely. This limit is defined when the fatigue curve becomes horizontal. For ferrous materials this limit is at 10 million cycles while for aluminum alloys it is at 500 million cycles. Fatigues limits for some aluminum PM alloys are about 50% of the comparable wrought alloys. This difference is due to the lower density of PM parts. Hot forging the aluminum PM part results in fatigue limits comparable to the wrought alloys. A distinguishing characteristic of PM Aluminum is its lighter weight

in comparison to other common PM materials. Aluminum enjoys better than a 3 to 1 weight advantage over iron, nickel and copper. After benefits of Aluminium powder evaluate on the fatigue strength, knowlodges about what to do can explain in the present study.

The aim of this work is to investigate effect of sintering and shot peening process on the mechanical and other properties such as metallurgic, chemical of Alumix 431 alloys. To determine the effect of sintering and shot peening process on the material, a lot of studies have been performed. These are listed in the following:

i. For experimental tests, 100 specimens were compacted at 400 MPa pressure and room temperature.
ii. After that, 50 specimens were sintered at 600 ºC and 620 ºC for each temperature value separately.
iii. Densities of sintered and green specimens were measured with Classical and Archimedes Methods, and then compared.
iv. 100 sintered specimens were prepared in turn in Computer Numerical Control (CNC) lathe impending 80 and 20 specimens for fatigue and tensile experiments, respectively.
v. 40 specimens which sintered at 600 ºC and 620 ºC temperatures were shot peened in 12 and 16 Almen (A) intensities separately.
vi. Tensile experiments were performed using shot peened and unpeened samples and Stress-Extension graphics were evaluated. These results were investigated in terms of mechanical properties.
vii. Vickers Micro-Hardness tests were made using sintered specimens to compare sintered and green samples in terms of effect increasing sintering temperature and measurements were evaluated using fractured tensile test samples. Also, Vickers Hardness (HV) versus Displacement (mm) curves was plotted.
viii. Fatigue experiments were made using shot peened and unpeened samples and then, S-N curves were evaluated. These results were investigated in terms of mechanical properties.
ix. Optical Microscope views of shot peened and unpeened samples were

performed in etched and unetched mediums using fractured samples. After that, these views were evaluated in respect to metallurgical investigation.

x. Scanning Electron Microscope views of shot peened and unpeened samples were performed using fractured samples prepared for fatigue tests and these views were evaluated with respect to a metallurgical investigation.

xi. Finally, all experimental works were conducted to improve and evaluate fatigue strength of Alumix 431 powder material.

2. PREVIOUS STUDIES

2.1. Processing, Properties, and Aplications of Powder Metallurgy Materials

Couchman and Cousino (1994) studied the processing, properties, and applications for aluminum powder metallurgy materials. They compared using the PM versions of 2014 and 6061 alloys and their wrought and cast counterparts. The manufacturing process is fairly typical for press and sinter PM. Process sequence may be seen in Figure 2.1.

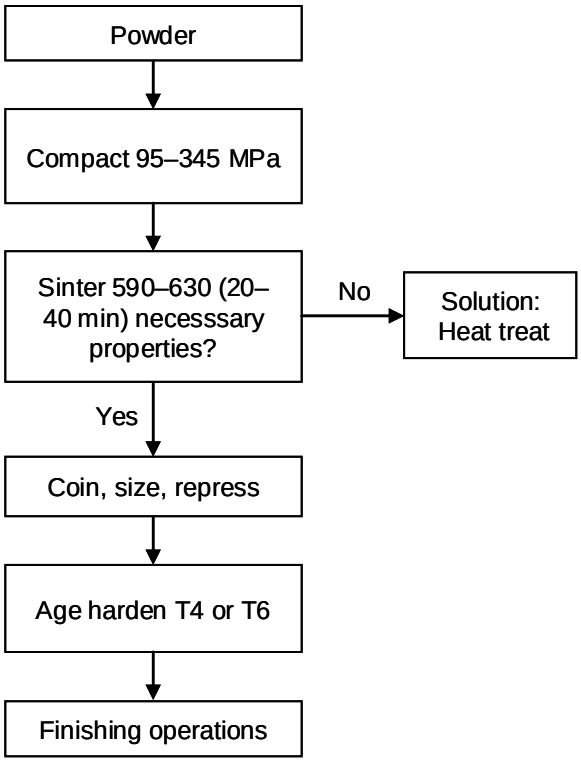


Figure 2.1. Process flow for aluminum PM process (Couchman and Cousino, 1994)

The starting point is an aluminum powder containing a master alloy to provide proper chemistry and addition of a waxy die lubricant to enable the compaction of the powder mix in a die under unaxial compaction. The compaction is done in relatively standard press and sinter PM. From the compaction operation the green compact will then be taken to the sintering operation. The sintering process is done under very tightly controlled conditions. Close process control is necessitated

by the need to remove the die lubricant at a rate such that the compact is not ruptured by the rapid evolution of vaporized wax lubricant, and in order to control the liquid phase present in the initial stages. Subsequent to the sintering, the part may be coined (or forged, or repressed as needed), solution treated and aged, machined, or coated to attain the necessary mechanical and physical properties. In addition, they reported mechanical and physical properties. Table 2.1 shows the typical ultimate tensile and yield strength values for alloys 601 and 201 compared to their counterparts, 6061 and 2014 in wrought, and to casting alloys 356 and 380.

Table 2.1. Typical tensile datas for Aluminum (Couchman and Cousino, 1994)

Alloy grade	Green density		Temper	Tensile strength, MPa	Yield strength, MPa	Elongation, %	Modulus of elasticity, GPa
	%	g/cm^3					
Alloy 601AB	90	2.42	T1 T4 T6	140 170 230	90 115 225	5.0 5.0 2.0	60
	95	2.55	T1 T4 T6	145 175 240	95 117 230	6.0 6.0 2.0	
6061			T6	310	276	17	69
356			T6	262	186	5	
380			F	330	165	3	
Alloy 201AB	90	2.50	T1 T4 T6	200 245 325	170 205 320	3.0 3.5 0.5	60
	95	2.64	T1 T4 T6	210 260 330	180 215 325	3.0 5.0 2.0	
2014			T6	483	414	13	72

Dynamic properties for aluminum PM products follow the typical density of material. Datas show that as density increases, so increase the impact and fatigue properties. Figure 2.2 and Figure 2.3 are the S-N curves giving a graphical display of the fatigue properties of these materials. The fatigue testing was done on a 500 million cycle basis on smooth rotating beams of 7,6 mm diameter.

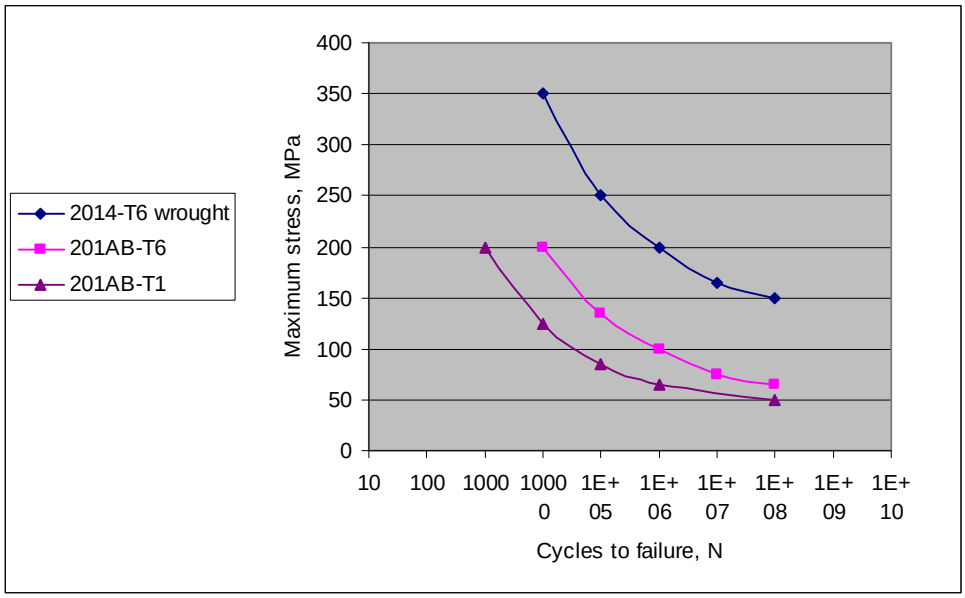


Figure 2.2. Fatigue curves for 201AB PM and 2014 aluminum alloys (Couchman and Cousino, 1994)

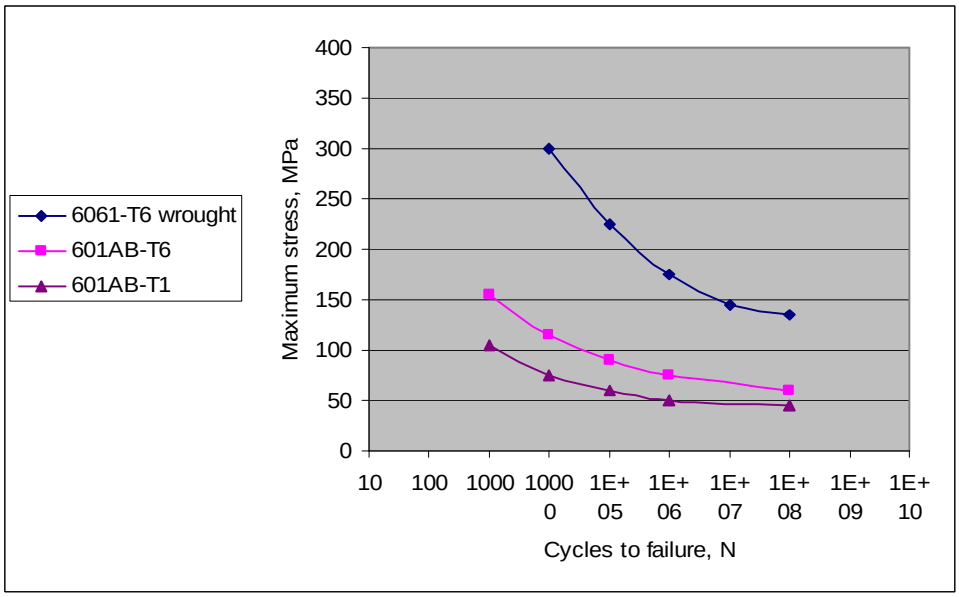


Figure 2.3. Fatigue curves for 601AB PM and 6061 aluminum alloys (Couchman and Cousino, 1994)

The PM bars were processed to 95% relative density. The average fatigue limits for 201AB and 601AB were about 41 N/mm^2 and 48 N/mm^2, respectively. This is far below 6061-T6 at 97 N/mm^2 and 2014-T6 at 124 N/mm^2. It is clear that conventionally processed aluminum PM should not be chosen for applications

involving high cyclic loading.

Schaffer and Huo (1999) studied on development of sintered 7xxx (Alumix 431) series aluminium alloys. They stated the sintering characteristics and the tensile properties of the 7000 series Al-Zn-Mg-Cu alloys, fabricated using elemental powders in conventional press and sinter powder metallurgy process. Steel usage has decreased substantially since the fuel crisis of the mid 1970s, in favour of aluminium and magnesium. In effect of composition other than lead section that alloys are generally designed to accommodate the manufacture of goods made from them as much as the properties required of them in service. Zinc was chosen as the principle alloying addition and sintering aid. Three reasons underpinned this decision. First, zinc provides the greatest contribution to the age hardening of aluminium without recourse to costly non-equilibrium techniques such as rapid solidification. Thus, the high strength 7xxx series aerospace alloys are based on the Al-Zn-Mg system. Second, zinc has the lowest melting point (420 °C) of those readily available alloying additions which can be used for age hardening. Brandes and Brook (1992) stated that zinc also forms a eutectic with aluminium at 380 °C. It therefore has the potential to enhance sintering by the generation of liquid phases which might persist for long periods but eventually dissolve in the matrix where it can contribute significantly to precipitation hardening.

Schaffer et al. (2006) studied the effect of the atmosphere and the role of pore filling on the sintering of aluminium. They stated that sintering of metals is typically conducted in a controlled atmosphere. The role of the atmosphere can include the sweeping of volatile reaction products from the furnace, the prevention of undesirable reactions and the enabling of desirable reactions. Amongst the latter is the reduction of the oxide present on most metal surfaces. For iron, this is readily achieved in conventional atmospheres such as dissociated ammonia. For aluminium, however, the oxide is thermodynamically very stable and requires an oxygen partial pressure of $<10^{-50}$ atm at 600 °C to be reduced. This is not attainable by conventional means. Consequently, the role of the atmosphere in the sintering of aluminium is often seen as simply limiting further oxidation. Any inert gas or vacuum should therefore be equally efficacious. Jha et al. (1988) stated that sintered

6061-Al_2O_3 composites in vacuum, nitrogen and argon. Their results indicated that there was little difference between argon and vacuum, while nitrogen was the least effective of the atmospheres. The difference between the gases was attributed to the lower dew point of the argon. Schaffer et al. (2006) reported that the difference between argon and nitrogen atmospheres on pore evolution is readily apparent in Figure 2.4. Both samples have a similar pore structure when the sintering temperature is first attained. While the porosity in the argon sintered sample does not change markedly over the next 60 min, the porosity in the nitrogen sintered sample is largely eradicated, at least in the interiorportion.

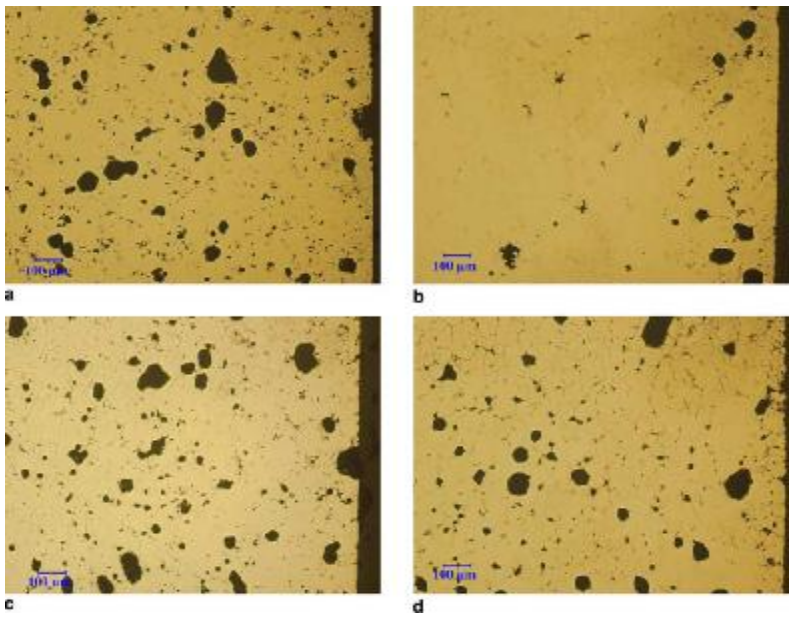


Figure 2.4. Unetched optical microstructures of Al–4Cu–0.6Si–0.1Mg without wax, compacted at 400 MPa with die wall lubricant and sintered in either nitrogen (a and b) or argon (c and d). Samples were either quenched as the sintering temperature was reached (a and c) or 1 h later (b and d). It is only the small pores that are removed under argon, whereas the large pores also disappear in nitrogen, except for those close to the surface (Schaffer et al., 2006).

Eksi and Yuzbasioglu (2004, 2007) studied effect of sintering and pressing parameters on the densification of cold isostatically pressed Al and Fe powders and in investigate sintering of Al specimens. They stated that increasing pressure causes higher density in non-sintered parts due to particle deformation and reducing pores.

When pores reduce, particles are yielded and volume is decreased. Thus, density is increased. Calculated densities with Archimedes Principle for 600°C, 620 °C, 640 °C and 20 min sintering for Al parts are shown in Figure 2.5. As can be seen in Figure 2.5, the highest density is obtained under 600 °C and 20 min sintering condition. Comparison of gren density and sintered density of 600 °C/20 min is shown in Figure 2.6. It shows increasing density after sintering operation. Density increased by only 1.5% after sintering operation with aluminum.

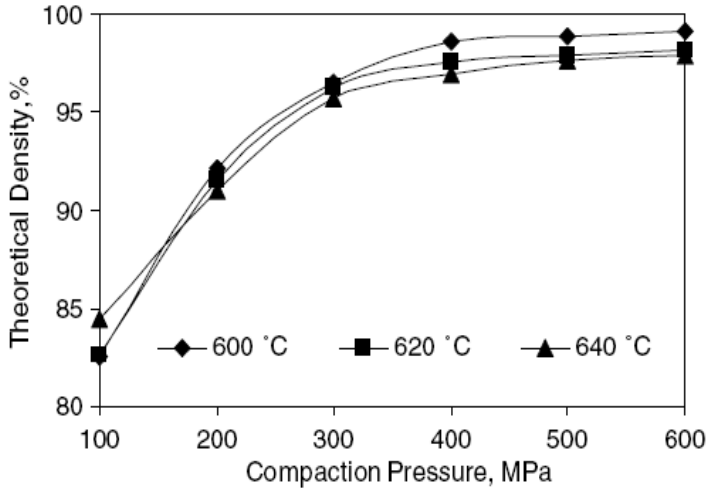


Figure 2.5. Comparison of % densities for 20 min sintered Al parts (Eksi and Yuzbasioglu, 2004 and 2007)

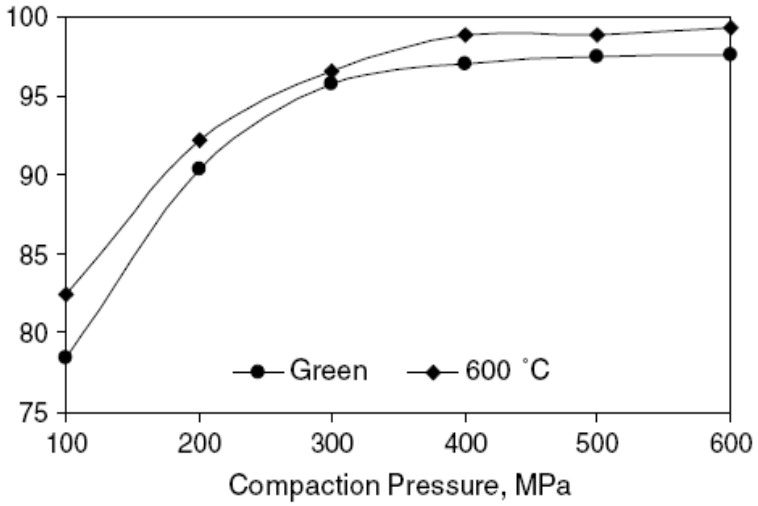


Figure 2.6. Comparison of % green density and 600 °C/20 min sintered Al parts (Eksi and Yuzbasioglu, 2004 and 2007)

Polmear (1995) investigated light alloys. He stated that Copper is added to the 7xxx series alloys principally to improve resistance to stress corrosion cracking.

Kehl and Fishmeister (1980) studied PM. They stated that copper is beneficial to sintering although it also has substantial transient aspect and increases the liquid volume through melting of the Al-Al_2 Cu eutectic.

Gradl et al. (2004) studied improvement in the sinterability of 7xxx based aluminium premix. They stated that the elemental powder blend up to pressures of 400 MPa is easier to compact resulting in higher green density and strength in green density and green strength versus compacting pressure for Alumix 431 alloys made as a result of the experiments.

Showaiter and Youseffi (2008) studied compaction, sintering and mechanical properties of elemental 6061 Al powder with and without sintering aids. They stated that the compaction characteristic at different compaction pressures in the range 250-770 MPa. The highest gren density of ~2.6 g/cm3 (96% TD) was obtained at a compaction pressure of ~510 MPa above which there was little increase in green density. The sintering curves for the premixed elemental (EL) Al alloy sintered under vacuum and pure nitrogen at 620 °C for 1 h, along with compaction curve in the range 250– 770 MPa processed with 0.6 wt% lubricant and no sintering aids are shown in Figure 2.7. The sintering results show that by increasing the compaction pressure the sintered density increases due to more particle bonding and presence of less void as the compaction pressure increases. The variation in sintered density with sintering temperature and presence of 0.12Pb, pressed at 340 and 510 MPa, and sintered for 1 h at different temperatures (580–640 °C) under vacuum. It can be seen that sintered densities decrease gradually after the optimum sintering temperature at 620 °C, but increase more rapidly before this temperature. These results, therefore, reveal that the optimum sintering condition is at a temperature of 620 °C for 60 min under pure nitrogen (or vacuum), which was chosen for the sintering of mechanical tensile bars.

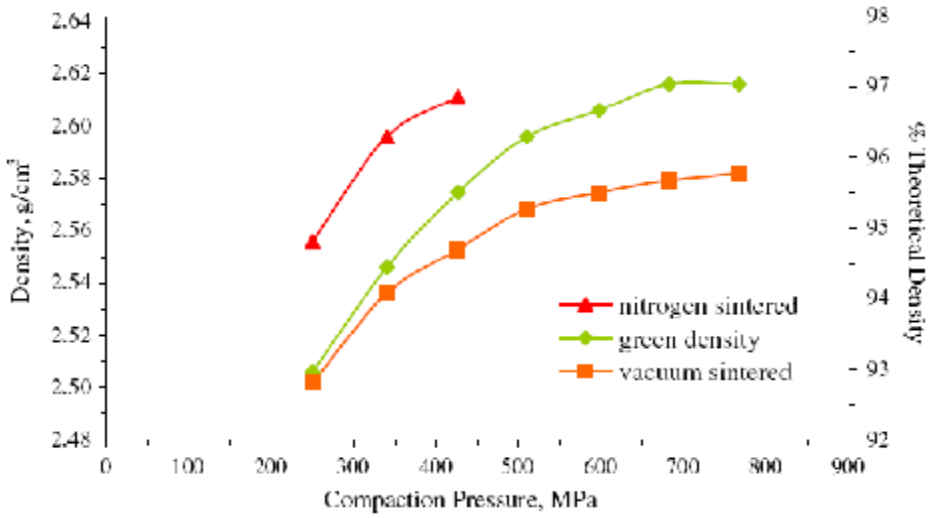


Figure 2.7. Variation in green and sintered densities with compaction pressure for the premixed elemental 6061 Al powder compacts sintered at 620 °C for 1 h (Showaiter and Youseffi, 2008)

2.2. Characteristic Properties of Fatigue Strength of Powder Metallurgy Materials

Many studies on powder metallurgy materials in connection with fatigue strength have made up to the present time. Esper et al. (1981) studied characteristic properties of powder metallurgical materials relevant to fatigue design. They stated that a Fe-Cu-C alloy was investigated in threes and a Fe-Cu-Ni alloy in four density levels. An important condition for investigations was a uniform microstructure within each sample as well as within a whole batch. Samples with the same density and composition showed an analogous fracture performance. A significant value for the estimation of the materials' behaviour is the cyclic 0.2% yield strength, especially in the case of porous materials where already, under small loads, plastic flow can occur in microscopic areas at the interface beneath the solid material and pores. Furthermore, there is also certain relationship between the cyclic yield strength and fatigue life under random loading which enables an evaluation of the materials' behaviour for such loadings. The fatigue strength for bending is generally higher than that for axial loading because of different stress gradients. The fatigue strength for bending is generally higher than that for axial loading because of

different stress gradients. The fatigue strength of the PM can be improved by increasing the tensile strength, because of higher densities.

Varol (1996) studied effect of heat and mechanical surface treatments on the fatigue properties of SAE 8620 steel. He stated that there are three reasons of effects of shot peening. These are work hardening of peened surface, developing a compressive stressed layer in surface and roughing of peened surface. But the main effect in improving the fatigue life is the compressive residual stress. Residual stress magnitudes are slightly changing in the hardened layer. However, for only shot peened specimens residual stresses reach a maximum value at 0.05-0.07 mm depth from surface, then falling rapidly to zero. Also, the maximum increase in fatigue limit is determined with shot peened specimens. Increasing in fatigue limit is found as 41% for only shot peened specimen group. These improvements are due to compressive residual stresses, increased hardness in the surface, and higher depth of hardened layer. The fatigue limit of surface-treated specimens increases due to retardation of crack propagation in compressive residual stress and hardened layer.

Hicyılmaz et al. (1999) studied mechanical properties of aluminum based on granular composites produced by PM. They stated that pressing and sintering process made twice according to the contiditions. First, the mixtures (Al alloys) were pressed at 350 MPa and sintered in nitrojen gas at 600 °C for 30 minutes and secondly, were sintered again in nitrojen gas at 600 °C for 30 minutes after the same of mixtures were pressed at 600 MPa. While the theoretical density was 80% as a result of first pressing-sintering process, in the second pressing-sintering was become 90%. Increase in density for each sample was about 10%. Tensile graphs did not show plastic zone in tensile tests and maximum extension at break was approximately 3%. Tensile Strength and Elongation curves of Al alloys increased as a linear and broke after reaching very small values of elongation (about 0.3% and 3.8%) before plastic transformation curve did not be see. Residual plastic transformation did not observe.

Sonsino and Huppmann (1985) studied fatigue design of PM components. They stated powder metallurgical component design procedure with two examples that are a conventionally sintered turbocharger bushing and a powder forged parking gear. In the case of the material for the turbocharger bushing, Fe-1.5%Cu, and

densities fewer than 7.2 g/cm^3 are manufactured by the single sintering technique and densities above 7.2 g/cm^3 up to 7.5 g/cm^3 by the more expensive double sintering technique. Sintering can also be carried out temperatures between 1120 and 1280°C, higher temperatures leading to a more homogeneous microstructure. In addition, Sonsino et al. (1982) studied influence of homogeneity on the fatigue properties of sintered steels. They stated that the endurance limit can be increased by about 10 to 20% in comparison to lower sintering temperature of 1120°C. Sonsino and Huppmann (1985) showed that the mechanical properties obtained on specimens with a cross section of 5x5 mm are given in Table 2.2 and on the example of the porous alloy Fe-1.5%Cu it can be seen that the properties are improved by increasing the density.

Table 2.2. Mechanical properties obtained on specimens with a cross section of 5x5 mm (Sonsino and Huppmann, 1985)

Material	Density (g/cm^3)	Young's modulus E (GPa)	$S_{0.2}$ (MPa)		S_{UTS} (MPa)	Elongation e (%)	Hardnes	Treatment
			Monotonic Tension	Cyclic Tension-Compression				
Fe-1,5% Cu*)	6.8 7,1 7,4	140 155 180	195 228 235	202 228 235	244 286 340	8 9 13	80 HB 96 HB 105 HB	as sintered
Fe-2% MnCrMo-0,2% C	7,8	206	325 -	410 -	590 -	24 -	20 HRC 55 HRC	forged case Hardened

*) Sintered at 1120 °C

Sonsino (1990, 1999) investigated fatigue behaviour of sintered materials and components under operational service. He stated that how best to fatigue design procedure was intended to create. The development of fatigue loaded PM parts requires knowlodge of material related design data such as S-N curves, influence of loading mode, notches, and mean stresss sensitivity on one hand, and on the other

hand knowlodge of the service loading and local stresses resulting in the most critical areas of the part.

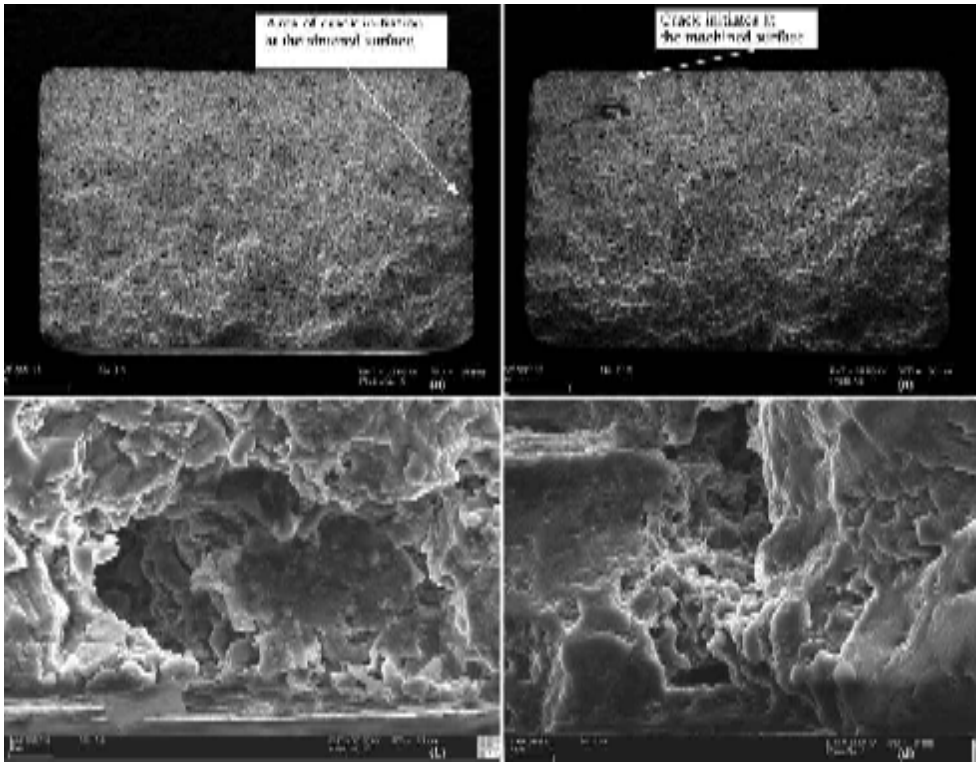
Sudhakar (2000) studied fatigue behaviour of high density PM steel. He stated that the fatigue property of a high density Fe–2%Ni based PM steel under different heat-treated conditions evaluate. For each material (A and B), four sets of samples were sintered and heat-treated. The first four sets of samples were used in the as-sintered (designated as 'AS') condition. The other four sets of samples were hardened and tempered at 813 K (designated as 'HT1') and 593 K (designated as 'HT2') to achieve hardness levels of approximately 30 and 40 HRC, respectively. It is readily seen that the endurance limit increased in the order AS, HT1 and HT2 (for both materials) in terms of stress values. Both materials A and B exhibited the maximum endurance limit value in the 'HT2' condition. This improved fatigue life was mainly attributed to the presence of tougher, tempered martensitic structure. In conclusions, he reported that the high density Fe–2% Ni based PM steel recorded the best endurance limit (~360 MPa in the present investigation) when heat treated to 'HT2' condition. Obviously, this particular grade of PM steel holds good potential for achieving better fatigue properties by suitably designing heat treatment schedules.

Sarıtas (2002) studied a critical review of the interaction of material and processing conditions made for sintered steels in relation to their microstructures and attendant fatigue properties. He stated that the study established for the optimization of material and processing conditions in terms of the fatigue life of PM steels. Aim increased density to develop fatigue properties at the same time. Pores that are surface of material and open pores formed on the surface of material are more dangerous. Therefore, surface plastic deformation, hardening, and covering methods are always beneficial.

Miura (2002) studied fatigue fracture behaviour of PM and PIM steels. He stated that study has been performed to clarify the relationship between the mechanical properties and the microstructures for strengthening the sintered low alloy steels through the conventional PM (die pressing) and new (PIM) techniques. In conclusion, the mechanical properties of sintered low alloy steel compacts are very dependent on the microstructures as well as the density and chemical

compositions. Generally, the homogeneous microstructure has been favorable for strengthening the steels in the conventional PM processings using prealloyed powder. On the other hand, mixed elemental powder compacts show the various heterogeneous microstructures because of the different diffusivities between alloying elements. But, if the good combination of resultant phases is obtained, the strength of mixed powder compacts will be significantly improved. In such a case, the higher density and the finer heterogeneous structure, the more effective for strengthening the steels.

Eksi et al. (2004, 2006, and 2007) studied tensile and fatigue properties of cold and warm compacted Alumix 431 alloy. They stated that tensile and fatigue properties of the Alumix 431 alloy (Al-5,5Zn-2,5Mg—1,5Cu) produced using the conventional press and sinter processes in different pressures and temperatures are investigated in experimental study. The studies carried out on the cold and warm compaction of Alumix 431 alloy static, tensile and fatigue properties makes. The highest densities have been obtained in sintering conditions: temperature; 620 °C, time; 30 min, atmosphere; N_2, heating rate; 5 K/min, cooling rate; freely cooled at room temperature and pressing pressure: at 400 MPa in RT and these results have been taken into consideration for tensile and fatigue specimens in order to obtain optimum results. Also, the sintering behaviour of Alumix 431 powder shows changes depending on the sintering temperature, heating rate and sintering time. In addition, the prosity has a significant effect on the mechanical properties and in the fatigue tests, it was observed in all SEM examinations that fracture started from the large pores and ductile fracture occurred. SEM photograps of fracture surfaces are showed in Figure 2.8. The endurable stress for both cold and warm compacted specimens was almost equal due to same densities, and the endurable stress at 10^5 cycles was 16% cycles for $R = \sigma_{min} / \sigma_{min} = -1$. It can also be expected, however, that significant static and fatigue property improvements can be achieved by increasing the density of specimens.



a, b 180 MPa/80°C; σ_a = 50 MPa, N_R = 4,3x10^5, R = -1; c, d 230 MPa/RT; σ_a = 60 MPa, N_R=4,1.10^5, R= -1

Figure 2.8. SEM photographs of fracture surfaces (Eksi et al., 2004, 2006, and 2007)

Sonsino (2007) studied light-weiht design changes using high-strength steels. He stated that the selection of a high-strength material will not improve the fatigue strength of a component in the presence of a high stress concentration; an improvement must be sought first by a reduction of the stress concentration. However, because of geometrical constraints this is not always possible. In such cases, an additional mechanical surface treatment i.e. shot peening or surface rolling can increase the fatigue strength significantly, especially when the treatment is applied to a high-strength material. Due to the higher yield strength the beneficial compressive resudial stresses generated in high strength materials are higher than in lower strength steels. Influence of material strength on the increase of fatigue strength is dislayed in Figure 2.9.

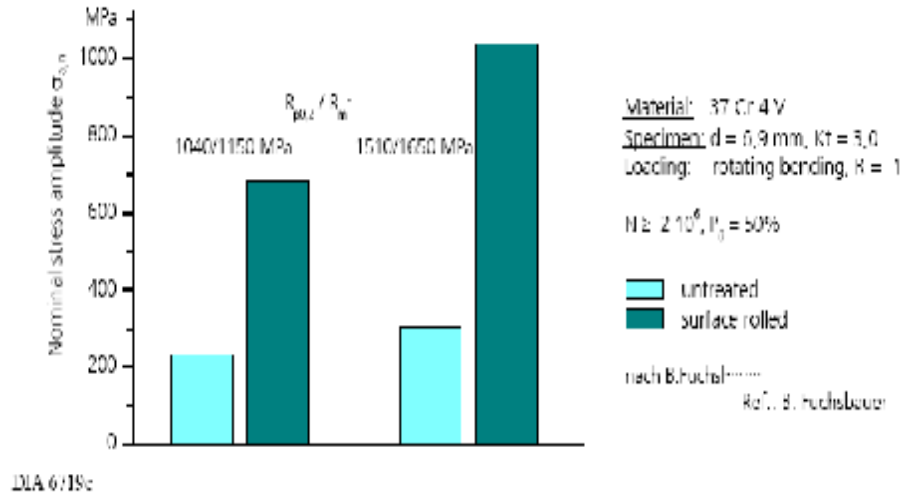


Figure 2.9. Influence of material strength on the increase of fatigue strength due to surface rolling (Sonsino, 2007)

Iynen et al. (2009) studied design and investigation of improvement of fatigue properties of machine elements produced by PM. They stated that PM introduced economic manufacturing ways that can be competed with convential materials to produce parts subjecting to fatigue loading.

2.3. Improvement of Fatigue Properties of PM Materials by Shot peening

There are considerable studies concerning shot peening process. Sarıtas et al. (1999) studied improvement of fatigue properties of PM steels by shot peening. They stated that focuses on the effect of shot peening parameters on the fatigue properties of Fe-2Cu–0.5C PM steel. As a result of examining of the mechanical properties of materials, shot peening improves the fatigue strengths of all. The materials have 10A, 20A, 25A, and 30A shot peening intensity parameters. Shot peening improves in the fatigue strength of pure iron and Fe-2Cu material saturate at 25A shot peening intensity but further peening is detrimental. For example, for Fe-0.5Cu material, improvement continues up to 30A intensity and then the fatigue strength starts degreasing. For all of the materials investigated, too much shot peening was not beneficial. Also, the present authors (1997) stated that too much shot peening removes the surface deformed layer in previous works. Thus, the hardness increased

layer produced by shot peening is eroded by excessive shot peening. The results showed that residual compressive stresses as well as superficial densification due to plastic deformation produced by shot peening contributed to the improvements in fatigue performance.

Akyıldız and Sarıtas (1999) studied improvement of fatigue strength of PM steel by shot peening. They stated that shot peening is the most economic method among surface process for fatigue life of PM steels. Sintered steel materials shot peened using 0.20mmA, 0.25mmA and 0.35mmA intensity, respectively. As a result of fatigue test, shot peening process were inceased fatigue strength. Shot peening provided a significant increase in fatigue life of material. This increase changed between 30–35% according to intensity of operation and material characteristic. Increase of fatigue life continued up to 0.35mmA intensity. When 0.35mmA intensity applied, it stopped almost and then decreased. This originated from effect of detrimental of too much shot peening intensity.

Akdemir et al. (1999) studied effects of surface treatments on fatigue strength using ferritic-pearlitic and pearlitic nodular cast iron materials. They stated that shot peening increases considerable fatigue strength of materials. Also, Varol (1990) studied effect of different shot peening parameters upon fatigue life of 2024 Al alloys and stated that fatigue strength limit of shot peened specimen increased 108% according to unpeened specimen. Fatigue strength limit of Al alloys increased by shot peening using appropriate intensities. In addition, Nakonieczny (1981) studied effect of shot peening on the fatigue life of machine elements and stated that shot peenind improved fatigue strength between 10%-60% on different machine elements.

Varol and Tunay (2001) studied the changes of wear properties of natural aged AA2024 aluminum alloy by shot peening. They stated that changes performed on aluminum alloy after shot peening process. Aluminum specimens were shot peened using S230, S170 steel shots and S13 glass beads to 16A-28A intensities. Surface roughness of unpeened and peened specimens was measured. It was seen that important increase in surface roughness were determined after shot peening. Surface hardness of peened specimens was also increased.

Tekeli (2002) studied enhancement of fatigue strength of SAE 9245 steel by shot peening. He stated that the effect of shot peening on fatigue life of SAE 9245 steel, which is used in endustry for helisel spring production, was investigated. The fatigue results for unpeened and peened conditions were compared. It was seen that shot peening improved fatigue life by about 30% and optimum peening intensities were in the range 20-25A. S-N curves for shot peened and unpeened specimens are shown in Figure 2.10 This improvement on fatigue life can be attributed to the formation of compressive residual stresses in the surface layer of the material. A further increase in the peening intensity beyond 20A–25A range resulted in a degrease fatigue strength. This decrease was due to overpeening which can form cracks at the surface and remove the compressive residual stressed layer.

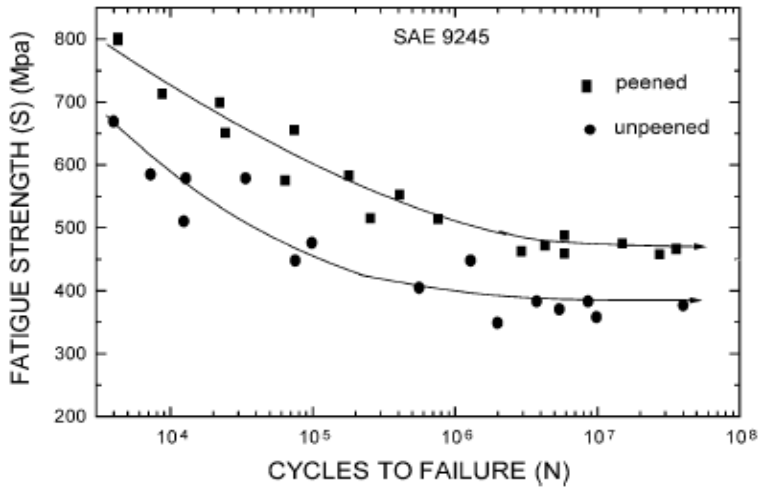


Figure 2.10. S –N curves for shot peened and unpeened specimens (Tekeli, 2002)

Torres and Voorwald (2002) worked an evaluation of shot peening, residual stress and stress relaxation on the fatigue life of AISI 4340 steel. They stated that the shot peening influence on the fatigue life, the behaviour of CRSF (compressive residual stress field) during the fatigue process and the crack initiation points of fatigued specimens were studied. The S-N curves for the base material and for the four peening conditions analyzed as shown in Figure 2.11. There was almost no difference in the fatigue limit between the lowest and the highest peening intensities tested 0.0027 and 0.0141 A. Yet, the shot peening for the studied conditions

represents an enhancement of the fatigue limit from 9% (0.0027 A) to 12% (0.0063 A) when comparing to the base material because of compressive residual stress formed on material.

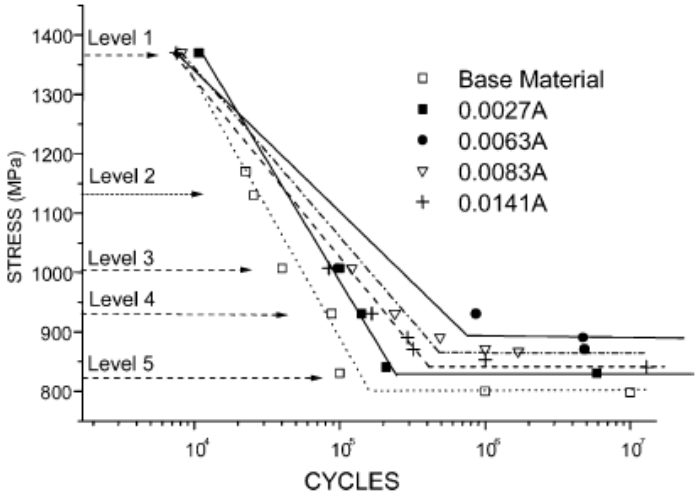


Figure 2.11. S–N comparative curves of the base materials and shot peening conditions (Torres and Voorwald, 2002)

Pavel et al. (2002) studied the influence of shot peening on the fatigue properties of PMs. They stated that a study of the kind in which surface mechanical treatment as shot peening may influence the fatigue strength of sintered materials based iron. Shot peening appear a material densification and particle deformation, as well as an improvement of the surface roughness. Also, shot peening increases the endurance limit of the Fe-Cu alloy by 42% according to results which were obtained for all three different almen intensities and there are in accordance with hardness. The surface will be more deformed if the shot intensity is greater; but the shot intensity can't be too big because the particles from the material surface can be broken. Examination of the fatigue fracture of a shot peened part revealed that in most cases failure initiated at a point below the peened surface.

Dulek et al. (2003) studied effect of residual stresses formed on AISI 1020 steel by shot peened. They stated that compression residual stresses formed on material surface were usually beneficial. It is known that compression stresses hinder detrimental which originated crack and tensile stresses. Shot peening performed

compression residual stresses, which are improved performance of materials, varied between 276 MPa (compression) to 363 MPa (compression) on material. In addition, the present authors (2005) investigated effects of shot peening on fatigue strength of AISI 1020 steel. Maximum compression stress obtained on surface material by shot peening of AISI 1020 steel in 0, 26 mm A intensivity. Compression residual stresses on surface decreased in intensivity above of this. While material is overpeening, compression residual stresses on surface of material can not increase. The reason for this, it was thought that surface layer was given detrimental by overpeening and surface of material was broken down as plastic deformed.

Basaran et al. (2007) studied investigation of effect of the shot peening and high temperature on the fatigue strength of PM steels. They stated that Steel PM parts containing copper (FC 0205) were shot peened using different parameters and the change of fatigue strength values was analyzed. The parts are kept at 560°C for 30 minutes and were applied rotating bending fatigue test. Then, S-N curve was plotted. The fractured surfaces were examined metallographic in order to explain the fatigue test results. Fatigue strength of PM specimen's appling different heat and surface treatments were observed an increase from 10% to 90% by shot peening when all group investigated. All of group show parallel each other. As long as shot peening intensity rises, in low cycle region of S-N curves were observed an increase.

Yılmaz et al. (2007) studied effect on fatigue behaviour of shot peening and bronizing on materials based iron. They stated that PM materials which based iron FeCu-graphite examined sintering, boronizing and shot peening process and compared fatigue properties by means of bending fatigue testing each other. When low cycle areas of S-N curves are investigated, fully dense materials are observed more horizontal and lower slope. This case can be explained the amount of pores or by the low of relative density of PM materials.

Baryy et al. (2009) worked effect of shot peening on the fatigue behaviour of cast magnesium A8. They stated that the fatigue life of sand-cast A8 magnesium alloy has been investigated before and after a shot peening treatment to investigate whether shot peening is beneficial for a component with this combination of

relatively low strength and relatively poor initial surface finish. The shot peening has many benefits on used material. These:

- The effect of shot peening on the fatigue behaviour of cast magnesium A8 has been investigated. Shot peening has been found to offer a significant improvement in the fatigue life, with an increase in the fatigue life of up to five times depending on the applied stress amplitude, and a 30% increase in the endurance limit of the material.
- The peened samples show a significantly higher surface roughness than the as-machined condition. However, crack initiation appears to occur from residual porosity in the samples, rather than from surface features that can be attributed to the peening. It can be surmised therefore that the compressive residual stresses act to retard the initiation and growth of fatigue cracking from the residual porosity and surface damage.
- Overall it can be concluded that the peening process provided a beneficial improvement in fatigue life, with the residual stres field acting to retard the initiation and growth of cracks. Initiation of fatigue damage was at areas of residual porosity, and the rougher surface introduced by the peening process did not have a negative effect on fatigue life.

3. MATERIAL AND METHOD

3.1. Material

Aluminum alloys are usually preferred to be used such as automotive, machine and airpcraft components due to their lightweight properties and suitability of their mechanical properties required by the related industries. Conventionally pressed and sintered aluminum powder metal parts have been commercially available for many years. PM has been recently the subject of renewed attention due to the combination of the lightweight of aluminum and the efficient material utilization of the PM process, which offer attractive benefits to the perspective end users. The influence of manufacturing parameters of the PM parts, such as alloy compositions, density, sintering conditions, mechanical and thermal surface treatments (carboning, tempering, quenching, shot peening, ultrasonic shot peening etc.) and heat treatment on the static (tensile) and dynamic (fatigue) properties play an important role. Commercially, available aluminum powder alloy compositions consist of blends of atomized aluminum powders mixed with powders of various alloying elements such as zinc, copper, magnesium and silicon.

The Alumix 431 (7xxx series) is one of the aluminum alloys of the most common heat-treatable grades and been used in this study. The Alumix 431 based on additions of zinc (Zn), magnesium (Mg) and copper (Cu) is a high strength aerospace alloy. The 7000 series alloys have the highest age hardening response of all the conventional aluminum alloys. Zinc provides the greatest contribution to the age hardening of aluminum without recourse to costly non-equilibrium techniques such as rapid solidification. Also, zinc has the lowest melting point (420 ºC) of these readily available alloying additions which can be used for age hardening. In addition, it forms a eutectic with aluminium at 380 ºC (Brandes and Brook, 1992). Copper is added to these alloys principally to improve resistance to stress corrosion cracking. Copper is beneficial to sintering although it also has a substantial transient aspect and increases the liquid volume through melting of the Al-Al_2-Cu eutectic. Magnesium even at the 0.5% level impact on shrinkage in a positive manner by reducing the

oxide allowing metal-metal contact at particle interfaces and facilitating diffusion (Schaffer and Huo, 1999).

Material used in this study was Alumix 431® powder from Ecka Granules in Germany. It is a mixture of 7xxx series aluminium alloys which is termed Alumix 431. The chemical composition and particle size characteristics of Alumix 431 powder are given in Table 3.1.

Table 3.1. Chemical composition and particle size characteristics of the Alumix 431 (ECKA Granulate GmbH & Co. KG, 2009)

Chemical Composition, % (Density: 2,786 g / cm^3)					Particle Size Characteristic*				
Al	Cu	Zn	Mg	Lubri-cant	D_{10}	D_{50}	D_{90}	S_w**	Mean Value
89	1,5	5,5	2,5	1,5	54,8	107,2	193,1	4,7	118,7

*Dimensions are in µm, **S_w: The particle size distribution slope

3.2. Method

3.2.1. The Pressing Process of Aluminum Alloys Powder Used in This Study

First of all, the components of powder (Al-5.5 Zn-2.5 Mg-1.5 Cu; elemental mixing is in weight%.) which are approximately weight of 15 g are mixed to put into blanks , together with lubricant, until a homogeneous mix is obtained using a 3-D Turbula Mixer. A homogeneous mix of Alumix 431® powder is shown in Figure 3.1.



Figure 3.1. Alumix 431 powder which have Al-5,5 Zn-2,5 Mg-1,5 Cu component powders

In the second step, the mix is then loaded into prismatic blanks which a die in

sizes of 10x10x55 mm^3 as shown in Figure 3.2 and cold compacted under 400 MPa pressure at room temperature (RT) using a single action press in PM Laboratory of Süleyman Demirel Universty in Isparta, Turkey.

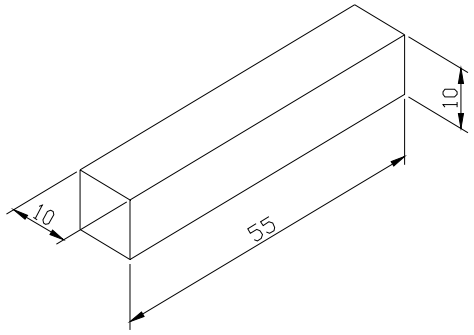


Figure 3.2. Compacted aluminium alloy used in this study

3.2.2. The Sintering Process of Compacted Aluminium Alloy Used in This Study

In the third step, sintering of all materials was performed in an automatic controlled high temperature gas atmosphere tube furnace using Protherm Electrical Furnace as shown in Figure 3.3, which is PTF 4/75/750 model, and can heat up to 1600 °C temperature in Gazi Universty's Mechanical Research Laboratory in Ankara, Turkey. Eksi et al. (2004) stated that in order to determine the optimum sintering result, the specimens were sintered under five different sintering conditions and 620 °C sintering was selected the best temperature to produce the samples for tensile and fatigue tests since it resulted in high density. They found that the the best sintering temperatures were at 600 °C and 620 °C temperatures. Based on this issue, the specimens were sintered at two different temperatures that was at 600 ºC and 620 ºC in this study. All specimens of pressed dies were sintered for 1 hour at 600 °C and 620 °C temperatures in groups of fifteen each, respectively. Temperature was increased by 5 °C/min until medium of furnace reached sintering temperature; and then specimens were kept in these temperatures (in turn at 600 °C and 620 °C) for 1 hour. After that, furnace was closed and temperature was decreased by 5 °C/min until medium of furnace was reached room temperature (RT, 22 °C). While the specimens were cooling, the furnace was also running in N_2 atmosphere, which is protective gas.

These operations were continued till medium of furnace was reached RT and sintering process ended up. Sintering conditions used in this work are given in Table 3.2.



Figure 3.3. Protherm automatic controlled high temperature gas atmosphere tube furnace

Table 3.2. Sintering conditions

Specimen	Atmosphere*	Heating rate, °C/min	Cooling rate, °C/min	Sintering temperature, °C	Sintering time, min
No.1	N_2*	5	5	600	60
No.2	N_2*	5	5	620	60

*=N_2, dry, clean, dew point lower -45 °C

Physical, chemical, compacting and sintering properties of Alumix 431 which are recommended from Ecka Granules are shown press-ready mix for aluminium sintered parts in Table 3.3 and 3.4. Due to the superior die filling behaviour and excellent compressibility, Ecka Alumix 431® is specially intended for the production of high-precision sintered components. Sintered parts of Ecka Alumıx® 431 are

particulary used, when high sintered strength is required. Due to the alloy composition AlZnMgCu material properties, typical for that alloy system can be reached by applying a heat treatment.

Table 3.3. Typical materials properties of the Alumix 431 (ECKA Granulate GmbH & Co. KG, 2009)

Physical characteristics		Chemical compositions	
Apparent density	1,10 - 1,25 g/cm³	Aluminium (Al)	Rest
Flowability	Max. 30 s	Zinc (Zn)	5,0 - 5,8%
Tap density	1,20 - 1,50 g/cm³	Magnesium (Mg)	2,2 - 2,8%
Sieve fraction < 45µm	Max. 35%	Copper (Cu)	1,4 - 1,8%

Lubricant: 1,5% amidwax

Table 3.4. Typical compacting and sintering properties of the Alumix 431 (ECKA Granulate GmbH & Co. KG, 2009)

Recommended compacting and sintering conditions				
Compacting	Compacting Pressure	400 MPa	Green density	2,65 g/cm³
Sintering	Dewaxing	directly to sintertemperature		
	Sintering temperature	600 - 610°C		
	Sintering time	20 min.		
	Atmosphere	N_2 dew point < -45°C		

3.2.3. Density Measurement of Green and Sintered Aluminium Alloy

The density of sintered and green Al alloys was evaluated at this stage. Densities of sintered and green (pressed) parts were measured by Classical Method and the Archimedes Principle (water displacement technique) using Precisa 320XT series for analytical and precision balances which has 1/10.000 precision of scale in Gazi University's Mechanical Research Laboratory in Ankara, Turkey. Archimedes Principle is easy to apply and results can be calculated rapidly. Especially, when precision balance is used the results can be confidential. In order to measure densities by Archimedes Principle, Precisa Density Measurement Set is also used. This set specially produced with this balance consist of liquid tube carrier table, specimen holder, glass liquid tube and fitted temperature for liquid. Pure water is used for

measuring media at room temperature, 22 ºC for this study.

There are a lot of the basic formulas related to density according to Classical Method and Archimedes Principle. These are given with symbols and explanations to determine densities of samples below:

a) Classical Method to determine the green density

ρ_{green} = Green density of specimen, g / cm ^{3}

m_{green} = Green mass of specimen, g

v_{green} = Green volume of specimen, cm ^{3}

$$\rho_{green} = \frac{m_{green}}{v_{green}} \tag{3.1}$$

b) Archimedes Method to determine the sintered density

x = Weight of specimen, g

y = Carrier material weight, g

z = Weight of specimen in the water, g

b = Difference of weight, g

a = Weight without carrier bond, g

$\rho_{sintered}$ = Sintered density of specimen, g / cm ^{3}

k = 0, 9999 (special constant for pure water at 18-26 °C temperature from handbook of the density measurement set)

$$a = z - y \tag{3.2}$$

$$b = x - a \tag{3.3}$$

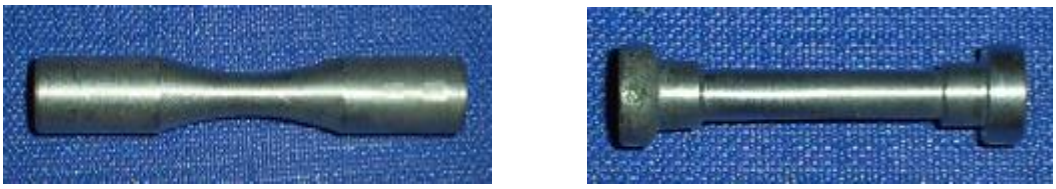
$$\rho_{sintered} = k.\frac{x}{b} \tag{3.4}$$

The densities have been calculated easily with the help of these equations to compare used all data in connecting with density in this work.

3.2.4. The Machining and Polishing Operations of Test Specimens

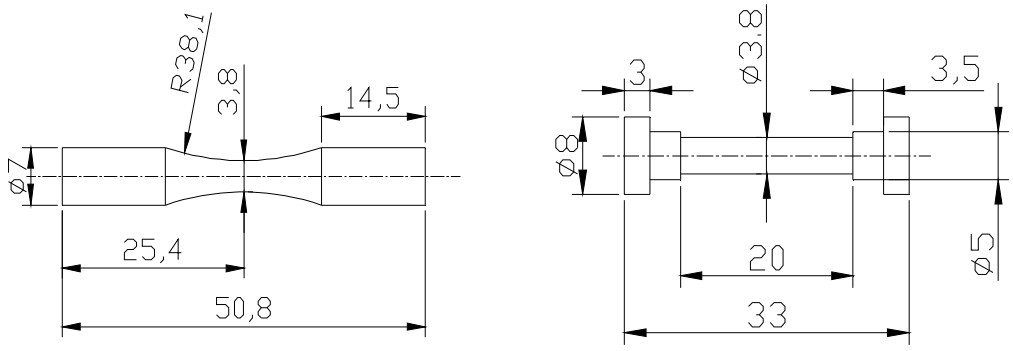
In this step, the sintered samples were conducted machining operations and

polishing operations using Computerized Numerical Control (CNC) turning lathe and metal polishing machine, in turn, to achieve optimum results for fatigue and tensile test produced by Işın Technical Machine Industry Limited Company and Uzeller Machine Industry Limited Company in Adana, Turkey. The tensile, fatigue specimens and S-N curves have been machined and performed according to the standard of ASTM E8M 'Standard Test Medhods for Tension Testing of Metallic Materials (Metric)', ASTM E468 'Standard Practice for Presentation of Constant Amplitude Fatigue Tests Results for Metallic Materials' and ASTM E739 'Standard Practice for Statistical Analysis of Linear or Linearized Stress-Life (S-N) and Strain-Life (ε-N) Fatigue Data at room temperature, respectively. Fatigue, tensile test samples and technical drawings are shown in Figure 3.4 and 3.5 separately.



(a) (b)

Figure 3.4. Fatigue and tensile test specimens; a) Fatigue test sample, b) Tensile test sample



(a) (b)

Figure 3.5. Technical representation of fatigue and tensile test specimens; a) Finished product (fatigue test sample), b) Finished product (tensile test sample) (Dimensions are in mm)

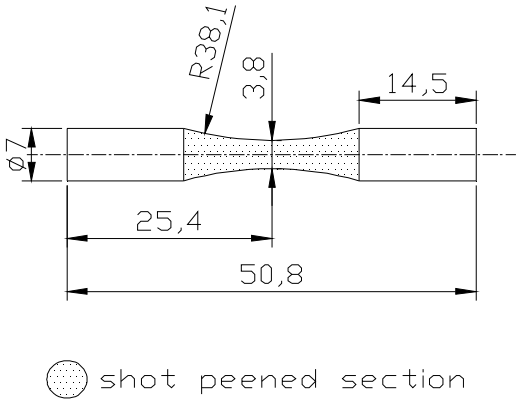
3.2.5. Shot peening

There are many ways to improve fatigue strength parts which are produced by PM like heat treatment, boronizing, and shot peening etc. The Shot peening that was one of the most economic surface processes that applied to increase fatigue life of material. To evaluate unpeened and peened parts in respect to mechanical properties, 15 samples were only sintered and other 15 samples are shot peened in 12A and 16A intensities separately according to literature to perform the best results using an air high-pressure type of equipment. Shot peening was conducted using S110 atomised steel shot with 45-55 HRC hardness. Almen peening intensity as the major peening parameter was applied 12A and 16A intensities. For providing this, peening procedure was carried out at 345 kPa nozzle air pressure. The impingement angle was chosen to be 90º and distance from the nozzle to the workpiece was constant at 100 mm. Fatigue specimens were rotated at 20 rev/min speeds during peening operation. Almen A strips and Almen gage were used to determine Almen intensity. Saturation rate was chosen as 100%. The shot peening parameters used in this work are given in Table 3.5. Figure 3.6 displays technical drawing of shot peened material. The shot peening studies were carried out using IEPCO Micropeen-Peenmatic 2000S Machine in Laboratory of 1st Air Supply and Maintanence Center (1. Hava İkmal Bakım Merkezi Komutanlığı) in Eskisehir, Turkey.

Table 3.5. Shot peening parameters used in this study

Specimen	Material, sintering temperature	Peening intensity, A (mm)	Shot material, shot diameter (mm)	Peening air pressure, psi (MPa)	Peening time, second (s)
No.1	Alumix 431, 600°C	12 (0, 30)	Steel, S 110 (0, 27)	50 (0, 34)	15
No.2	Alumix 431, 620°C	16 (0, 40)	Steel, S 110 (0, 27)	50 (0, 34)	27





(a) (b)

Figure 3.6. Shot peened specimen for fatigue test; a) Shot peened material, b) Technical representation of shot peened material

3.2.6. Mechanical Tests

3.2.6.1. Tensile and Fatigue Tests

In this study, to examine the static and dynamic properties of used samples, tensile and fatigue tests were conducted. Tensile tests were carried out on sintered and shot peened specimens prepared according to different sintering, shot peening conditions. Outcomes of tensile experiments were plotted as Stress (MPa) versus Extension (mm). Fatigue tests were conducted using same way and outcomes of fatigue experiments were plotted as Nominal stress amplitude, $\sigma_{a,n}$ (MPa) versus Cycles to rupture, N_R (Number). Tensile and fatigue tests were executed at room temperature using Instron® with a controller Fast Track® 8800 series connected to a computer and a servo hydraulic. Typical materials properties of ECKA Alumix 431® sintered parts are shown in Table 3.6.

Table 3.6. Typical materials properties of sintered parts

Typical material properties of ECKA ALUMIX® 431 sintered parts (Green density: 2,65 g/cm³)					
Sintered density	Dimension change		Tensile strength	Brinell*/Vickers HB*/HV Hardness	Elongation A_5
1	-0,5%	T_{1a}	270 N/mm²	100*/105	4%
		T_{76}	400 N/mm²	150*/160	2%

The tolerance accuracy of the sintered parts can be increased by calibration; T_{76} treatment is leading to improve material properties. * Astral (Brinell) values are converted to Vickers and Vickers values are approximately values.

For tensile and fatigue tests, the experiments were done by means of Bluehill® 2 and Single Axis (SAX), Multi Axis (MAX) software systems, respectively. Typical screen layout of Bluehill® 2 and SAX or MAX software are shown in turn in Figure 3.7 and 3.8.

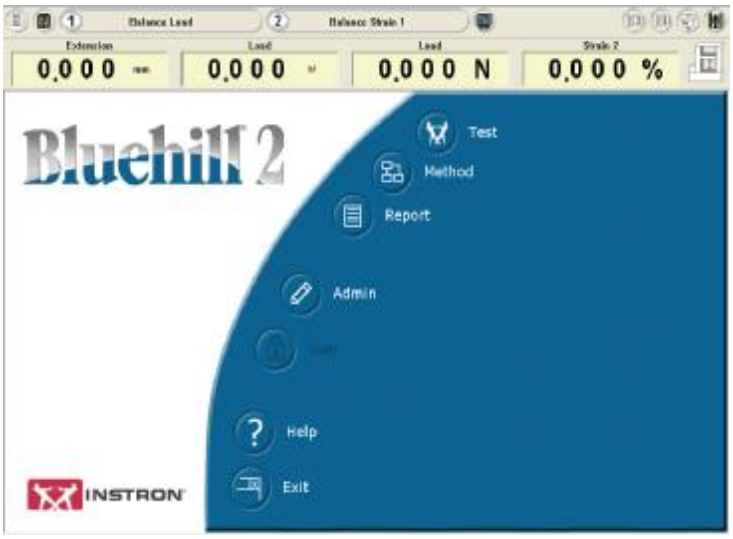


Figure 3.7. Typical screen layout of Bluehill® 2 software

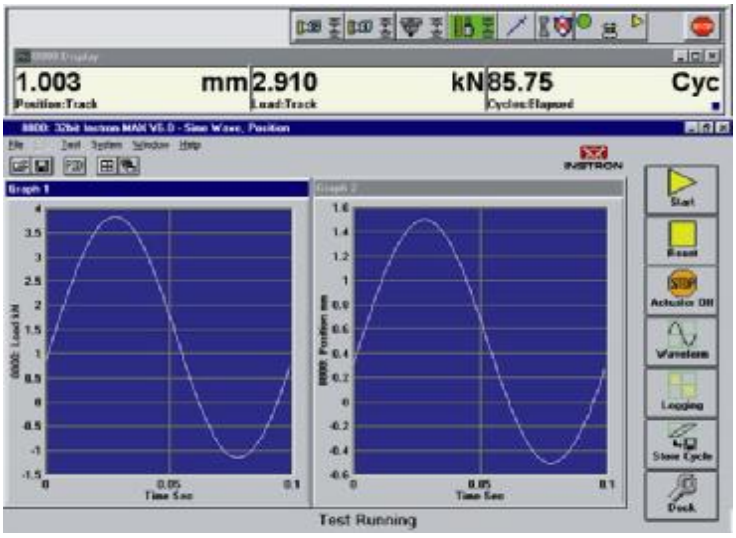


Figure 3.8. Typical main screen of SAX or MAX software

All the experiments of fatigue tests were conducted in the axial load control which is more severe than bending under fully reversed loading (stress or load) ratio $R = \frac{s_{\min}}{s_{\max}} = -1$ which is sine (cyclic) waveforms using 15 specimens for the determination of each S-N (Wöhler) curve. The fatigue tests were performed at the constant frequency of $f = 10Hz$. One stress ratios (R = -1) were investigated on the unnotched ($K_t = 1$) specimens. Sine (cyclic) waveforms as shown in Figure 3.9 are used. The cyclic group of waveforms all start at a setpoint, proceed to a peak amplitude, either negative or positive, before reversing direction, passing through the setpoint to the opposite peak amplitude. The signal will then return to the initial starting position, ready to commence the next cycle. The sine waveform follows a sinusoidal path, defined by the amplitude and frequency parameters.

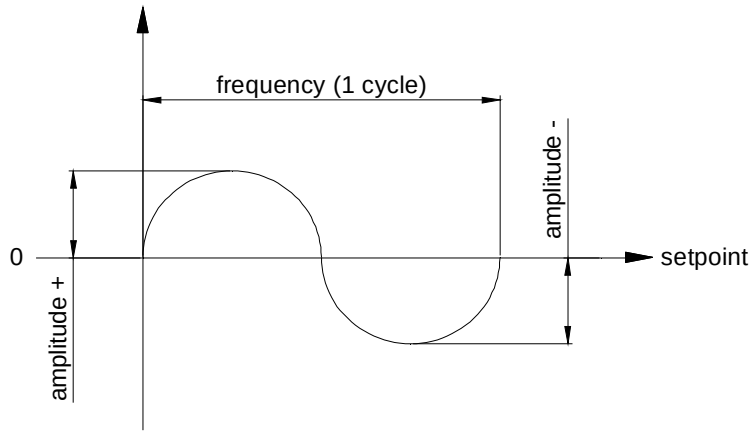
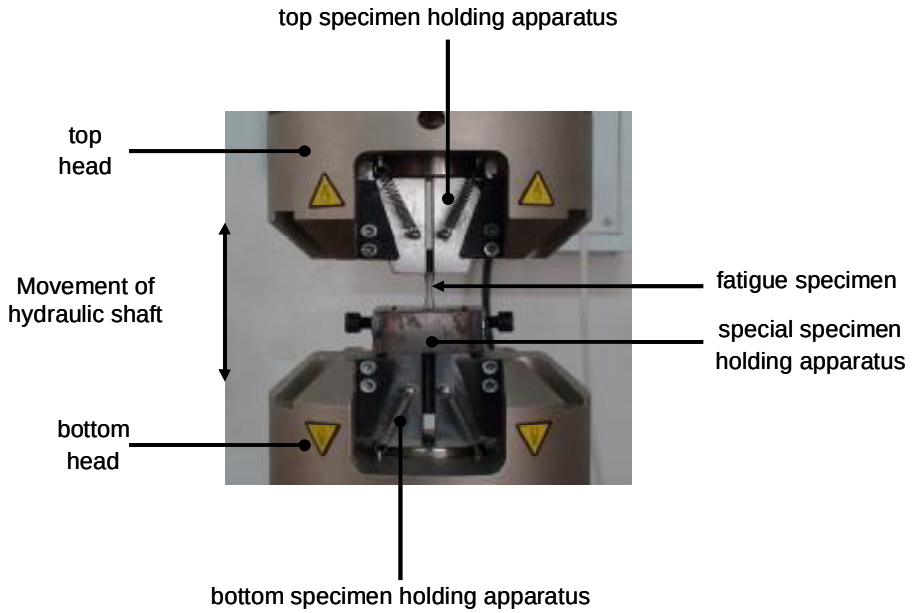


Figure 3.9. Typical sinusoidal waveform

All the tensile and fatigue experiments were carried out in the Materials Laboratory of Department of Mechanical Engineering of Cukurova Universty in Adana/Turkey. Figure 3.10a and 3.10b show all the main equipment and set-up used to perform the tests separately. For the tensile experiments, three tensile tests were made for each condition to obtain the best efficient results.



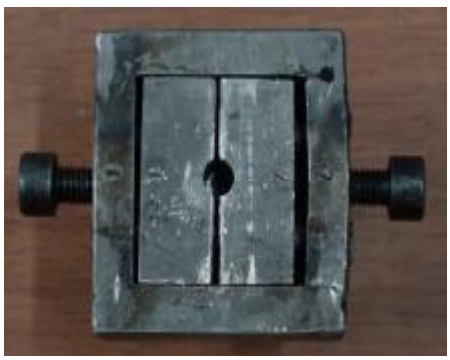
(a)



(b)

Figure 3.10. The main equipment used to perform tensile and fatigue tests; a) General appearance of laboratory arranged for tensile and fatigue experiments, b) Set up of apparatus of specimen

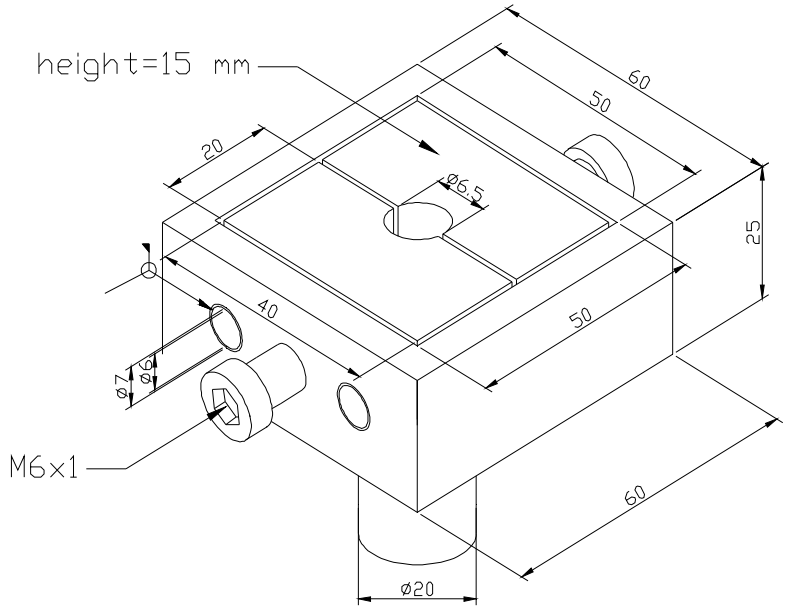
In the tensile test, Action Velocity of Instron® Machine was taken v = 0, 3 mm/min as vertical movement and this velocity was kept constant during experiments. Averages of these tests were taken and besides, graph of the results were evaluated in different colors and type for each test. Top and bottom specimen holding apparatuses have coupling ability up to diameter of 12 mm. Special specimen holding apparatus were produced coupling ability diameter of 7 ± 0,5 and 8 ± 0,5 mm special for tests used in this work. Special apparatus machined for tests are shown in Figure 3.11.



(a)



(b)



(c)

Figure 3.11. Special apparatus machined for tests; a) Top view, b) Side view, c) Isometric view (Dimensions are in mm)

3.2.6.2. Hardness Tests

After fatigue and tensile tests, the most important experimental study is hardness tests for evaluation of mechanical properties of material. Vickers Micro-Hardness tests were achieved using Model HV-1000 Micro-Hardness Tester Machine in Machine Experiment Laboratory of Tarsus Technical of Education Faculty in Tarsus/Mersin, Turkey. The Vickers Hardness (HV) number is calculated

by the ratio F/A where F is the force applied to the diamond and *A* is the surface area of the resulting indentation. A can be determined by the formula below:

$$A = \frac{d^2}{2.\sin(136^0/2)} \tag{3.5}$$

which can be approximated by evaluating the sine term to give

$$A \approx \frac{d^2}{1{,}854} \tag{3.6}$$

$$HV = \frac{F}{A} \approx \frac{1{,}854.F}{d^2} \tag{3.7}$$

where

d: the average length of the diagonal left by the indenter, mm

A: surface area of the resulting indentation, mm^2

F: the force applied to the diamond, N

HV: Vickers hardness scale, N/mm^2

The Vickers hardness profile of fractured parts obtained as a result of static tests was measured at five different points and intervals of 3 mm on longitudinal-section using a Vickers intender with a 25 g load for time of 10 s as displayed in Figure 3.12.

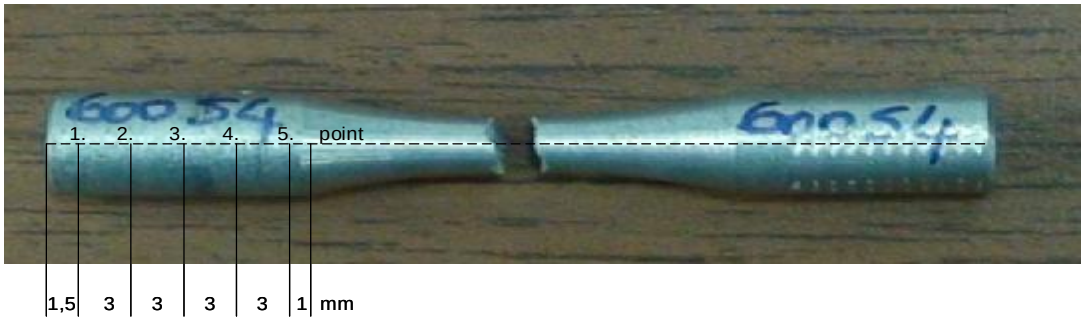


Figure 3.12. Fractured sample during tensile test for Vickers Micro-Hardness experiment

The procedures employed for hardness testing are conducted in accordance

with ASTM E 10-93 (Standard Test Method for Vickers Hardness of Metallic Materials) along the center of the cylindrical samples and the variations in the measured hardness values were plotted by Microsoft Excel® programme.

3.2.7. Microstructure Analysises

In order to analyze the morphology and microstructure of materials which were sintered and shot peened in different conditions, specimens were examined by Optical Microscopy (OM) and Scanning Electron Microscopy (SEM). For this reason, the significant rupture surfaces of materials were prepared by standard metallographic techniques unetched and etched with reagent in order to study the grain structure and allow microscopy characterization of sintered and shot peened materials.

3.2.7.1. Optical Microscopy

Specimen preparation has become a long established art in the optical microscopy of materials, particularly in the fields of metallurgy and mineralogy. The specimens are prepared ideally representative of the structure of interest and free from damage and contamination. In this study, preparation of specimen has five steps and all these steps are illustrated schematically in Figure 3.13. After preparation steps, all specimens investigated with optic microscope and photographed. Preparation and photographing of specimens were managed in TEMSA GLOBAL Sanayi ve Ticaret A. Ş. Calibration Laboratories which has Akreditasyon No: AB-0043-K from Türk Akreditasyon Kurumu (TÜRKAK) in accordance with TS EN ISO/IEC 17025:2005 standard in Adana, Turkey.

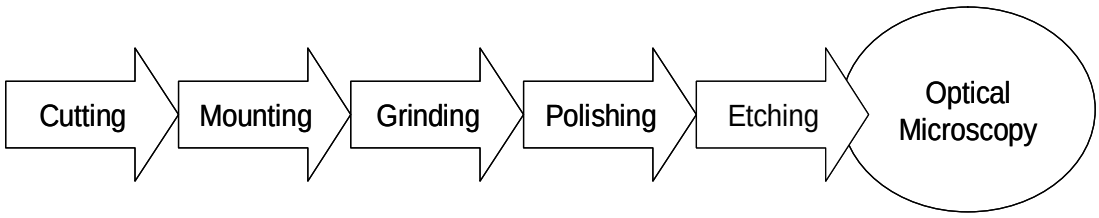


Figure 3.13. Specimen preparation steps for Optical Microscopy (Dilek, 2006)

For cutting operation with a little deformation as possible, a method is required to facilitate and expetide further preparation. Consequently, the most appropriate sectioning method is Abrasive Wet Cutting, which will introduce the least amount of damage on the cut specimens that are sintered and shot peened parts, and specimens were cut with this method. Buehler Abrasive Wet Cutting Test Machine is used in this study.

Mounting of samples are embedded in bakalite to facilitate their handling and improve the preparation result. Specimens that need perfect edge retention or propection of layers require mounting. For the best possible result, samples were cleaned prior to mounting. And, the surface is made free from contaminants for the best possible adhesion of bakalite to sample. Samples are put in to hole on the machine through the plain surface then bakalite powder added. Cover is closed and after machine stared, heating bakalite formed and covered the parts. Buehler (simpliment) Mounting Press Machine is used in this study.

Struers Labopol Polishing Machine is used for grinding and polishing operation. On the grinding sand paper with different abrasive dimensions which are 1000 μm (P1000), 800 μm (P800), 600 μm (P600), 400 μm (P400), 200 μm (P200), 100 μm (P100) is used, respectively. Specimens are polished with polishing machine on the different layer. Struers Labopol Polishing and Grinding Machine are used in TEMSA GLOBAL Sanayi ve Ticaret A. Ş. Calibration Laboratories.

Finally, two different mediums were conducted impending unetched and etched. Etching process was executed according to TSE CR 12361/April 1999 (Destructive Tests on Welds in Metallic Materials- Etchants for Macroscopic and Microscopic Examination) standard. All etched specimens were performed by Keller's reagent that has a mixture of nitric acid (25 ml, HNO_3), hydrochloric acid

(15 ml, HCl), and hydrofluoric acid (10 ml, HF) and water (950 ml, H_2O), is used to etch aluminum alloys to reveal their grain boundaries and orientations for etching time of a few seconds at RT. As the latest: Microscopic Images of unetched and etched parts were attained by Olympus PME3 Microscope in TEMSA GLOBAL Sanayi ve Ticaret A. Ş. Calibration Laboratories.

3.2.7.2. Scanning Electron Microscopy

The Scanning Electron Microscopy is commonly used to examine the microstructure of bulk specimens. It is an electron optical instrument which uses a source of electrons to illuminates the specimen. These electrons are accelerated down the column and pass through a combination of electromagnetic lenses and apertures to form a fine probe at the surface of the specimen in the chamber area. Both the column and the chamber are held under vacuum to avoid high voltage discharge and scattering of the electrons along their path by residual gas atoms. A variety of signals are produced as a result of the interaction of the beam with the specimen, which may be collected by appropriated detectors. There is a trade off between good count rate and low noise images and ability to see very fine specimens detail (Mccall and Mueller, 1973).

In order to obtain well researchable images from the parts, compacted specimens were broken and cracked surfaces were investigated. Plastic and elastic particle deformations, effects of cracks can be seen easily with SEM photos. SEM investigations are organized in Nigde University Mechanical Research Laboratories in Nigde/Turkey and Carl Zeiss AG - EVO® 40 Series Computer Controlled Digital Scanning Electron Microscope is used in this study.

4. RESULTS AND DISCUSSION

4.1. Evaluation of Physical, Chemical, Metallurgical and Mechanical Properties

4.1.1. Evaluation of Density Measurements

In this study, sintering process was carried out at 600 °C and 620 °C temperatures. Compaction process was executed constant pressure of 400 MPa and at RT. First, after compaction process, green densities were obtained 2,53 g/cm^3 evaluating average of fifteen specimens pressed at 400 MPa. Then, sintered densities were measured 2,42 and 2,50 g/cm^3 the average of fifteen specimens at 600 °C and 620 °C, respectively. Green and sintered densities were measured in pure water using Archimedes Principle as seen in Table 4.1.

Table 4.1. Density values of prismatic samples compacted with axial die at RT formed from the Alumix 431

Theoretical density (TD), g/cm^3	Compression pressure, MPa	Green (Pressed) density, g/cm^3	Sintering conditions	Sintered densities, g/cm^3
			Atmosphere: N_2 Heating rate: 5 ºC/min, 600 ºC Cooling rate: 5 ºC/min, 600 ºC Sintering time: 60 min, 600 ºC, No.1	2,42
2, 786	400	2,53	Atmosphere: N_2 Heating rate: 5 ºC/min, 620 ºC Cooling rate: 5 ºC/min, 620 ºC Sintering time: 60 min, 620 ºC, No.2	2,50

Increasing temperature causes higher density in sintered parts because of reducing pores. When pores reduce, particles are yielded and volume is decreased. Therefore, the density is increased. Densities of No.1 and No.2 samples are different despite of fact that temperature raises a small difference such as 20 ºC. Hence, No.2 have higher density than No.1. Besides, as comparison of theoretical and sintered densities, No.1 and No.2 have approximately 86%, 90% of theoretical density, respectively. Consequently, sintering density increased roundly 5% on account of increase of temperature. Results show clearly that the sintered densities under N_2

protective gaz atmosphere were marginally lower the green densities even increasing sintering temperature. This is because of fact that the porosity was not completely eliminated, despite it was significantly reduced.

4.1.2. Evaluation of Tensile and Hardness Test

In the present study, all Al sintered powder parts were subjected to tensile test after sintering and shot peening process. All samples are symbolized for definition of samples according to conditions as temperatures 600 ºC (designaed as 'A') and 620 ºC (designaed as 'B'); as process sintered (designaed as 'S') and shot peened (designated 'P') as shown in the Table 4.2. Each samples for tensile test have test length of 20 mm, test diameter of 5 mm, shoulder diameter of 8 mm and the the total size of 33 mm.

Table 4.2. Symbols of material used in this work

A	states material sintered at 600 ºC
B	states material sintered at 620 ºC
S	states only sintered of material
P	states shot peened after sintered of material
Numbers	states sequence of material

The Vickers hardness tests were conducted using the static (tensile) test parts to assess according to sintering temperature on surface of specimens. The hardness tests were performed with the averages of five measurement points for each specimen at intervals of 3 mm. The variations in the measured hardness values are respectively plotted in Figure 4.1-4.3.

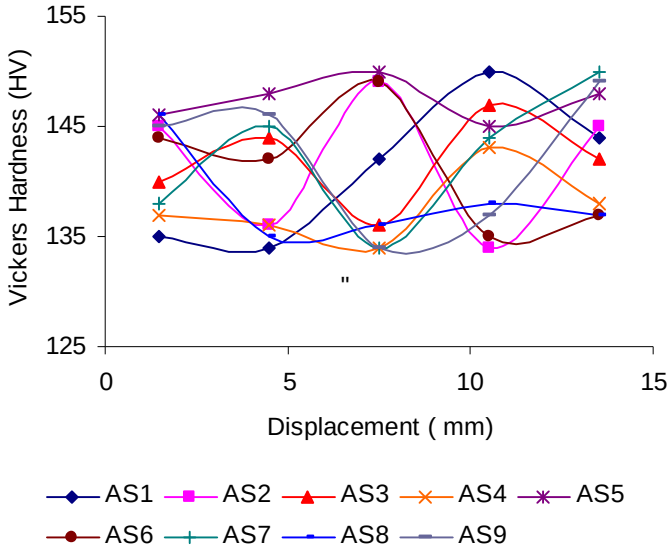


Figure 4.1. The variations in hardness for sintered specimens at 600 ºC

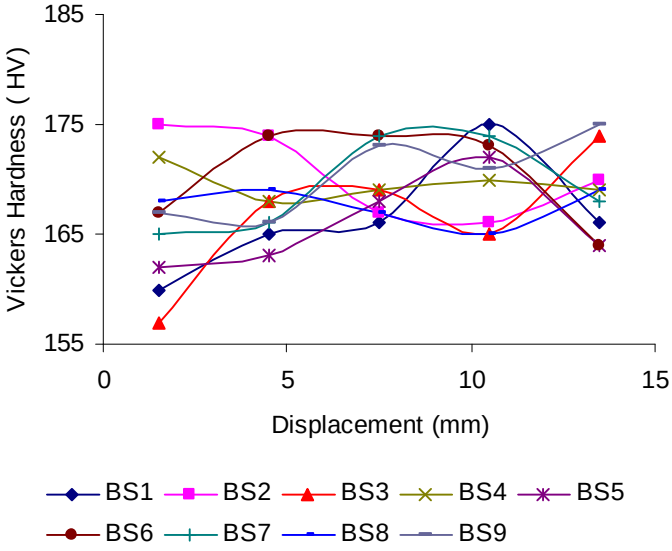


Figure 4.2. The variations in hardness for sintered specimens at 620 ºC

As sintering temperature from 600 ºC to 620 ºC increases, homogenization of the microstructure occurs. Nevertheless, poor bonding between the powder particles is strengthened and porosity content that is the most important properties of PM decreases even if the density increases slightly. For reason, the microhardness values were increased from 141 to 168 HV for No: 1 (AS) and No: 2 (BS) samples because of fact that pore voids was closed as can be seen in Figure 4.3, respectively. In

addition, the hardness distribution on each part was showed roughly homogeneous values and was mainly governed both density of material and the pore content.

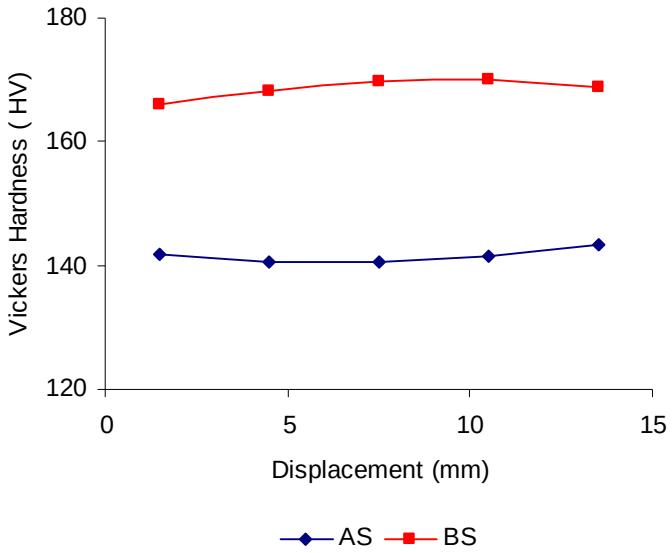


Figure 4.3. Comparison of the variations in hardness for sintered specimens at 600 and 620 ºC

The tensile behaviour of Alumix 431 material which was peened and unpeened was examined by conducting tensile tests on specimens of each type. Velocity of 0, 3 mm/min for the tensile test was kept constant in the entire tensile test. Each experiment was repeated 3 times and the average value was accepted for tensile strength. Tensile test values were plotted as shown in Figure 4.4-4.8. As tensile tests indicate a little plastic region in accordance with characteristic of Alumix 431 powder because of fact that graphics of all tensile have slightly slope as horizontal as can be seen in Figure 4.4-4.8, extension at break were represented at maximum load. That is, the datas for yield strength could not be obtained from tensile tests. Table 4.3 shows characteristic properties of used specimens according to the datas obtained from this study. In the hardness results, the hardness was increased because of fact that the density was raise. Sintering and shot peening processes were provided the density increases. The more density rise, the more tensile strength increases as stated in literature. Therefore, the ultimate tensile strength were indicated slowly increase in accordance with sintering temperature and

shot peening intensity as shown in Figure 4.8. Also, these are seen as 132, 157, 170 and 185 MPa in Table 4.3, respectively.

Table 4.3. Characteristic properties of used specimens

Conditions	Sintered Density, (ρ) g/cm^3	Young's Modulus(E), GPa	Ultimate Tensile strength (UTS), MPa	Strain (A), %	Hardness (HV), MPa
AS	2,42	36	132	0,24	141
AP	-	40	157	0,36	-
BS	2,50	46	170	0,57	168
BP	-	52	185	0,63	-

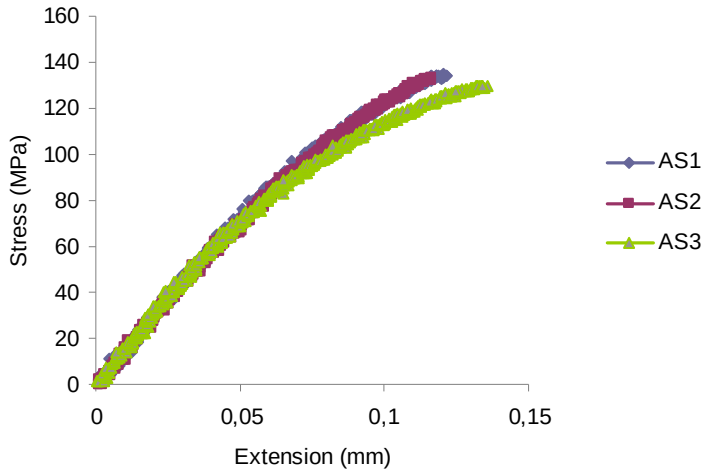


Figure 4.4. Tensile stress curves of samples sintered at 600 ºC

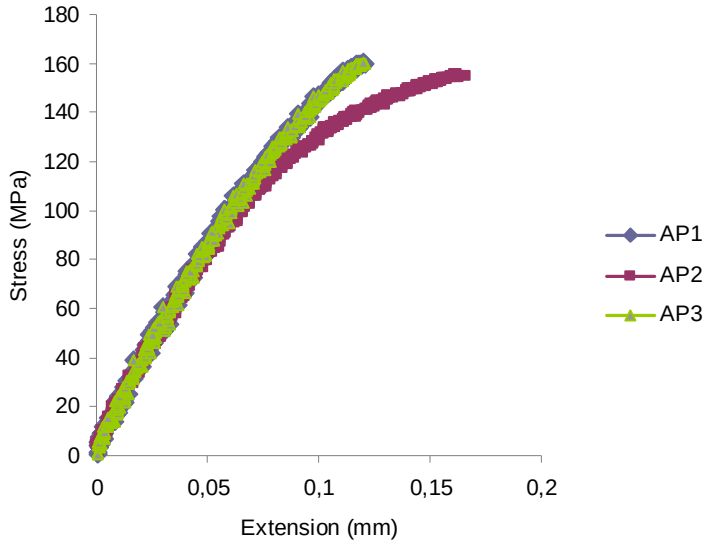


Figure 4.5. Tensile stress curves of samples shot peened at 600 ºC

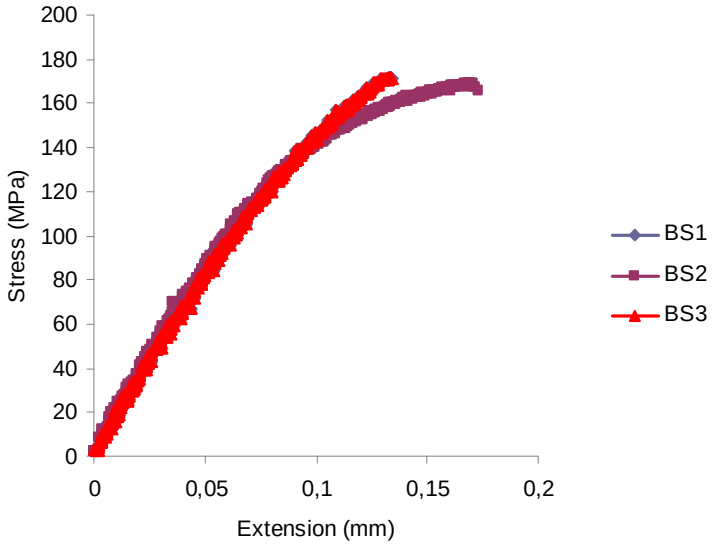


Figure 4.6. Tensile stress curves of samples sintered at 620 ºC

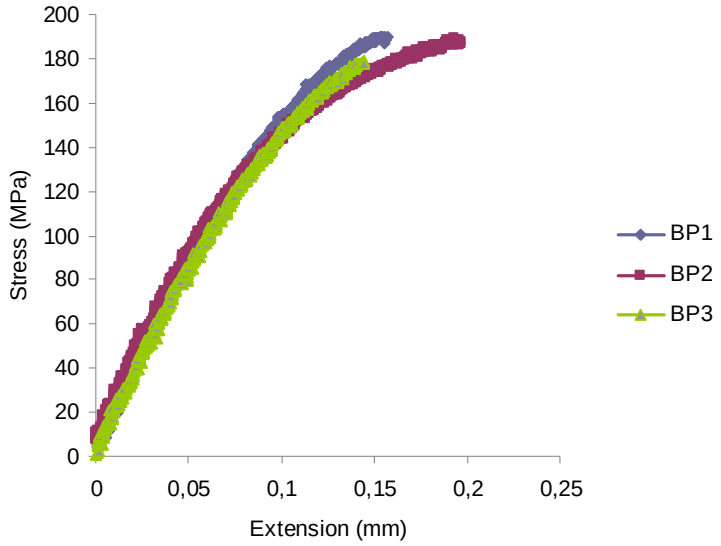


Figure 4.7. Tensile stress curves of samples shot peened at 620 ºC

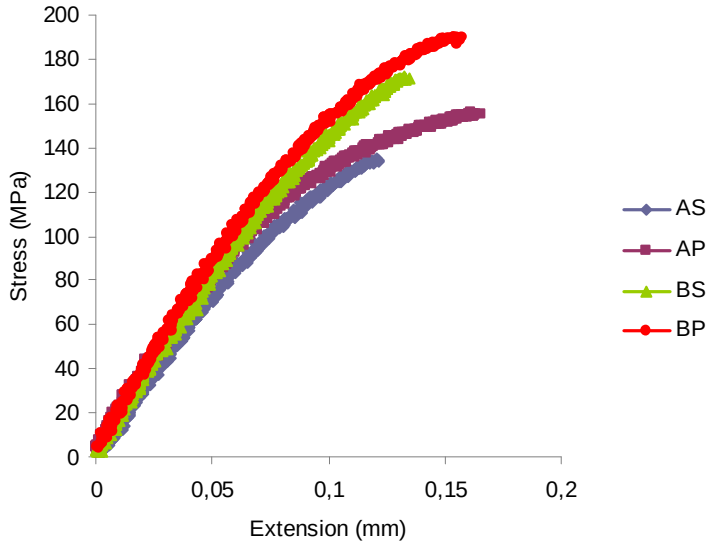


Figure 4.8. Comparison of tensile stress curves

4.1.3. Evaluation of Fatigue Test

All the tests were conducted to failure and the specimen design respects the standard requirements. Successively, the significant rupture surfaces were prepared by standard metallographic techniques and etched with Keller's reagent, in order to

study the grain structure of the sintering material and to allow Optical Microscopy and Scanning Electron Microscopy characterization.

For the values resulted of axial fatigue tests, Wöhler curves were plotted correspond the greatest cycle values by Microsoft Excel® program. The fatigue test machine including clamping of the specimen used in this investigation is seen in Figure 3.10b. Datas for the determination of each S-N curves are shown in Figure 4.9-4.15 and Table 4.4-4.7. Average stresses in the interval of 30–120 MPa were tested. The Wöhler curves, presented in terms of Nominal stress to amplitude $\sigma_{a,n}$ and Cycles to rupture N_R, were statically evaluated. In all tests, cycle number have been constant to be $N_R = 2x10^6$ as boundary cycle number that proposed in literature (Dilek, 2006) and run-out was defined as no failure after $2x10^6$ fatigue cycles.

Table 4.4. S-N datas for all unpeened specimens at 600 ºC

Specimen no	Condition	S, stress to failure (MPa)	N, cycles to failure (Number)	Observation
AS1	unpeened	100	1205	Failed
AS2	unpeened	95	3050	Failed
AS3	unpeened	90	5761	Failed
AS4	unpeened	85	7846	Failed
AS5	unpeened	80	8002	Failed
AS6	unpeened	75	15029	Failed
AS7	unpeened	70	20306	Failed
AS8	unpeened	65	50203	Failed
AS9	unpeened	60	110303	Failed
AS10	unpeened	55	245457	Failed
AS11	unpeened	50	528000	Failed
AS12	unpeened	45	890078	Failed
AS13	unpeened	40	1507802	Failed
AS14	unpeened	35	2005905	Run-out
AS15	unpeened	30	2500873	Run-out

Table 4.5. S-N datas for all unpeened specimens at 620 ºC

Specimen no	Condition	S, stress to failure (MPa)	N, cycles to failure (Number)	Observation
BS1	unpeened	105	1316	Failed
BS2	unpeened	100	3145	Failed
BS3	unpeened	95	6578	Failed
BS4	unpeened	90	11404	Failed
BS5	unpeened	85	9678	Failed
BS6	unpeened	80	17576	Failed
BS7	unpeened	75	23456	Failed
BS8	unpeened	70	34567	Failed
BS9	unpeened	65	78005	Failed
BS10	unpeened	60	268886	Failed
BS11	unpeened	55	479903	Failed
BS12	unpeened	50	923445	Failed
BS13	unpeened	45	1606005	Failed
BS14	unpeened	40	2139067	Run-out
BS15	unpeened	35	2590873	Run-out

Table 4.6. S-N datas for all peened specimens at 600 ºC

Specimen no	Condition	S, stress to failure (MPa)	N, cycles to failure (Number)	Observation
AP1	12A	115	1265	Failed
AP2	12A	110	3150	Failed
AP3	12A	105	5690	Failed
AP4	12A	100	7856	Failed
AP5	12A	95	8040	Failed
AP6	12A	90	16029	Failed
AP7	12A	85	20050	Failed
AP8	12A	80	50030	Failed
AP9	12A	75	110608	Failed
AP10	12A	70	245457	Failed
AP11	12A	65	528000	Failed
AP12	12A	60	890078	Failed
AP13	12A	55	1507800	Failed
AP14	12A	50	2005900	Run-out
AP15	12A	45	2600870	Run-out

Table 4.7. S-N datas for all peened specimens at 620 ºC

Specimen no	Condition	S, stress to failure (MPa)	N, cycles to failure (Number)	Observation
BP1	16A	120	1405	Failed
BP2	16A	115	3256	Failed
BP3	16A	110	5769	Failed
BP4	16A	105	7745	Failed
BP5	16A	100	8242	Failed
BP6	16A	95	16029	Failed
BP7	16A	90	22067	Failed
BP8	16A	85	52307	Failed
BP9	16A	80	120607	Failed
BP10	16A	75	239486	Failed
BP11	16A	70	528055	Failed
BP12	16A	65	880078	Failed
BP13	16A	60	1547878	Failed
BP14	16A	55	2005900	Run-out
BP15	16A	50	2646878	Run-out

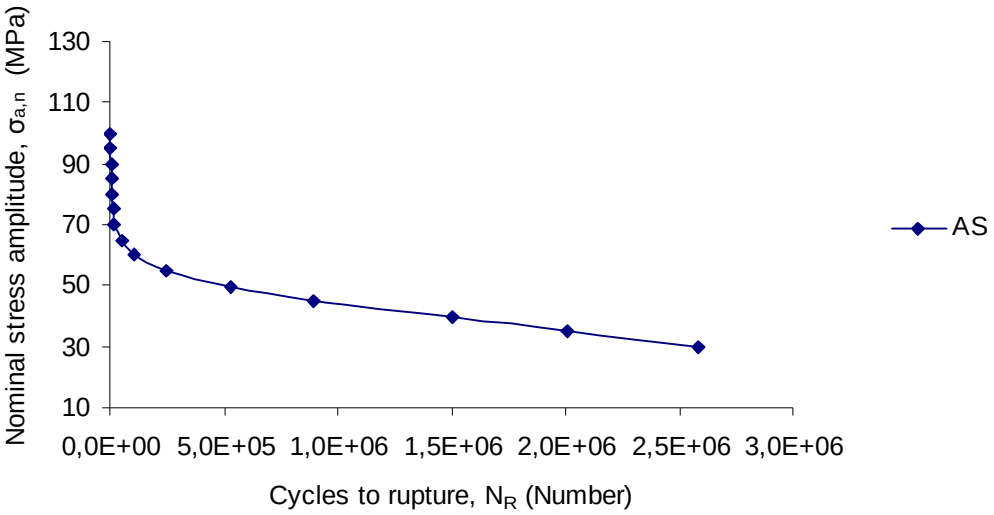


Figure 4.9. S-N curves for all unpeened specimens at 600 ºC

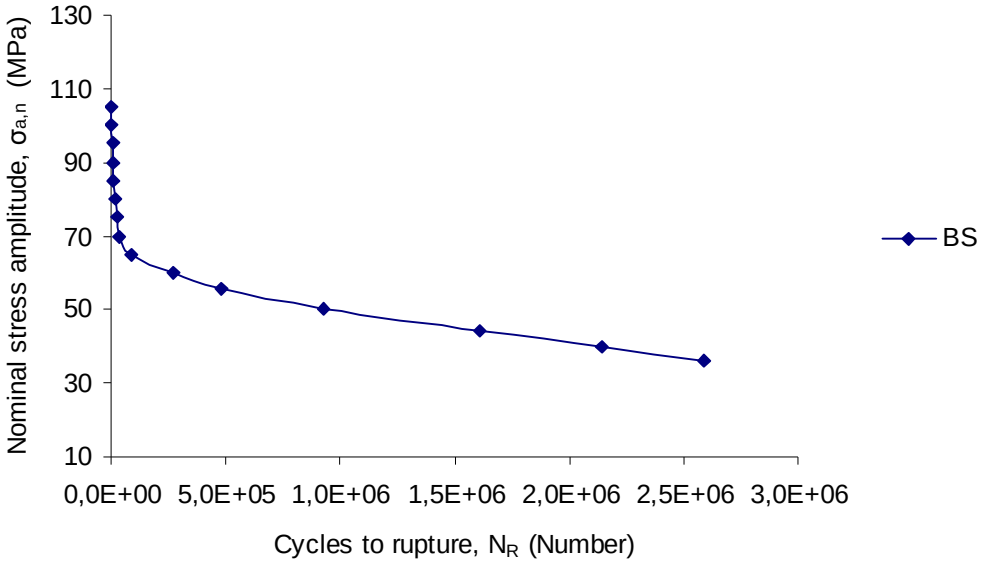


Figure 4.10. S-N curves for all unpeened specimens at 620 ºC

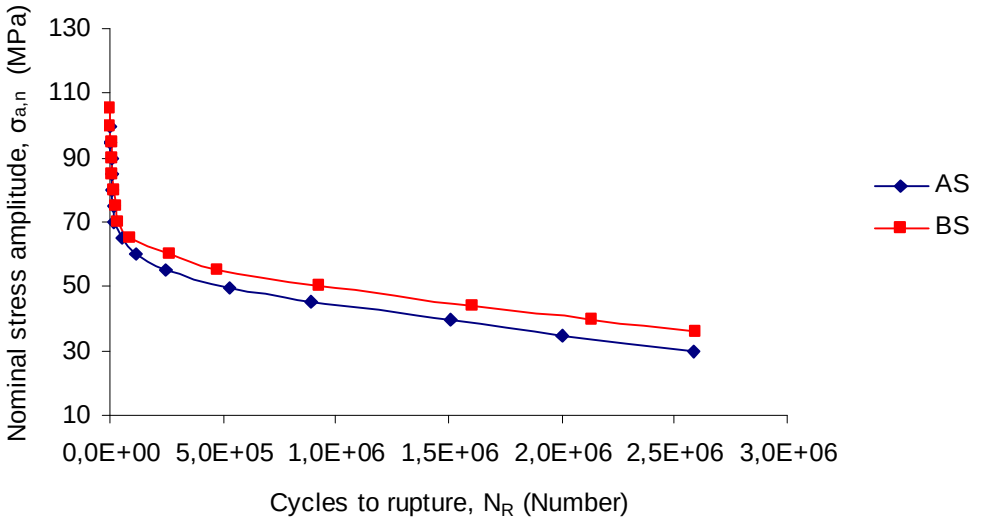


Figure 4.11. Comparison of S-N curves for all unpeened specimens at 600 ºC and 620 ºC

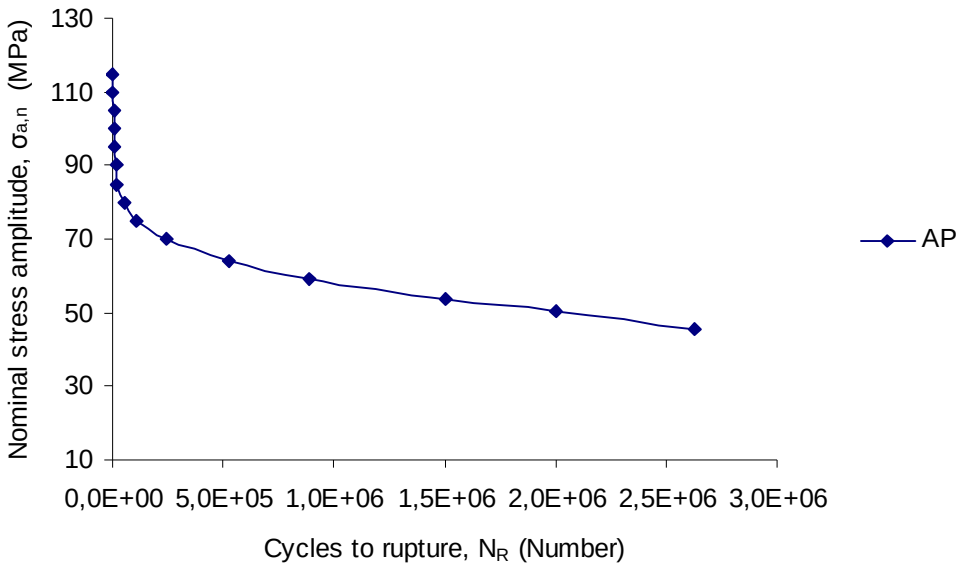


Figure 4.12. S-N curves for all peened specimens at 600 ºC

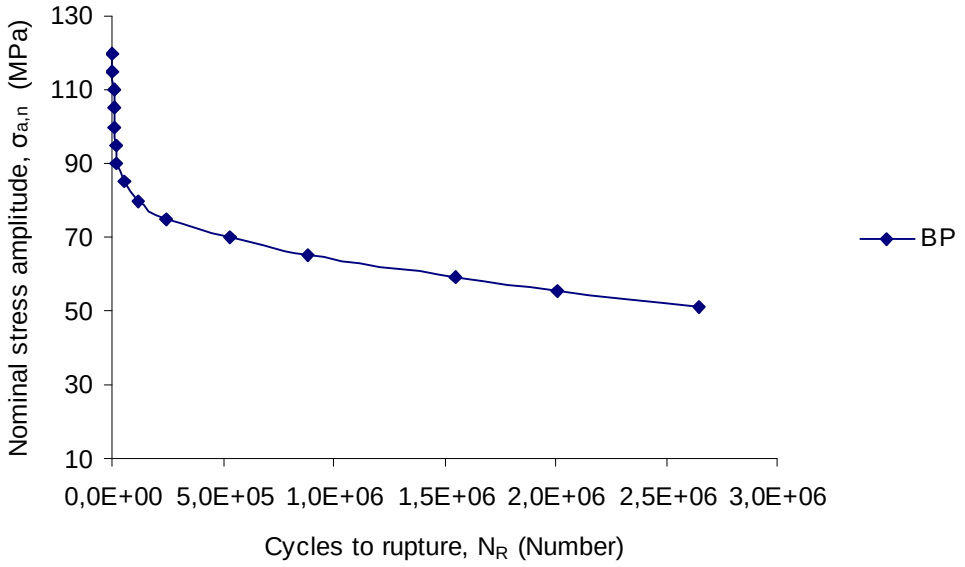


Figure 4.13. S-N curves for all peened specimens at 620 ºC

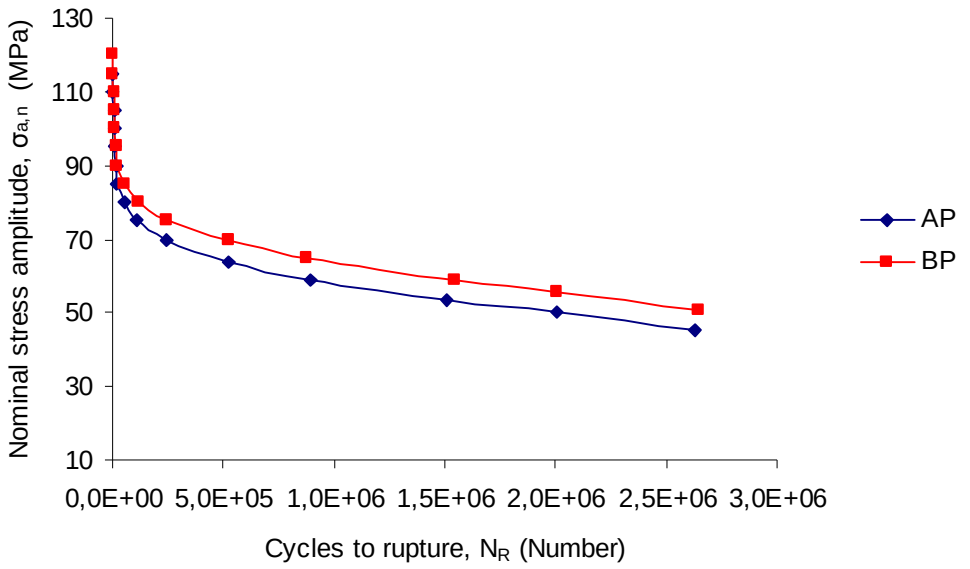


Figure 4.14. Comparison of S-N curves for all peened specimens at 600 ºC and 620 ºC

In this study, the effect of shot peening on fatigue life of Alumix 431 aluminium alloys was investigated. To assign the effect of peening on the fatigue strength, the fatigue samples were shot peened in various intensities. It is known that residual compressive stress on the surface has the effect of increasing the fatigue strength of materials. In addition, shot peening causes residual compressive stress on the surface of material. In other words, because of fact that surface intensity of material rises and also, weight is usually steady, whole density of material increases. Hence, it has improvement in fatigue strength depending compressive residual stress and peening intensity. The fatigue results for unpeened and peened conditions were compared. As mentioned in literature, it was seen that shot peening improved fatigue life by about 10%, 15% using 12A, 16A intensities according to sintered material as displayed in Figure 4.15, respectively. Fatigue strength increased from 100 MPa for unpeened specimens to maximum of approximately 115 MPa for the specimens peened to 12A and from 105 MPa for unpeened specimens to maximum of approximately 120 MPa for the specimens peened to 16A at this the same as shown in Figure 4.15. It was thought that shot peening was improved fatigue strength because of compressive residual stress and rising of peening intensity.

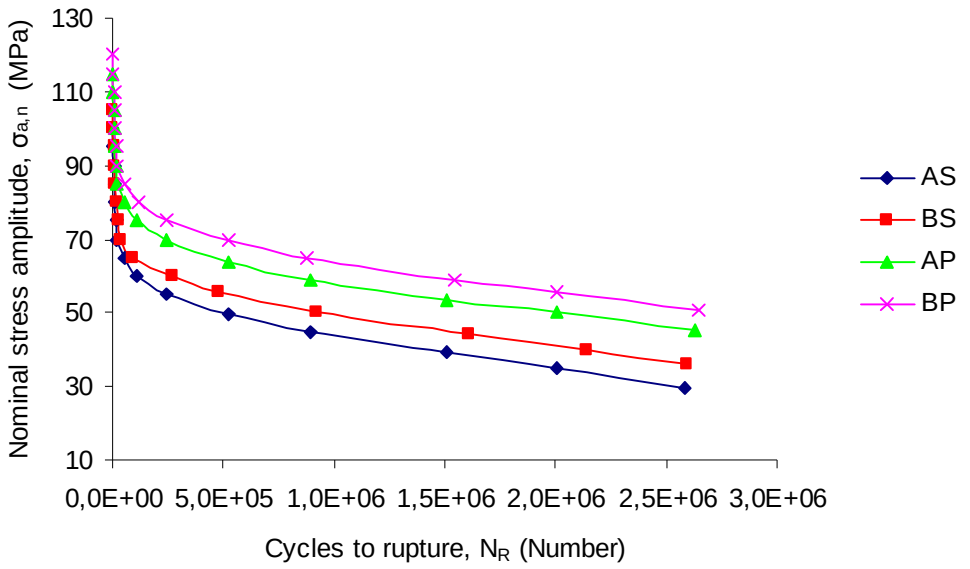


Figure 4.15. Comparison of S-N curves for all peened and unpeened specimens

4.1.4. Evaluation of Optical Microscope Images

Optical Microscopy observations have been done on the sintered at 600 ºC and 620 ºC and shot peened in 12A and 16A intensities materials. These processes were observed getting part of 5mm from shoulder section of samples as displayed in Figure 4.16. Etched and unetched Al parts photographed to investigate for this study. Optical photographs are taken in 50X and 100X scales from optic microscope with video capture. General pore structures on the surface can be seen clearly with 100X scaled photographs. Structure of sintered Al alloys is shown in Figures 4.17-4.20.

As seen in the sintering Figures, structures are become homogeneous and pores between the powder particles are reduced with increasing from 600 ºC to 620 ºC temperature. Also, grain boundaries appeared notably in Figures 4.18b, 4.20b. Grain necks are constituted notably and homogeneous structure obtained. In addition, smooth and less porosity surface can be seen due to increasing of sintering temperature in Figures 4.18, 4.20. Because of sintering treatment, pore structures change and thus, micro and macro pore structures occur. Macro and micro pore structures are signed on Figures 4.18b, 4.20b.

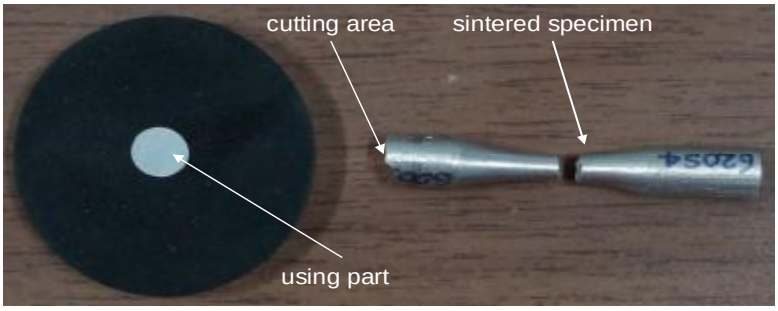
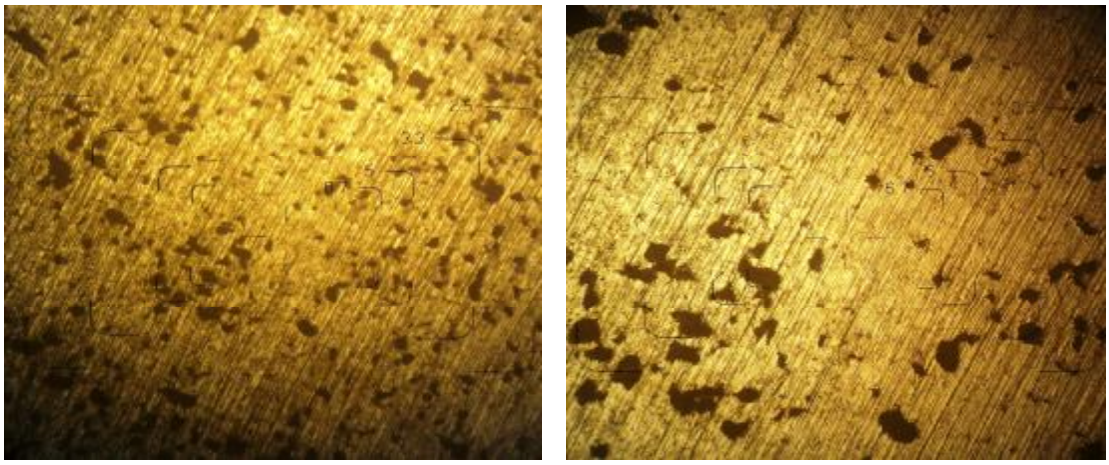
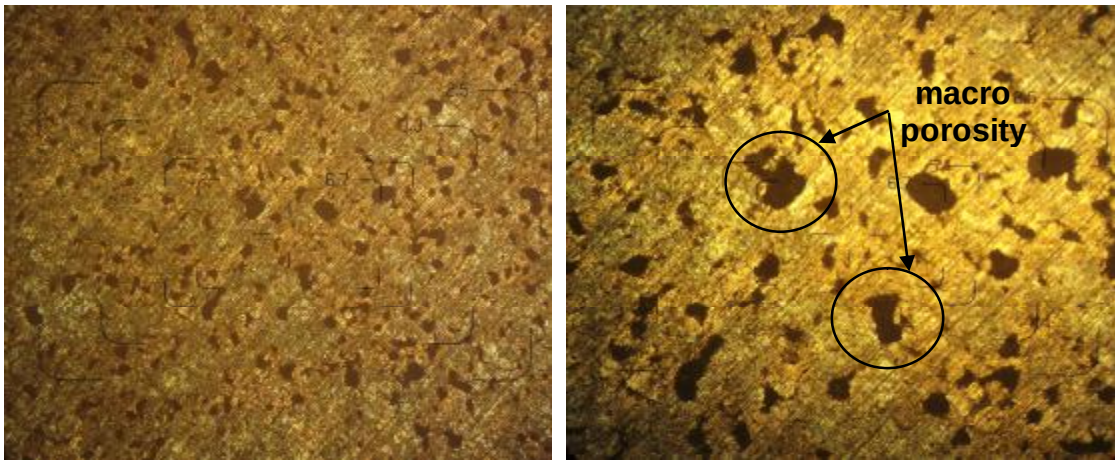


Figure 4.16. Sintered specimen prepared in bakalite for Optical Microscope Images



(a) (b)

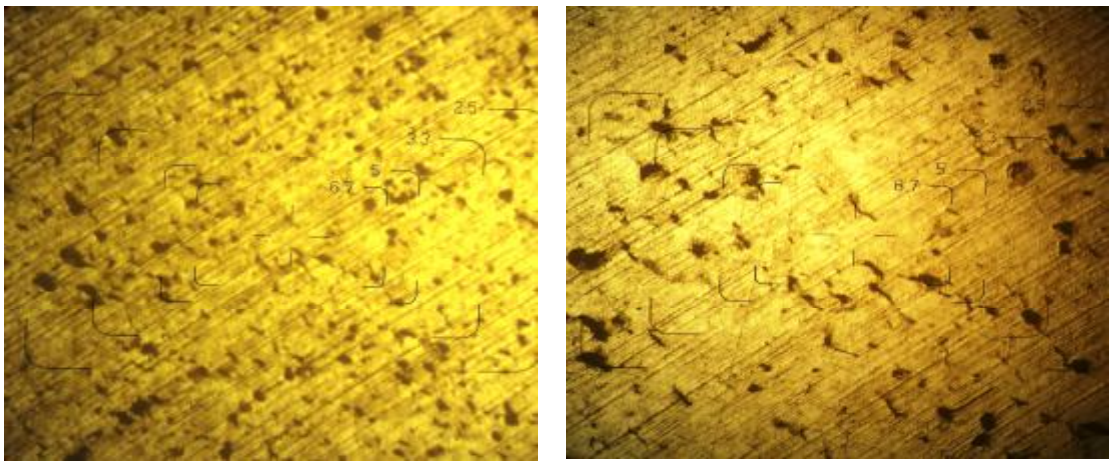
Figure 4.17. Optical Microscope analysis of unetched only sintered parts at 600 ºC; a) 50X, b) 100X



(a) (b)

Figure 4.18. Optical Microscope analysis of etched only sintered parts at 600 ºC; a) 50X, b) 100X

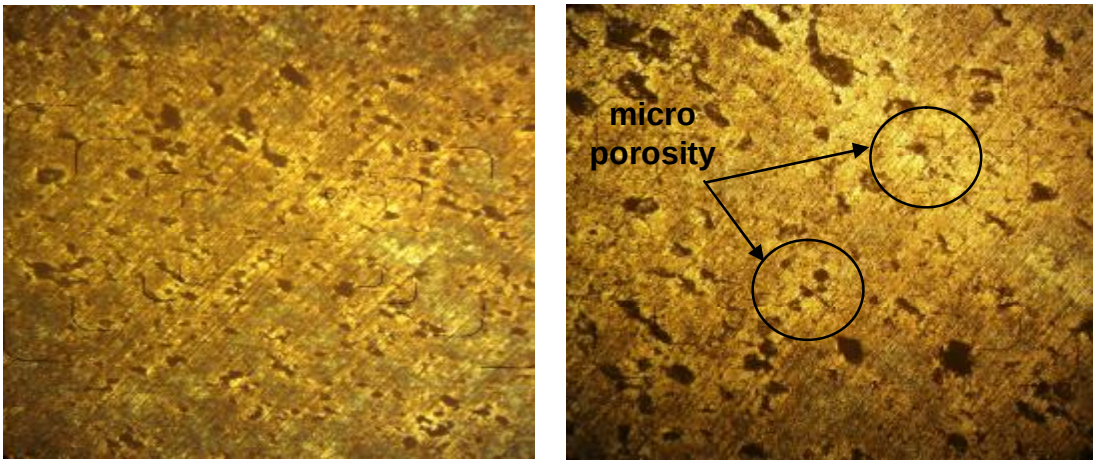
The sintering results show that as the sintering temperature is increasing from 600 ºC to 620 ºC, the sintered density increases because of more particle bonding and presence of fewer voids as more clearly seen in etched Figures 4.18b and 4.20b. Comparing the microstructure of sintered parts at 600 ºC and 620 ºC temperatures, it is obvious that a more uniform porosity and smaller pore size at 620 ºC in spite of high temperature as signed in Figures 4.18b and 4.20b. Also, a better homogeneity of the alloying elements is visible and besides, less precipitatios at the grain boundaries.



(a) (b)

Figure 4.19. Optical Microscope analysis of unetched only sintered parts at 620 ºC; a) 50X, b) 100X

From that point of view, it can be seen from sintering Figures that while the sintering temperature increases; pores are closed during sintering treatment and are eventually reduced or eliminated in pore of size or content. On the one hand; in spite of fact that pores structures are minimized more clearly as shown in sintering Figures, volume shrinkage increases. Thus, weight gain occurs and the sintered density increases. These are an advantages in terms of material properties. That is; the bigger the weight gain, the higher the sintered density and the larger the weight gain, the larger the sintering shrinkage as mentioned in literature.

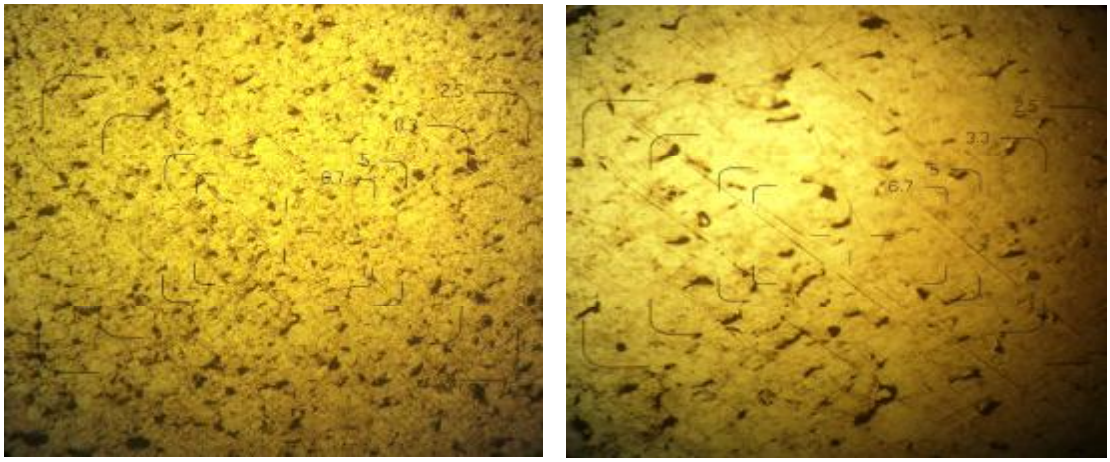


(a) (b)

Figure 4.20. Optical Microscope analysis of etched only sintered parts at 620 ºC; a) 50X, b) 100X

On the other hand; if present pore structures formed in material are evaluated according to mechanical properties, poor bonding between the powder particles and present pore content is strengthed because of sintering temperature and filling of pores. Therefore, the structure of homogeneous of material was leaded to a better strength values as explained in tensile and fatigue evaluations. As a result, the strengths should rise as sintered density increase or as the porosity content decreases.

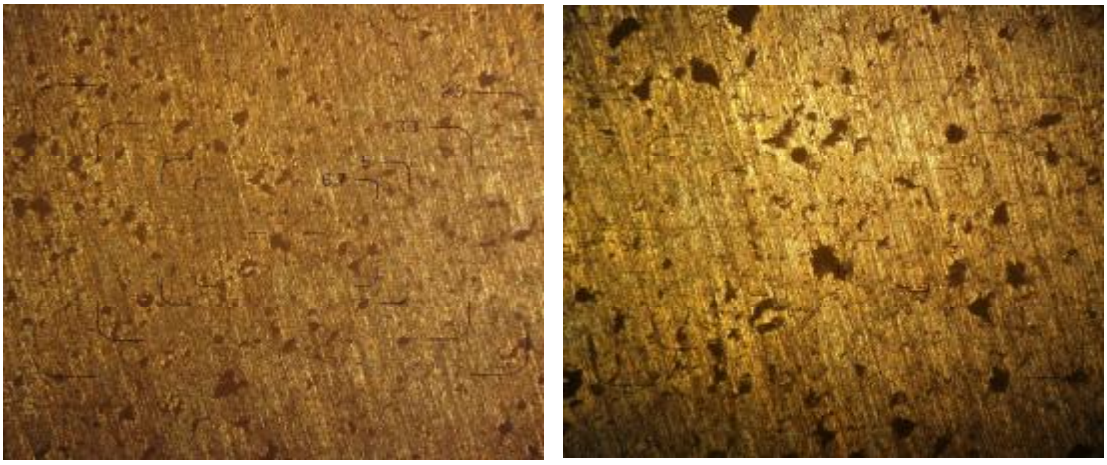
To define the improvement resulted from shot peened, it was done a work to compare the fatigue behaviour of some unpeened specimens with that one of those shot peened. Also, to investigate influence of shot peening on the microstructure, optical microscope analysises were prepared on shot peened parts and shot peened parts were photographed by Optical Microscopy as shown in etched and unetched Figures 4.21-4.24.



(a) (b)

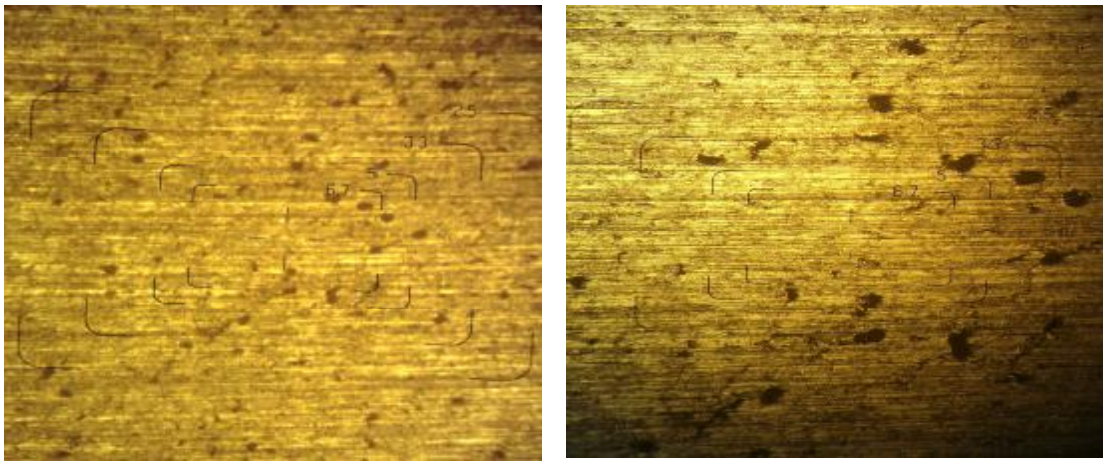
Figure 4.21. Optical Microscope analysis of unetched shot peened parts in 12A intensity at 600 ºC; a) 50X, b) 100X

As displayed in shot peening Figures 4.21-4.24, there is deformation state of the surface as a function of the shot peening for the tested specimens. Because of the shot peening, on the specimen surfaces will appear a densification and deformation of the grains as well as an improving of the surface roughness obviously as shown in etching Figures 4.22b and 4.24b. It is well known that shot peening process allows densification at and under surface of material owing to compressive residual stress formed on material. In addition, with rising of peening intensity, surface intension of shot peened material increases if peening intensity rise not over as mentioned in literature in accordance with used material properties. This situation improves strength in favour of material as an advantage.



(a) (b)

Figure 4.22. Optical Microscope analysis of etched shot peened parts in 12A intensity at 600 ºC; a) 50X, b) 100X

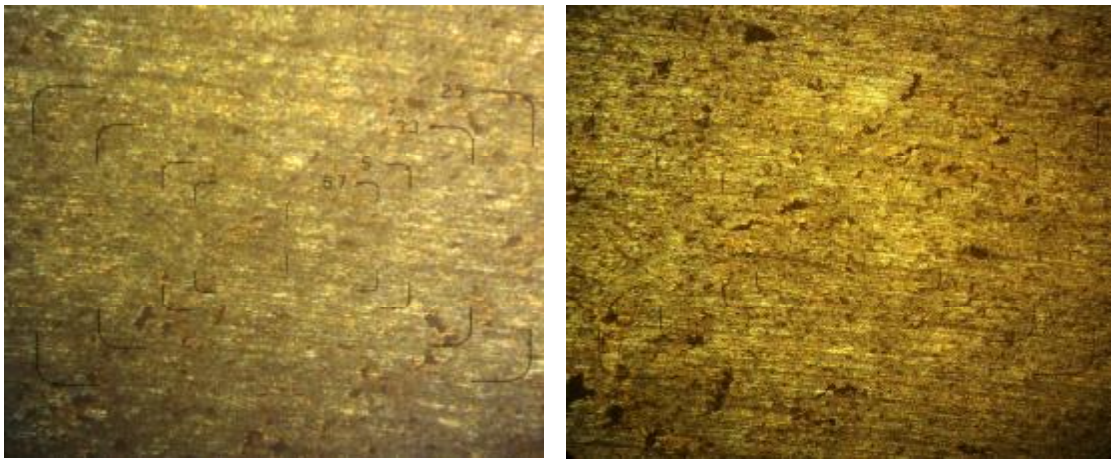


(a) (b)

Figure 4.23. Optical Microscope analysis of unetched shot peened parts in 16A intensity at 620 ºC; a) 50X, b) 100X

As shot peened specimens are comparing according to 12A and 16A intensities, the surface was more deformed and densification occurred closing pores for the higher peening intensity as can be seen in Figures 4.22b and 4.24b. As indicate in literature, mechanical properties depend on pore of quantity, size, shape, distributions and to be bonding each other. Figure 4.24b has more intense microstructure at 16A intensity than shown in Figure 4.22b at 12A intensity. Thus, as explained in mechanical properties evaluations; when shot peening intensity

increases, strength of material improves.



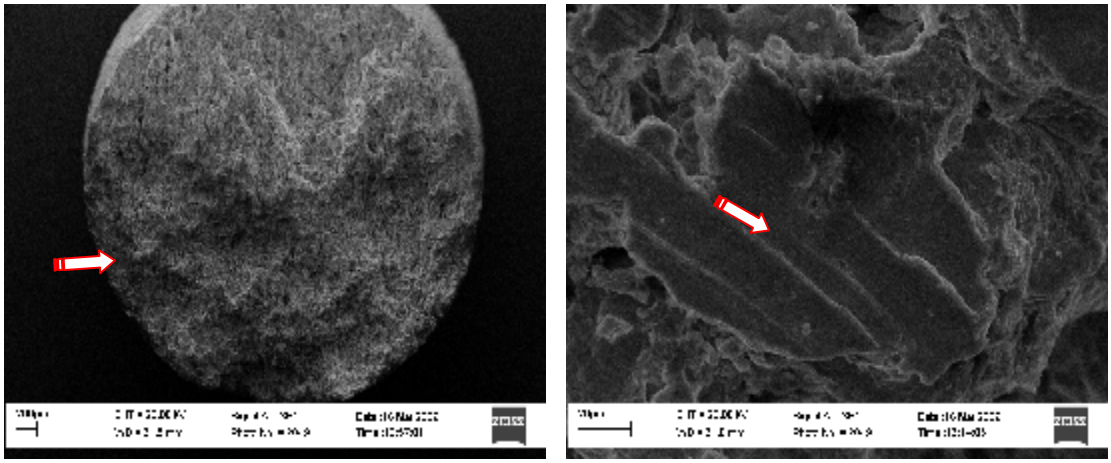
(a) (b)

Figure 4.24. Optical Microscope analysis of etched shot peened parts in 16A intensity at 620 ºC; a) 50X, b) 100X

4.1.5. Evaluation of Scanning Electron Microscope Images

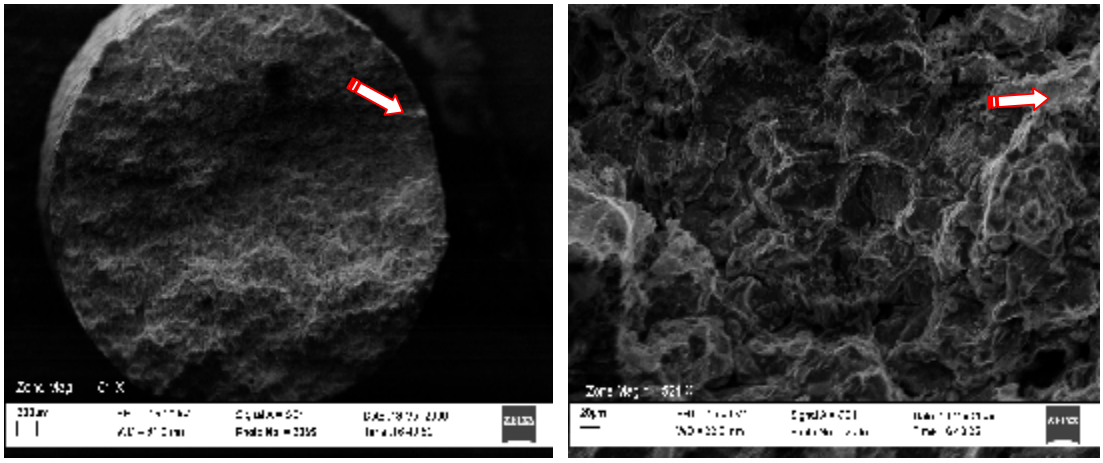
The Scanning Electron Microscope images of the fatigue specimens are used 50X to 500X scales in this investigation after sintering and shot peening process. The sintered and shot peened Alumix 431 specimens are examinated as shown in Figures 4.25-4.28 and it is enough to show the structure clearly.

In order to identify the zones of crack propagation, final rupture of fatigue test specimens under fully reversed loading were conducted. Fatigue cracks were initiated at the large pore area. They started sometimes at the sintered and the shot peened surface or a point shot peened surface below. The final rupture is ductile and shows dimples as displayed in SEM images. These crack initiations and zones predicted are signed with arrows on the SEM Figures.



(a) (b)

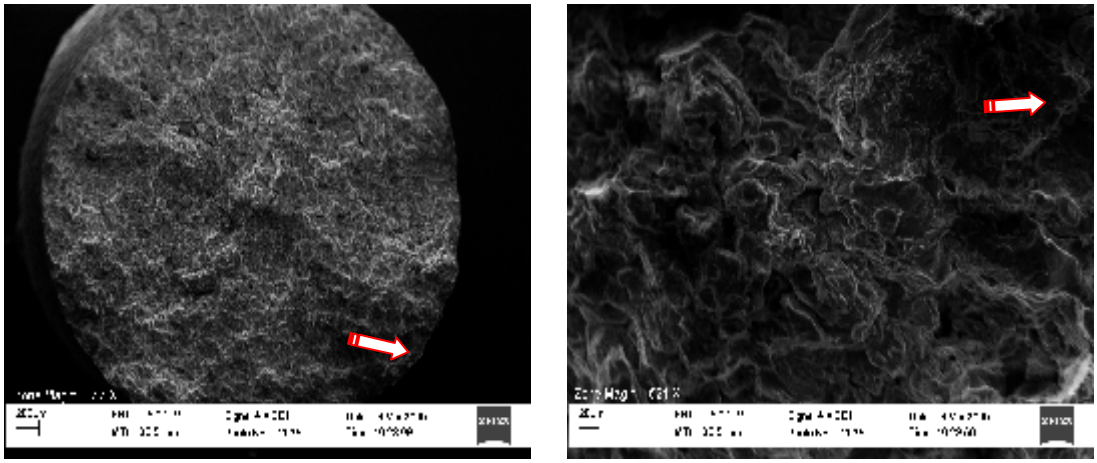
Figure 4.25. SEM views of fracture surface of unpeened specimen at 600 ºC; a) 50X, b) 500X



(a) (b)

Figure 4.26. SEM views of fracture surface of peened specimen at 600 ºC in 12A; a) 50X, b) 500X

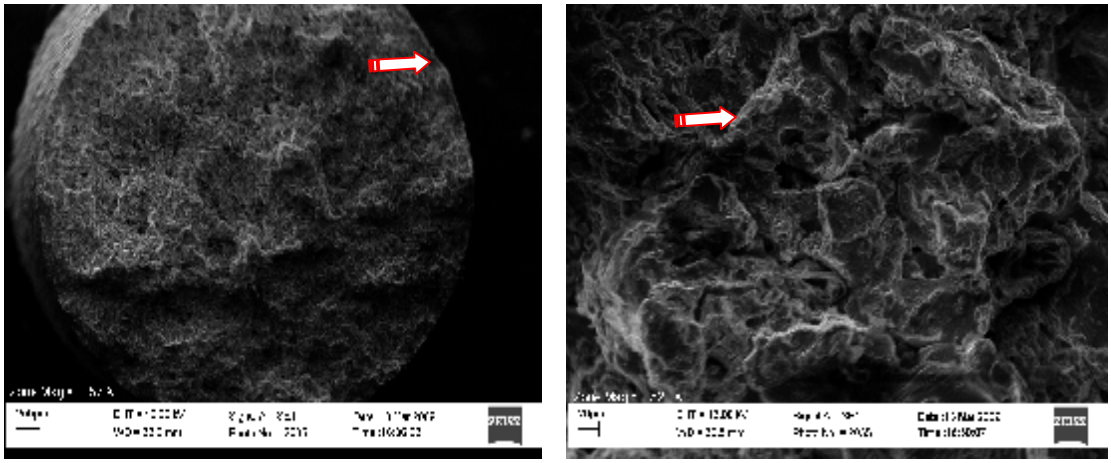
It is known that most of the pores in the surface layers are closed due to plastic deformation induced by shot peening. Shot peening contrubutes to the densifications of the porous surface and is more resistant to pore opening. As may be seen in SEM Figures, surface of peened sample has more intensitive structure than unpeened sample. Fracture surfaces of sintered and shot peened Alumix 431 materials show a familiar surface for PM materials where cracks propagate from powder particle boundaries as may seen in Figures 4.25-4.28.



(a) (b)

Figure 4.27. SEM views of fracture surface of unpeened specimen at 620 ºC; a) 50X, b) 500X

As mentioned in literature, in general, fatigue crack initiation occurs on the surface or points beneath the compressive residual stress zone and in addition, on the surface of material. In this study, fractured surface of used specimens for the fatigue experiments show obviously the effect of sintering and shot peening. Sometimes, crack sources are pushed under surface of material due to effect of compressive residual stress created by shot peening. Crack initiation points take places many times from surface and many times beneath surface as shown with arrow in SEM Figures. This crack initiation points and zones formed because of effects of sintering and shot peening processes were estimated.



(a) (b)

Figure 4.28. SEM views of fracture surface of peened specimen at 620 ºC in 16A; a) 50X, b) 500X

5. CONCLUSION AND FUTURE STUDIES

5.1. Conclusion

In the present work, Alumix 431 aluminum alloys have been successfully machined and experimental studies have been carried out to evaluate the effect on the behaviour of material by sintering and shot peening operations. The following processes have been applied. Also, conclusions were formed and proposal for further work are recommended.

i. Al powders have been pressed at 400 MPa, RT and prismatic blocks have been performed.
ii. Al powders have been sintered at 600 ºC and 620 ºC temperatures after pressing process. Densities have been measured for specimen of each type. Then, evaluations have been done.
iii. Aluminum alloy specimens have been successfully sintered at 600 ºC and 620 ºC temperatures and shot peened in intensities of 12A and 16A separately. These specimens have been subjected to tensile test. The tensile behaviors of sintered and shot peened Al powder specimens have been examined by conducting tensile tests. After that, evaluations have been done.
iv. The Vickers Micro-Hardness tests have been conducted on sintered specimens at 600 ºC and 620 ºC temperatures. Afterwards, evaluations with relation to the results have been done.
v. Fatigue tests have been conducted in the axial loading mode, which is more severe than bending. The Wöhler curves have been plotted and then, presented in terms of Nominal stress amplitude, $\sigma_{a,n}$ versus Cycles to rupture, N_R for sintered (unpeened) and shot peened specimens, respectively. Sinusoidal load-time function has been in fatigue test. Frequency was 10 Hz and one stress ratio was investigated with the unnotched specimens ($K_t = 1.0$) under fully reversed loading ($R = \sigma_{min} / \sigma_{max} = -1$) using 15 specimens for the determination of each S-N curve.
vi. Etched and unetched optical microscopy observations have been done on

sintered at 600 ºC, 620 ºC and shot peened in 12A, 16A (almen) intensities specimens with 50X and 100X scales separately. Evaluations regarding view have been done.

vii. Scanning Electron Microscope photographs have been investigated on fracture surface of sintered and shot peened specimens with 50X and 500X scales for fatigue test specimens separately. Comparison relating to graphs have been done and evaluated.

The results from the obtained experimental study are below:

- The density measurements of Alumix 431 aluminum alloys sintered at 600 ºC and 620 ºC have been performed in turn and comparison of green and sintered specimens has been done. The results show that highest density has 2, 50 g/cm^3 on sintered specimen at 620 ºC, 400 MPa, RT.
- The porosity reduced and structures became homogeneously with arising temperature. The density is effected directly reducing porosity. Shrinkage of pores was decreased volume of sintered parts, and weight did not change. Thus, the density was increased. High density means that has high strength of sintered parts, and it is desirable feature with powder metallurgy because of fact that high density also effects mechanical properties like strength, toughness, and hardness etc.
- The tensile test results show that tensile strength increases in spite of fact that sintering temperature and peening intensity arises. Shot peening and sintering process is indicated positive effect on material. For reason, Ultimate Tensile Strength was represented an increase between 132 MPa and 185 MPa.
- Sintered materials were indicated uniform values on same specimen and at temperatures in hardness tests. While sintering temperature increases, the hardness profile on samples indicates increasing values because of density rise and these are roughly homogeneous values. The homogeneity in hardness was mainly governed dislocation density, and the distribution as well as the size of small particles. For reason, hardness tests were represented an increase between 141 MPa and 168 MPa.
- Fatigue stresses in the interval of 100 MPa-120 MPa have been tested. Shot

peening gives a marked improvement in the fatigue strength over as the machined condition, with around an order of magnitude increase in cycle life. Shot peened materials were improvemed 10% and 15% in the fatigue strength in terms of unpeened specimens in 12A and 16A intensities, respectively because of fact that shot peening causes increase of density of part. Thus, fatigue strength increased from 100 MPa for unpeened specimens to maximum of approximately 115 MPa for the specimens peened to 12A and from 105 MPa for unpeened specimens to maximum of approximately 120 MPa for the specimens peened to 16A.

- As a result of sintering and shot peening processes, OM observations show that structures are generally become homogenous and pore. Also, grain boundaries appeared notably in etched views. Grain necks are constituted notably and homogeneous structure obtained. Besides, smooth and less porosity surface in spite of fact that sintering temperatures and shot peening intensity arise from 600 ºC to 620 ºC and from 12A to 16A, respectively. Also, shrinkage of the pore was initiated due to sintering and shot peening process.
- SEM observations show that specimens that were sintered and shot peened failed in a ductile manner in terms of properties of PM materials. Cracks were initiated at the large pore area and started sometimes at the sintered or the shot peened surface. The crack initiation zones or points beneath and at shot peened and sintered surface were estimated.

5.2. Future Studies

5.3. Recommendation of Future Studies

This study has been concentrated on the investigation in properties of sintered and shot peened Alumix 431 aluminum alloys.

In the future, the following considerations could be improved:

- More work is required to develop fatigue life and the effect of shot peening

must evaluate more accurately in different shot peening intensties.

- The powder particles among the pores cause voids and this problem can be solved with changing of sintering parameters such as temperature, pressure.
- Different fatigue frequences could be applied.
- Compressive residual stress and roughness created by shot peening could be evaluated in terms of used material.
- Different shot peening parameters could be used like peening time and air pressure.

REFERENCES

ABRASIVE FINISHING COMPANY INCORPORATED, 2009, http://abrasivefinishingcompany.com/.

ASTM E 10-93, 2003, 'Standard Test Method for Vickers Hardness of Metallic Materials'.

ASTM E8M, 2004, 'Standard Test Medhods for Tension Testing of Metallic Materials (Metric)'.

ASTM E468, 2004, 'Standard Practice for Presentation of Constant Amplitude Fatigue Tests Results for Metallic Materials'.

ASTM E739, 2004, 'Standard Practice for Statistical Analysis of Linear or Linearized Stress-Life (S-N) and Strain-Life (ε-N) Fatigue Data at Room Temperature'.

AKYILDIZ, H. K. and SARITAS, S., 1999, 'Bilyalı Dövmenin Fe+%2Cu+%0,5C TM Çeliğin Yorulma Dayanımına Etkisinin Araştırılması', Uluslar arası Katılımlı 2. Ulusal Toz Metalurjisi Konferansı, 15-17 Eylül 1999, ODTÜ, Ankara, Turkey, pp. 519-527.

AKDEMIR, A., TARAKCIOGLU, N. and DEGER, M., 1999, 'Ferritik-Perlitik ve Perlitik Küresel Grafitli Dökme Demirlerde Yüzey işlemlerinin Yorulma Dayanımına Etkileri', 4. Ulusal Kırılma Konferansı, 18-20 Ekim 1999, YTÜ, Istanbul, Turkey, pp. 138-150.

ALMEN, J. O. and BLACK, P. H., 1963, 'Residual Stresses and Fatigue in Metals', New York, NY, McGraw-Hill Education, pp. 226.

ASM HANDBOOK, 1998, 'Powder Metal Technologies and Applications', Vol. 7, ASM International.

BARRY, N., HAINSWORTH, S. V. and FITZPATRICK, M. E., 2009, 'Effect of Shot peening on the Fatigue Behaviour of Cast Magnesium A8', Materials Science and Enginering A, 507, pp. 50-57.

BASARAN, A., VAROL, R., PIRGE, G., BASTURK, S. and VAROL, H., 2007, 'Bilyalı Dövme İşlemi ve Yüksek Sıcaklığın, Bakır İlaveli Toz Metal Çelik Parçaların Yorulma Dayanımına Etkisinin İncelenmesi', Prooceedings of 8th

International Fracture Conference, 7-9 November 2007, Istanbul, Turkey, pp. 242-252.

BRANDES, R. M. and BROOK, G. B., 1992, 'Smithells Metals Reference Book', Eighth Edition, Oxford, Great Britain, Butterworth Heinemann.

COUCHMAN, K. and COUSINO, C., 1994, 'The Processing, Properties, and Applications for Aluminium Powder Metallurgy Materials', SAE Technical Paper Series, 940428, pp. 1-13.

DİLEK, M., 2006, 'Mechanical Properties of Different Aluminum Alloys Joined by Friction Stir Welding', Master Thesis, Cukurova University Institute of Naturel and Applied Sciences, Adana, Turkey.

DULEK, E., ORMAN, S., KARATAS, C. and SARITAS, S., 2005, 'Bilyalı Dövme Parametrelerinin Ç1020 Çeliğinin Yorulma Dayanımına Etkisi ve Oluşan Kalıcı Gerilmenin Katman Kaldırma Yöntemi ile Araştırılması', J. Fac. Eng. Arch. Gazi Univ., Vol. 20, No. 3, pp. 289-295.

DULEK, E., KARATAS, C. and SARITAS, S., 2003, 'Bilyalı Dövülmüş Ç1020 Malzemede Kalıcı Gerilmenin Katman Kaldırma Yöntemi ile İncelenmesi', J. Fac. Eng. Arch. Gazi Univ., Vol. 18, No. 3, pp. 107-116.

EKSI A. K. and YUZBASIOGLU, A. H., 2007, 'Effect of Sintering and Pressing Parameters on the Densification of Cold Isostatically Pressed Al and Fe Powders', Materials and Design, 28, pp. 1364-1368.

EKSI, A. K., VELT, G., PETZOLDT, F., LIPP, K. and SONSINO, C. M., 2004a, 'Tensile and Fatigue Properties of Cold and Warm Compacted Alumix 431 Alloy, Powder Metallurgy, Vol. 47, No.1, pp. 60-64.

EKSI, A. K., BIRCAN, D. A. and SONSINO, C. M., 2007, 'A Study of Cold and Warm Compacted Alumix 431 (Al 7xxx) Powders', J. Fac. Eng. Arch. Gazi Univ., Vol. 22, No. 2, pp. 337-345.

EKSI, A. K., BIRCAN, D. A. and SONSINO, C. M., 2006, 'Static and Fatigue properties of the Cold and Warm Compacted Sintered Aluminium Alloy Alumix 431 (Al-5.5 Zn-2.5 Mg-1.5 Cu)', Wiley Inter Science, 37, No. 5, pp. 374-382.

ESPER, F. J., LEUZE, G. and SONSINO, C. M., 1981, 'Characteristic Properties of

Powder Metallurgical Materials Relevant to Fatigue Design', Powder Matallurgy International, 13, No. 4, pp. 203-208.

GERMAN, R. M., 1997, 'Powder Metallurgy Science', Metal Powder Industries Federation, New Jersey, USA, pp. 472.

GOI, K. L. S., BUTLER, D. L., JARFORS, A. E. W, YONG, J. M. S. and LIM, D. C. S., 2008, 'Elastic Modulus of Sintered Porous Ti-Si-Zr, Using Activation by Ti-Si Mechanically Alloyed Powder and TiH_2 Powder', Materials Science and Enginering A, 475, pp. 45-51.

GRADL, J., NEUBING, H. C. and MÜLLER, A., 2004, 'Improvement in the Sinterability of 7xxx based Aluminium Premix', Euro PM2004 PM Lightweight and Porous Materials, Vol. 4, pp. 13-19.

HABIBI, S. M., JANGHORBAN, K., KHORSAND, H. and YOOZBASHIZADE, H., 2002, 'Axial Fatigue Behaviour of MoNiCu Alloyed Sintered Steel', 3rd International Powder Metallurgy Conference, September 4-8, 2002, Turkish Powder Metallurgy Association, Gazi University, Ankara, Turkey, pp. 398-407.

HICYILMAZ, N., AYDIN, S. and SARITAS, S., 'Toz Metalurjisi ile Üretilmiş Aluminyum Esaslı Tanecikli Kompozitlerin Mekanik Özellikleri', 1999, Uluslararası Katılımlı 2. Ulusal Toz Metalurjisi Konferansı, 15-17 Eylül 1999, ODTÜ, Ankara, Turkey, pp. 621-629.

IYNEN, O., EKSI, A. K., BIRCAN, D. A. and DILEK, M., 2009, 'Design and Investigation of Improvement of Fatigue Properties of the Machine Elements Produced by the Powder Metallurgy', 5th International Advanced Technologies Symposium (IATS'09), May 13-15, 2009, Karabuk, Turkey.

SEROPE, K., SCHMID, S., 2008, 'Manufacturing Processes for Engineering Materials', Prentice Hall, Pearson Education, 4th Edition, pp. 976, New Jersey, USA..

METAL POWDER INDUSTRIES FEDERATION, 2009, http://www.mpif.org/.

METAL IMPROVEMENT COMPANY, 2009, http://www.metalimprovement.com/.

MCCALL, J. L. and MUELLER, W. M., 1973, 'Microstructural Analysis Tools and Techniques', Plenum Press, New York, London, Great Britian.

MIURA, H., 2002, 'Fatigue Fracture Behaviou of PM and PIM Steels', 3rd International Powder Metallurgy Conference, September 4-8, 2002, Turkish Powder Metallurgy Association, Gazi University, Ankara, Turkey, pp. 47-55.

PAVEL, C., BRANDUSEN, L. and MURESAN, R., 2002, 'The Influence od Shot peening on the Fatigue Properties of Powder Materials', 3rd International Powder Metallurgy Conference, September 4-8, 2002, Turkish Powder Metallurgy Association, Gazi University, Ankara, Turkey, pp. 698-701.

SARITAS, S., DOGAN, C. and VAROL, R., 1999, 'Improvement of Fatigue Properties of PM Steels by Shot peening', Powder Metallurgy, Vol. 42, No. 2, pp. 126-130.

SARITAS, S., 2002, 'Toz Metal Çeliklerin Yorulma Özellikleri', 3rd International Powder Metallurgy Conference, September 4-8, 2002, Turkish Powder Metallurgy Association, Gazi University, Ankara, Turkey, pp. 1207-1220.

SCHAFFER G.B. and Huo S.H., 1999, 'On development of Sintered 7xxx Series Aluminium Alloys, Powder Metallurgy', Vol. 42, No. 3, pp. 219-226.

SCHAFFER, G. B., HALL, B. J., BONNER, S.J., HOU, S.H. and SERCOMBE, T. B., 2006, 'The Effect of the Atmosphere and the Role of Pore Filling on The Sintering of Aluminium, Acta Materialia, 54, pp. 131-138.

SHOWAITER, N. and YOUSEFFI, M., 2008, 'Compaction, Sintering and Mechanical Properties of Elemental 6061 Al Powder with and without Sintering Aids', Materials and Design, 29, pp. 752-762.

SONSINO, C. M. A. and HUPPMANN, W. J., 1985, 'Fatigue Design of PM Automotive Components', International Journal of Vehicle Design, Vol. 6, No. 3, Printed in UK, pp. 297-309.

SONSINO, C. M. A. and HUPPMANN, W. J., 1990, 'Fatigue Design for Powder Metallurgy', Powder Metallurgy, Vol. 33, No. 3, pp. 235-245.

SONSINO, C. M. A. and HUPPMANN, W. J., 2007, 'Light-Weight Design Changes Using High-Strength Steels', Metallwissenschft und Technik, Vol. 38, Issue: 1, pp. 9-22.

SUDHAKAR, K. V., 2000, 'Fatigue behaviour of a High Density Powder Metallurgy Steel', International Journal of Fatigue, 22, pp. 729-734.

TEKELI, S., 2002, ‘Enhancement of Fatigue Strength of SAE 9245 Steel by Shot peening’, Materials Letters, 57, pp. 604-608.

TORRES, M. A. S. and VOORWALD, H. J. C., 2002, ‘An Evaluation of Shot peening, Residual Stress and Stress Relaxation on the Fatigue Life of AISI 4340’, International Journal of Fatigue, 24, pp. 877-886.

TSE CR 12361, 1999, ‘Destructive Tests on Welds in Metallic Materials- Etchants for Macroscopic and Microscopic Examination’.

TURKISH POWDER METALLURGY ASSOCIATION (TTMD), 2009,http://www.turkishpm.org/.

THE EUROPEAN POWDER METALLURGY ASSOCIATION, 2009, http://www.epma.com/.

UYGUR, E. M., 1996, ‘Present Status of Powder Metallurgy In Turkey’, I. International Powder Metallurgy Conference, 16-17 September 1996, Gazi Universty, Ankara, Turkey, pp. 653-660.

VAROL, R., EKSI, A. K. and BEDIR, F., 2003, ‘The Effects of Bronizing on the Surface and Fatigue Properties of PM Steel’, Metallwissenschft und Technik, 57. Jahrrang. 10/2003, pp. 636-639.

VAROL, R., 1996, ‘Effect of Heat and Mechanical Surface Treatments on the Fatigue Properties of SAE 8620Steel’, Metallwissenschft und Technik, 50, Jahrgang, Nr. 4/96, pp. 257-259.

VAROL, R. and TUNAY, R. F., 2001a, ‘Bilyalı Dövülmüş AA2024 Aluminyum Alaşımın Aşınma Özellikleri’, Mühendis ve Makine, Haziran 2001, 42 (497), pp. 40-44.

_____2001b, ‘AA2024-T4 Alüminyum Alaşımının Yorulma Dayanımına Ilık Bilyalı Dövme İşleminin Etkisi’, TBMMOB Makine Mühendisleri Odası Konya Şubesi Makine Tasarım ve İmalat Teknolojileri Kongresi (MATİT), 02-03 Kasım 2001, pp. 53-57.

YILDIRIM, S., KELESTIMUR, M. H. and AKSOY, M., 1999, ‘Toz Metalurjisi Yöntemi ile Üretilen Fe/Ferrokrom Malzemesinin Yorulma Davranışının İncelenmesi, 4. Ulusal Kırılma Konferansı, 18-20 Ekim 1999, YTÜ, Istanbul, Turkey, pp. 160-170.

YILMAZ, S. S., UNLU, B. S. and VAROL, R., 2007, ‘Borlama ve Bilyalı Dövmenin Demir Esaslı TM Malzemelerde Yorulma Davranışına Etkisi’, Makine Teknolojileri Elektronik Dergisi, 2007 (1) pp. 61-68.

YÜZBAŞIOĞLU, A. H., 2004, ‘Sintering of Cold Isostatically Pressed Metal Powders’, Master Thesis, Cukurova University Institute of Naturel and Applied Sciences, Adana, Turkey.

CURRICULUM VITAE

Oğur İYNEN was born in Adana, 1979. After being graduated from Seyhan 19 Mayıs Lisesi, Adana, he enrolled in Harran University, Mechanical Engineering Department of Engineering. He graduated from Harran University as a Mechanical Engineer on June 2002. He started his Master of Science (MSc) education in Çukurova University Institute of Natural and Applied Sciences Mechanical Engineering Department Construction & Manufacture Division in 2005.